Title
The Toxicity of Chemical Flame-retardants and Silver Nanowires: An "omics" approach

Author
Scanlan, Leona Dance

Publication Date
2012

Peer reviewed|Thesis/dissertation

The Toxicity of Chemical Flame-retardants and Silver Nanowires: An "omics" approach

By

Leona Dance Scanlan

A dissertation submitted in partial satisfaction of the

requirements for the degree of

Doctor of Philosophy

in

Molecular Toxicology

in the

Graduate Division

of the

University of California, Berkeley

Committee in charge:

Professor Christopher D. Vulpe
Professor Leonard F. Bjeldanes
Professor David L. Sedlak

Fall 2012

ABSTRACT

The Toxicity of Chemical Flame-retardants and Silver Nanowires: An "omics" approach

Leona Dance Scanlan
Doctor of Philosophy in Molecular Toxicology
University of California, Berkeley
Professor Christopher Vulpe, Chair

Chemical contaminants are being detected with increasing frequency in the environment, both as a result of better analytical monitoring techniques and from increasing contaminant concentrations. It is important to understand if un-monitored "emerging contaminant" chemicals can affect or cause toxicity in organisms of ecological importance or affect ecological health. Acute toxicity testing is a usual first step to determine contaminant effects on model organisms. In this work, the nominal acute LC_{50} (concentration that kills fifty percent of animals tested) was established for chemicals from two classes of emerging contaminants, silver nanowires and chemical flame-retardants, on freshwater crustacean, *Daphnia magna*. Gene expression studies were then done with microarray technology at sub-acute 1/10 nominal LC_{50} concentrations to determine genes differentially expressed in exposed animals as compared to control. Results were computationally analyzed with KEGG gene ontology pathway analysis to determine biological pathways affected, and with HOPACH clustering to determine similarities between different gene expression profiles. In each class of contaminant, each different exposure elicited a largely unique gene expression profile.

Further studies on characterization of the nanowires in *Daphnia* growth media and on nanowire uptake were conducted, and high-throughput, short-read sequencing was done on *Daphnia magna* RNA samples. A *de novo* transcriptome was assembled and used for differential gene expression analysis of sequenced RNA from control and silver nanowire-exposed daphnids. The silver nanowires investigated in this study were long and short polyvinylpyrrolidone-coated silver nanowires (PVP AgNW) and long and short silica-coated silver nanowires (SiO_2 AgNW). Ionic silver (Ag^+) was also tested.

Silver nanowires were not as toxic as ionic silver, and toxicity varied as a function of size and of coating and in different *Daphnia* growth media. Toxicity could not be attributed to the concentration of dissolved silver in media, but might be caused by internal silver dosing and by a nanowire-specific effect, perhaps related to nanowire shape. The short SiO_2 coated AgNWs caused the most similar response to Ag^+, and were also the most toxic of the nanowires. The long PVP AgNWs were the least toxic material under most conditions, and caused the most unique gene expression profile. This is the first study to show what appears to be uptake and *in vivo* modification of nanowires into an animal and the first to show toxic effects of a silver nanomaterial both caused by and independent of silver.

De novo assembly of short-read sequencing data resulted in a robust *Daphnia magna* transcriptome. Over 101,000 unique transcripts were identified, which illustrated the power of new sequencing technologies and computation algorithms to identify alternate splicing of RNA transcripts. The generated transcriptome was used as a scaffold on which short-read sequencing data were aligned to analyze differential gene expression in control versus AgNW-exposed animals. Preliminary results showed that gene expression analysis with sequencing data resulted in different numbers of differentially expressed genes than were determined with microarray techniques. A combination of four align-and-count methods were subsequently used, which all resulted in different sets of differentially expressed genes. Further work on confirming which method is best for this dataset will need to be done before the sequencing results can be further compared to microarray results. To date, it is unclear whether gene expression studies using sequencing data are more robust or informative than studies with microarray data. However, the assembled transcriptome represents a significant *Daphnia magna* genomic contribution.

The chemical flame-retardant nominal LC_{50} values ranged from 58 μg/L (pentaBDE) to 3.96 mg/L (octaBDE). These chemicals are not very soluble in water, so the LC_{50} values only represent the amount of chemical added to the exposure system, not the amount of chemical dissolved in water or the amount of chemical available to the animals. These nominal LC_{50} values likely underestimate toxicity of FRs to *Daphnia magna*. Chemical flame-retardants tested were Firemaster® 550 (FM550), Firemaster® BZ54 (BZ54), pentabrominated diphenyl ether (pentaBDE), octabrominated diphenyl ether (octaBDE), triphenyl phosphate (TPP), tetrabromobenzoate (TBPH). The un-brominated analog to TBPH, phthalate di(2-ethylhexyl) phthalate (DEHP), was also tested. Gene expression profiles had little similarity between chemicals, indicating potentially unique biological effects instead of general toxicity, such as by narcosis. Additional lipidomic and metabolomic studies with FM550 and pentaBDE at 1/10 LC_{50} showed distinct differences between effects of the two compounds. Genomic results indicate that FM550 exposure may affect transcription and translation of mRNA in *Daphnia magna*, but further studies are warranted to determine exact mode of toxicity.

Both chemical flame-retardants and silver nanowires are highly toxic to *Daphnia magna* and cause unique molecular responses. However, exposure concentrations used in this study are typically higher than concentrations detected in environmental samples. Further studies are needed at lower concentrations to confirm the lower limits of effect, and to further investigate specific modes of toxicity. Distinct biological processes were affected by exposure to each chemical and by exposure to different concentrations of one chemical, FM550. This work was limited by lack of annotation of the *Daphnia* genome and by limited characterization of the *Daphnia* proteome. Molecular studies in *Daphnia* were limited, as *Daphnia* cell lines do not exist. This work contributes, however, to basic knowledge about acute toxicity and molecular effects of environmental contaminants.

DEDICATION

This dissertation is dedicated to my family: Dad, Mom, Joan, Greg and Summer-twin. It is also dedicated to my grandmothers Virginia, Ernestine, Jane and Naomi, and my grandfathers Bill, Donald and Earl Daniel Scanlan, Sr.

TABLE OF CONTENTS

LIST OF TABLES

LIST OF FIGURES

LIST OF ACRONYMS

TSCA – Toxic Substances Control Act, 1976
DGE – differentially expressed genes
mRNA – messenger RNA
RNA – ribonucleic acid
DNA – deoxyribonucleic acid
cDNA – complimentary deoxyribonucleic acid
qPCR – quantitative polymerase chain reaction
SAGE – serial analysis of gene expression
HTS – high throughput sequencing
PBDE – polybromonated diphenyl ether
FM550 – Firemaster® 550
FR – flame-retardant
AgNW – silver nanowire
NM – nanomaterial
NW – nanowire
NP – nanoparticle
Ag^{+} – ionic silver
pentaBDE – pentabromo diphenyl ether
octaBDE – octabromo diphenyl ether
TBPH – tetrabromo phthalate
TBB – tetrabromo benzoate
TAP – triaryl phosphate
TPP – triphenyl phosphate
DEHP – di(ethylhexyl) pthalate
BZ54 – Firemaster® BZ-54
PVP - polyvinylpyrrolidinone
SiO_2 – silicon oxide
NR – nanorod
NF – nanofiber
LC_{50} – lethal concentration that kills 50% of animals tested
LD_{50} – lethal dose that kills 50% of animals tested
ICP-MS – inductively coupled plasma mass spectrometry
TEM – transmission electron microscopy
STEM – scanning transmission electron microscopy
SEM – scanning electron microscopy
DLS – dynamic light scattering
COMBO – *Daphnia* culture media
EPA – Environmental Protection Agency, second *Daphnia* culture media
spICP-MS – single particle inductively coupled plasma mass spectrometry
NCBI – National Center for Biotechnology Information
BLAST – Basic Local Alignment Search Tool
KEGG – Kyoto Encyclopedia of Genes and Genomes
HOPACH - Hierarchical Ordered Partitioning And Collapsing Hybrid
S-SiO_2 – short silica-coated silver nanowire

L-SiO_2 – long silica-coated silver nanowire
S-PVP – short PVP-coated silver nanowire
L-PVP – long PVP-coated silver nanowire
$AgNO_3$ – silver nitrate
ATP – adenosine triphosphate
SRS – short read sequencing
EST – expressed sequence tag
NR – non-redundant protein database
Exp – eXpress computational program for aligning and counting differential gene expression short read data
L1, L2, L3 – names of high-throughput, short-read sequencing runs
NMR – nuclear magnetic resonance
TOSCY – total correlation spectroscopy
PCA – principal components analysis
PLS-DA – partial least squares discriminant analysis
DMSO – dimethyl sulfoxide
GC/ECNI-MS – gas chromatography mass spectrometry operated in negative chemical ionization mode
Jak-STAT – Janus kinase-signal transducer and activator of transcription

ACKNOWLEDGEMENTS

First and foremost, I thank Chris Vulpe, my advisor. Thank you for giving me the opportunity to work on so many different, interesting and important projects and for the financial and intellectual support, friendship, fun and travel opportunities. I am forever grateful and I will miss working with you.

Thank you to the professors who served as academic committee members throughout my graduate career. Len Bjeldanes, David Sedlak, Inge Werner, Terry Machen, Dale Johnson and Benito Delumen: I appreciate your advice, input, criticism, patience and effort through my successes and failures.

This work was not possible without the Vulpe laboratory members. Numerous undergraduate student interns contributed significant effort to my endeavors and became experts on laboratory techniques including *Daphnia* culture, microarray preparation and RNA handling: Daniel Nowinski, Christine Tran, Charlotte ter Haar, Michael Guzman, Jonah Kornbluh, Monica Eng, Tina Cun, Jeff Nathan, Audrey Arai, Nadeeka Karunaratne, Erica Lachenauer, Xin Xin Lin, Pauline Luong, Katie Dailey, Rosa Chan, Casey Wang, Jessica Hsu, and Namuun Bayara. Laboratory members who gave me advise and support include postdoctoral researchers Stela MacLachlan, Matthew North, Hun-Je Jo, Seonock Woo, and William Jo. Don Pham, Candace Clark and Marianna Augustine were invaluable research technicians and allies. Visiting scholars Huijun Chen and Zouhair Attieh kept me laughing and on my toes. Special thanks to senior scientist Abderrahmane (Mani) Tagmount, who rescued both my experiments and my moral and who was my hero on more than one occasion.

I also thank the Department of Nutritional Sciences and Toxicology, the Graduate Group in Molecular Toxicology, the NIH Genomics Training Grant and the Center of Integrated Nanomechanical Systems (COINS) for funding, support, and intellectual debate.

I am indebted to my collaborators. Ben Gilbert at Lawrence Berkeley National Lab performed all nanowire characterization and helped write the first nanowire manuscript. Philipp Antczak at University of Birmingham, UK, performed all KEGG pathway analysis. John Herbert, also at UB, performed the final transcriptome assembly and differential gene expression analysis with sequencing data. I am grateful to Phil and John's advisor Francesco Falciani for his collaboration and encouragement. Robert Reed at the Colorado School of Mines performed the spICP-MS analysis under the direction of James Ranville and Christopher Higgins. Heather Stapleton and Katie Douglas at Duke University performed the analytical analysis of FM550 accumulation. Heather also provided ongoing advice for the flame-retardant project. Quincy Teng at the U.S. EPA analyzed all metabolomics data. Shaul Aloni performed energy dispersive spectroscopy on the nanowires. Mary Roth and the Kansas State University Lipidomics Research Center did the lipidomic profiling. Arlene Blum and Susan Klosterhaus both provided advice and insight on flame-retardants. Thank you everyone for your contribution. We will be publishing soon.

Finally, I am thankful for my family and friends. My parents, stepparents, grandparents, twin sister and extended family loved and supported me for the last five and a half years, even when they did not understand the work that was causing me joy or frustration. Mom and Dad: thank you for raising me into the inquisitive, stubborn, literal and ethical scientist I am. Cantisano-Kampas and Severt families: You are my favorite. Thank you for feeding me. I love you forever. Mahim Lakhani: Thank you for the love, support and the long walks to clear out my head. Phin: You're the cat. Twin: I'm not sure what you'll do when I can no longer bring you dry socks. I think you'd better keep a spare set on campus.

INTRODUCTION

Background

Industries in the United States (U.S.) manufacture or import 42 billion pounds of chemicals daily for use in commercial processes and products.[1] These chemicals are found in products ranging from pharmaceuticals to building supplies, cosmetics and electronics. They enter the environment through use and subsequent disposal. The Toxic Substances Control Act (TSCA) inventory, created in 1976 to regulate chemical use and testing, registered more than 80,000 chemicals for commerce in the U.S.; approximately 2000 chemicals are added each year.[1] TSCA, in theory, protects humans and the environment from harm from chemical exposure, but it does not actually require chemical producers to generate or disclose toxicity or environmental data.[1] As a result, information on the toxicity of commonly used commercial chemicals and environmental contaminants is sparse.

Two classes of environmental contaminants are emerging contaminants and legacy contaminants. Emerging contaminants are naturally occurring or manmade chemical, microbial or radiological substances that are not commonly monitored in the environment. They have the potential to enter the environment and cause adverse ecological or human health effects. Limited toxicological information is available on these chemicals, and they may only have been detected in the environment due to advances in analytical techniques.[2], [3] Examples of emerging contaminants include personal care products and nanomaterials: commercial products that are now in or will likely enter the environment through manufacture, use or disposal.

Legacy contaminants are chemicals that are banned or severely restricted by government agencies.[4] These chemicals, such a polychlorinated biphenyls and polybrominated diphenyl ethers, are often persistent and bioaccumulative, have known toxicities and have been in commercial use for long periods of time. It is important to both test and understand the toxicity of legacy and emerging contaminants in ecologically relevant organisms. This process, ecotoxicology (ecotox), can inform on the sensitivity of organisms to a toxin, the ecological risk due to exposure and the general health of an ecosystem.

Ecotoxicogenomics

Traditional methods for assessing ecotox typically measure mortality, reproduction, phenotypic changes, and growth, but do not inform on the molecular mechanisms behind toxicity.[5], [6] Because gene expression is altered in toxicity, either as a direct or indirect result of exposure,[7] the combination of traditional methods with gene expression and other genomic studies (protein expression, metabolite profiling) can be highly informative. Toxicogenomics uses genomic phenomena to help understand toxicity, and results reflect both the toxicity process and the adaptive response to a toxin.[6], [8], [9] Ecotoxicogenomics is the integration of genomics and ecotox studies: effects of toxicants on organisms of ecological importance assayed with genomic

technology.[6] It can enhance the understanding of modes of toxicity by revealing biological pathways that may contribute to toxicity.[8], [10] These techniques have potential for use in monitoring of contaminant levels, identification of chemicals responsible for toxicity and for ecosystem protection.[8], [11]

After exposure to a contaminant, gene expression changes first, followed over time by changes in protein levels and finally by levels of metabolites. Differential gene expression (DGE) analysis, or comparing gene expression in an exposed system to a control system, therefore gives a rapid snapshot of changes occurring in an organism, tissue or cell. There are numerous techniques for analyzing mRNA expression. The simplest technique is quantitative polymerase chain reaction (qPCR). This technique, based on a process invented by Kary Mullis in 1983, uses a reverse transcriptase enzyme and DNA primers to copy RNA and amplify a single segment into DNA.[12] Fluorescent dyes intercalate into the DNA fragments, emit light, are detected by instrumentation and correlated to expression levels through comparison to an unchanging "housekeeping" gene. Only one gene is assayed per reaction, which limits the amount of data generated. qPCR is further limited by the need for *a priori* knowledge of specific nucleotide sequences of each gene, which are used to develop the DNA primers. qPCR is commonly used to look at the expression of a few genes of interest, but not for global (omic) transcriptome studies. Another quantitative technique for assaying DGE is serial analysis of gene expression (SAGE).[13] In this process, mRNA is processed into "di-tagged" complimentary DNA (cDNA, reverse transcribed from RNA), which is then concatenated, cloned into plasmids and sequenced. SAGE results in counts of partial mRNA sequences. A widely used approach for assaying global gene expression is the microarray technique. Microarrays consist of short cDNA or synthesized oligonucleotide DNA sequences attached to a glass slide with a molecular linker. Numerous copies of each DNA are attached in distinct clusters with a discrete, identifiable location. RNA is amplified, labeled with fluorescent dye, hybridized onto the array and scanned. Expression from a treated sample is then compared to that from a control sample, and DGE is determined.

Recent advances in high throughput sequencing (HTS) technology such as Illumina/ Solexa[14] may, however, make HTS the new gene expression analysis standard. In this process, an RNA sample is processed into short cDNA fragments and sequenced. The short fragments are then aligned to a reference genome and counted as a number of reads per kilobase of exon model (gene) per million mapped reads.[15] If a reference genome is not available, the sequences can be *de novo* assembled with computational algorithms into a transcriptome (collection of longer and full-length transcripts), which can then be used in place of a genome. HTS sample preparation is time consuming, but the cost per base sequenced has decreased significantly and sample preparation will soon have a similar cost to microarray technology.

Genomic methods have been used to help elucidate mechanisms of toxicity in ecologically relevant organisms and in biologically relevant cell lines. For example, Wintz *et al*. found exposure to munitions compound 2,4-dinitrotoluene affected expression of genes involved in lipid metabolism in fathead minnows, which was

confirmed by measuring liver lipids.[16] Ludwig *et al*. used DGE to assay effects of 1,3-dinitrobenzene on male rats, saw changes in gene expression related to plasma testosterone and testicular steroidogenesis, and confirmed hormone effects with a steroidogenesis assay.[17] Poynton *et al*. combined DGE assays with a metabolomic assay and determined that exposure to cadmium caused a decrease in expression of digestion enzymes and a corresponding decrease in absorption of nutrients in *Daphnia magna*.[18]

Model organism – *Daphnia manga*

The goal of this work was to use toxicity and genomic assays to understand the toxic effects of emerging environmental contaminant silver nanowires (AgNWs) and legacy contaminant polybrominated diphenyl ethers (PBDEs) as well as the emerging contaminant and PBDE flame-retardant replacement Firemaster® 550 (FM550) and related compounds on freshwater crustacean *Daphnia magna* (**Figure I**). Freshwater crustacean *Daphnia* sp. (daphnids) are considered a keystone species in freshwater food webs, are an important model for ecological, evolutionary and toxicological research and are the best characterized aquatic invertebrate.[19] They are used extensively to study organismal response to pollutants and are widely distributed in the environment, where they are constitutively exposed to chemicals.[20] They are sensitive to chemical exposure and are commonly used for toxicity testing. Ecotoxicogenomic studies on *Daphnia* can establish relationships between chemical exposure and adverse effects, identify biomarkers of exposure, and help elucidate molecular mechanisms of toxicity.[20] *Daphnia* is the second arthropod, after *Drosophila*, recognized by the US National Institutes of Health as a model organism for biomedical research (http://www.nih.gov/science/models).[19] "Daphnids" reproduce via cyclic parthenogenesis (female daphnids give birth to identical female clones), which makes it a model for epigenetic studies[21] and for investigating environmental effects. Daphnids are biologically interesting, easy to culture and maintain, and environmentally relevant. They are therefore ideal for studying the effects of environmental contaminants.

Chemicals studied

The two types of contaminants under study in this work are silver nanowires (AgNWs) and chemical flame-retardants (FRs). Nanowires (NWs) are a high-aspect-ratio nanomaterial (NM), or a material in which one dimension (length) is significantly larger than the others (height, width) as a result of preferential growth during synthesis. Nanowire height and width is on the nanometer scale while length is on the micrometer scale. NMs are increasingly used in technological materials and consumer products and NWs may have toxicological characteristics distinct from other nanoparticles (NPs). Hundreds of commercial products exist that contain NMs and the number of such products is growing. There is especially widespread use of silver nanoparticles NPs as antimicrobial agents,[22] and many types of metallic and semiconductor NPs are used in cosmetics, food products, children's toys and electronics.[23] The use of NWs is expected to increase due to an increase in technological applications.[24] For example, engineering of NW diameter can tune important properties such as optical band gap of

semiconductors or surface plasmon resonance frequencies of metals.[25] Individual NWs and their aggregates possess anisotropic properties, particularly for the transfer of charge or heat. Areas of NW commercialization include thermal shielding, optoelectronic devices and chemical sensors.[26], [27] AgNWs are not yet commercialized nor are they found in the environment. NMs from commercial products can be released into the environment during manufacture, use or disposal, but their environmental and toxicological impact is poorly understood.[28], [29] NM contaminants can also enter the environment through wastewater treatment plant effluent and activated sludge.[22], [30] Determining potential environmental impact requires study of the toxicity of NMs on relevant biota, but research on the toxicity of NWs is extremely limited.[31] NWs are not yet in the environment, as their use in commercial products is only now developing. This therefore represents a preemptive toxicity study of potential environmental contaminants.

Chemical flame-retardants (FRs) are used extensively in consumer products such as furniture foam, upholstery, and electronic casings. The chemicals are not covalently bound to the materials in which they are added, so they distribute into the environment and are globally distributed in sediment, water and air. However, very little data exists about the toxicity of FRs in environmentally relevant organisms such as *Daphnia magna*. In the 1970s, the state of California passed Technical Bulletin 117, which mandated all upholstered furniture for sale in the state to meet flammability standard criteria.[32] Manufacturers used chemical flame-retardants such as penta brominated diphenyl ether (pentaPBD) to meet this mandate. However, over the next 30 years, pentaBDE was found to be persistent and bio-accumulative, caused toxic effects and displayed potential for long-range environmental transport.[33] In the 2000s, PentaBDE and components (tri, tetra, hexa and heptaBDE) were banned from use in the European Union (EU) and were added to the Stockholm Convention as Annex A chemicals slated for elimination.[34], [33] Polybrominated diphenyl ethers (PBDEs) are found globally at low levels in soil, sediment, coastal waters and lakes, [35], [36] sewage sludge and wastewater effluent,[37] and animals including sea turtles (*Caretta caretta*), lake trout, Chinook salmon, humpback dolphins, falcon eggs and wild frogs [38], [39], [40], [41], [42]. PBDEs are also found in human breast milk,[43], [44], [45], [46] house dust, [47] the atmosphere,[48] and the Arctic.[49] Global data indicate increasing levels of PBDE congeners in animals with higher trophic positions.[33] In some locations, the levels of PBDEs are still increasing.[35] Human exposure has been linked to consumer products and to food.[47], [50]

A new chemical flame-retardant formulation, Firemaster®550 (FM550), in 2004 replaced pentaBDE in furniture foam and fabric.[51] FM550 is a proprietary mixture of four different chemical flame-retardants: two brominated components, tetra-bromo phthalate (TBPH) and tetra-bromo benzoate (TBB), and two organophosphate compounds, triphenyl phosphate (TPP) and isopropylated triaryl phosphate (TAP).[52], [51] Much less information is available on environmental load or toxicity of FM550 than for PBDEs. To date, FM550 has been detected in house dust and polyurethane foam from furniture and baby products in the US, marine mammals in Hong Kong, and sediment and mysid shrimp in the Netherlands.[53], [52], [40], [54], [55] Bearr *et al.* conducted accumulation and DNA damage studies of TBB and TBPH on fathead minnow[56] and

investigated *in vitro* hepatic metabolism of TBB and TBPH in the fathead minnow, common carp, mouse and snapping turtle.[57] There is a lack of toxicity data on FM550.

Scope of this work

This work used toxicogenomic techniques to understand the effects of AgNWs and FRs on *Daphnia magna* (**Figure I**). **Table I** lists all chemicals tested in this study. The manuscript is divided into three sections: Toxicity of AgNWs, Transcriptomics, and Toxicity of FRs. Acute LC_{50} values were determined for each molecule after a 24 hour (AgNWs) or 48 hour (FRs) exposure. The LC_{50} values are nominal, not actual values, due to the characteristics of chemicals tested, and likely underestimate the toxicity of FRs and AgNWs to *Daphnia*. Microarray technology was used to assay gene expression in animals exposed to each contaminant as compared to controls. Exposure concentrations are higher than those currently detected in the environment. Gene expression data was then combined with other chemical, molecular and biochemical techniques to investigate the toxicological effects of each contaminant. Chemical concentrations used in this study elicit a sub-acute response in the animals but are not ecologically relevant.

TABLES AND FIGURES

Chemical Name	Chemical Class	Chemical Abbreviation
Long PVP-coated silver nanowire	Nanowire	L-PVP-AgNW
Long silica-coated silver nanowire	Nanowire	L-SiO_2-AgNW
Short PVP-coated silver nanowire	Nanowire	S-PVP-AgNW
Short silica-coated silver nanowire	Nanowire	S-SiO_2-AgNW
Ionic silver	Metal	Ag^+
Firemaster® 550	Flame-retardant	FM550
Firemaster® BZ54	Flame-retardant	BZ54
Pentabrominated diphenyl ether	Flame-retardant	PentaBDE
Octabrominated diphenyl ether	Flame-retardant	OctaBDE
Triphenyl phosphate	Flame-retardant	TPP
Tetrabromobenzoate	Flame-retardant	TBPH
Di(2-ethylhexyl) phthalate	Plasticizer	DEHP

Table I. List of the emerging silver nanowire (AgNW) and legacy and replacement flame-retardant (FR) environmental contaminant chemicals tested in this study.

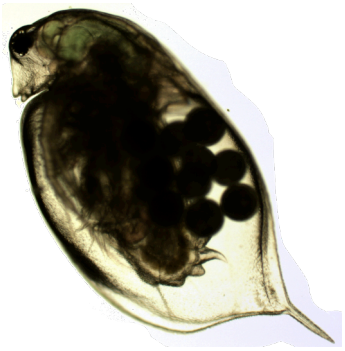

Figure I. Two-week old *Daphnia magna* with embryos in her brood chamber. Her second antenna is not visible. Image acquired with a Zeiss Axioimager M1 microscope.

Chapter 1.

The Toxicity of Silver Nanowires on *Daphnia magna*

INTRODUCTION

The toxicity of silver nanowires (AgNW) (**Figure 1**) to *Daphnia magna* was compared to each other and to the toxicity of ionic silver (Ag^+). A total of four AgNWs were investigated with two different dimensions and two different surface coatings (**Table 1**). The coatings were organic polyvinylpyrrolidone (PVP) or inorganic amorphous aluminum-doped silica (silica or SiO_2). The mean dimensions of the NW were either 2 μm (length) x 30 nm (diameter) or 20 μm x 60 nm, referred to as "short" (S) or "long" (L) NW, respectively. A relationship was sought between acute (24-hour) toxicity and NW characteristics such as length or type of coating. For example, silica coating had been shown to prevent release of metal ions from other nanomaterials, [58], [59] and was expected to minimize the contribution of media-dissolved Ag^+ to toxicity from AgNWs. Differential gene expression (DGE) between treated and control daphnids was analyzed and used to investigate modes of toxicity. Toxicities were expected to be similar between the different AgNWs but different than Ag^+.

Nanowires are considered a nanofiber (NF). The current state of nanofiber toxicological research lacks studies that are biologically or environmentally relevant. Studies that do exist fall into two distinct classes of NF toxicological papers. The first class consists of papers written on the design and manufacture of a NF that also include at least one toxicological assay but do not actually investigate molecular phenomena or mechanisms of toxicity. The second class of paper delves more deeply into the molecular and biological effects of a NF and may or may not contain data on the manufacture or characterization of the NF.

Non-molecular papers often include a single cellular viability test and no other toxicological assays, such as the paper by Jeon *et al*. on nickel-gold core-shell and nickel nanowires (NW).[60] NWs were synthesized and characterized, attached to a fluorescent dye and incubated with Panc-1 human pancreatic carcinoma cells at one concentration. The numbers of dead and live cells were counted microscopically at 8-40 hours. Jeon *et al*. concluded that the Ni-Au NWs may be useful in biomedical applications, and are now investigating whether the NW cause death via apoptosis (programmed cell death) or necrosis (extreme cell damage). This paper illustrates a common lack in the NF toxicity field – results are not biologically or environmentally meaningful. Will this one tested dose be relevant to animal (or human) exposure? Will pancreatic cancer cells be the only cells exposed to this NW? No LC_{50} (concentration that kills 50% of cells exposed) was established, no molecular assays were done, and only one cell kind of cell line was tested.

More thorough work by Kopwitthaya *et al*. combined *in vitro* and *in vivo* assays to look at the toxicity and utility of PEGylated gold nanorods (NR) in female mice.[61] They studied distribution of the NR and mouse body weight and blood markers of kidney

and liver function and concluded that the NR "revealed no mortality, adverse effects or weight changes," although some of the blood markers appeared to be in the "not normal" range. Furthermore, detailed data from a higher dose that did elicit partial mortality (~40%) and decreased body weight were not discussed. The group could have determined the LD_{50} in mice or in cells with a few more treatment groups, and would have then had a common metric for comparison of toxicity to other NFs. While their work contains animal and cell assays, it does not help understand how or why the NR are toxic. Work by Chen *et al* used molecular techniques as proof-of-concept for NF function. The techniques could easily be adapted into a toxicity assay.[62] Ultimately, however, in this type of study understanding the amount of NF required to cause toxicity and molecular effects of the NF are not a priority.

More thorough research articles by NF developers exist and show a deeper understanding of molecular mechanisms, such the work by Ahamed *et al.* on zinc oxide nanorod-induced apoptosis in human alveolar adenocarcinoma.[63] In this study, the ability of zinc oxide NR to induce cytotoxicity, form reactive oxygen species, cause oxidative stress and activate apoptotic signaling molecules was investigated with cellular, chemical and protein immunoblot assays. The work was both dose- and time-dependent and included an ionic zinc control. The work first tells a story of cell damage and then elucidates some of the mechanisms behind the damage. However, other cell lines will need to be tested to determine if the zinc NR toxicity is cancer cell-specific.

Nanofiber toxicity research is also lacking when compared to toxicity research on nanotubes, a similarly shaped nanomaterial that has a hollow core. A higher percentage of articles published on nanotubes are related to toxicity and there is larger breadth and depth of toxicological studies. For example, Begum *et al.* looked at the phytotoxicity of nanotubes,[64] while Larue *et al.* looked at uptake in wheat and rapeseed.[65] LD and LC_{50}s were established, such as for carbon nanotubes on freshwater crustacean *Ceriodaphnia dubia*.[66] Biologically relevant experiments were conducted, such as the pulmonary toxicity of nanotubes on rats[67] following a relevant, intra-tracheal route of exposure. There is also more frequent hypothesis testing[68] and use of a larger variety of cell lines, such as human intestinal cells.[69] Not all research done on nanotubes is thorough and biologically meaningful, but overall, research on the toxicity of nanotubes is more complete than that of nanofibers.

This dissertation in part addresses one gap in the nanofiber toxicology field, the toxic effects of silver nanowires on an environmentally relevant organism, *Daphnia magna*. This work is molecular and aims to begin investigation of the toxicity of nanowires by using molecular "omics" techniques. Environmental risk of AgNWs to aquatic cladocerans such as *Daphnia magna* is especially great as invertebrates are more sensitive than vertebrates to silver.[70] In the presence of dissolved O_2, silver NMs oxidize and release ionic silver (Ag^+).[71] Silver is highly toxic to aquatic species. The acute toxicity of Ag^+ is usually attributed to inhibition of a sodium-potassium adenosine triphosphatase (Na^+/K^+ ATPase) in the gill or the gut.[72], [73], [74] This is the first study to look at the toxicity of silver nanowires in any organism.

METHODS

Silver nanowire characterization

Silver nanowires were purchased from nanoComposix (San Diego, CA). Stock solutions were deoxygenated by bubbling in N_2 for one hour and were stored in rolled, lightproof bottles in an anaerobic chamber. The silver concentration of each solution was measured in triplicate using inductively coupled plasma mass spectrometry (ICP-MS) after digesting 100-µL AgNW aliquots in concentrated nitric acid. Silver concentrations were approximately 2 g/L. Nanorod impurities were detected and quantified by removing nanowires via filtration and measuring total silver in filtrate with ICP-MS. 200 uL of stock solution was added to 25 mL ultrapure water and stirred for about 10 minutes. Aliquots of each solution were passed through 0.45 µm or 0.02 µm diameter filters that retained just the nanowires, or the nanowires and nanorods, respectively. **Table 2** summarizes nanorod impurities. All characterization and imaging of wires was conducted by Dr. Benjamin Gilbert at Lawrence Berkeley National Laboratory.

Transmission electron microscopy (TEM) and scanning transmission electron microscopy (STEM) were used to measure the morphology and dimensions of the nanowires and their surface coatings (**Figures 2 & 3**). The TEM (JEOL 2100F) was equipped with OXFORD INCA energy dispersive x-ray spectroscopy suite (EDS). STEM was equipped with Gatan's Digiscan II. TEM was also used to investigate the effects of aqueous medias on silica coating integrity. To do this, short SiO_2-coated AgNWs were immersed in exposure media for two hours. A droplet of the solution was placed on a lacey carbon grid, dried, and imaged.

Dynamic light scattering (DLS) (Precision Detectors) was performed to measure the stability against aggregation of short AgNW suspensions in *Daphnia* media and in pure water. 25-mL AgNW suspensions of 12 mg/L (111 µM) Ag were placed in covered beakers. 1-mL aliquots were extracted for DLS analysis over a 48-hour period. All solutions were modestly stirred (1x5 mm stir bar at ~200 rpm) to limit NW settling. Long AgNW were too large for DLS analysis, so AgNW and their aggregates were collected from solution and imaged with scanning electron microscopy (SEM) on silicon wafers. At 12 mg/L Ag, collection time of 1-2 hours achieved a surface coverage of NW suitable for SEM imaging. The relative rates at which AgNW settled in unstirred 4-mL volumes of 12-mg/L suspensions were estimated in closed 1-cm path-length cuvettes monitored by optical absorption spectroscopy (Ocean Optics).

To measure Ag^+ release into aqueous solution, AgNWs were added to ultrapure water or to *Daphnia* media and the dissolved silver concentration was measured at intervals with ICP-MS. AgNWs were filtered from aliquots using a 0.02-µm pore size, 25-mm diameter syringe filter (Whatman Anotop) and the filtrate was acidified and analyzed for total silver. Preliminary trials revealed that all filters effective at separating all AgNW also significantly retained the Ag^+ ion. Retention dropped for successive 1-mL aliquots of solution passed through the same filter (**Figure 4**), indicating saturation of the Ag-binding groups. Therefore, the AgNW solutions were analyzed by passing four

consecutive 1-mL aliquots through the same filter, measuring the silver concentration in each, and taking the highest value of the 3rd or 4th aliquot as the best highest estimate of dissolved silver.

Daphnia magna culture

Genetically homogeneous *Daphnia magna* originally obtained from Aquatic Research Organisms (Hampton, NH) were cultured in a growth chamber (Conviron Adaptis) at 21C with 16 hours of light and eight hours of dark per day. Daphnids were grown in nutritive COMBO media[75] or in a moderately hard water formulation referred to as "EPA"[76] and were fed *Pseudokirchneriella subcapitata* (formerly *Selenastrum capricornutum)* and yeast cereal-leaf and trout chow mix (Aquatic Research Organisms) three times per week following renewal of media. Media was aerated overnight before use to increase dissolved oxygen levels. COMBO pH was maintained at 7.4-7.8; EPA was maintained at pH 7.80-8.0. **Table 3** summarizes media chemical composition.

Toxicity assays

Acute, 24-hour toxicity assays were conducted similarly to the U.S. EPA Whole Effluent Toxicity protocol.[76] Five first instar (<24 hours old) *D. magna* were placed in 35 ml aliquots of media. Each aliquot of media contained a different concentration of a single nanowire. Four replicates of five concentrations and a media-only control were typically tested at one time. Silver nitrate (99.999% trace metals basis) was obtained from Sigma-Aldrich. Lethality was measured after 24 hours. At least three sets of four replicates were conducted for each AgNW and for Ag^+. Acute LC_{50}s were determined using probit statistical program.[76] Assays were performed with and without shaking on an orbital shaker to determine if NW settling affected the LC_{50}. Raw acute data for both long and short PVP AgNW were compared with a Student's t-test in Excel (Microsoft) with two tails, assuming equal variance. There was no statistical difference in animal lethality between still or shaken NW exposures (p=0.824 short-PVP, 0.940 long-PVP). Subsequent exposures were done without shaking. The amount of dissolved ionic silver (Ag^+) in each media was estimated with the Geochemist's Workbench (Rockware), using the default database of thermodynamic constants (**Table 4**).

The presence of AgNWs in *Daphnia* hemolymph fluid was investigated at the SEM and with single particle inductively coupled plasma mass spectrometry (spICP-MS). For SEM and spICP-MS studies, adult *Daphnia* were exposed in COMBO media at the LC_{50} concentration for 24 hours and transferred to MilliQ water to remove any wires adhering to the carapace. Hemolymph was extracted as in Mucklow *et al.*[77] Care was taken to avoid the intestine during removal of hemolymph and to limit unnecessary needle and pipette contact with the daphnid carapace. For SEM, approximately 1 µL of hemolymph was dried on a hydrophilic Si wafer, resulting in extensive precipitation of salt crystals. Samples were coated with graphite prior to SEM analysis. For spICP-MS, samples were assayed on standard ICP-MS instrument, but data was collected over a longer reading time to detect single nanoparticles instead of single metallic ions. A dissolved metal calibration curve was used to determine metal mass – to – instrument

intensity relationship, determine the mass of nanoparticle "pulse" and estimate size. Samples were collected from daphnids exposed to LC_{50} and to 1/10 LC_{50} of L- SiO_2 and S-SiO_2 AgNW and Ag^+ with extraction immediately after exposure and subsequent water rinse or after a 1.5 hour depuration period with or without feeding. Exposure media (both EPA and COMBO) was also analyzed. This experiment represents a proof-of-concept for analysis of *Daphnia* hemolymph after exposure to nanomaterials. spICP-MS was done by Robert Reed at the Colorado School of Mines.

Molecular assays

Exposures were done with 15-20 adult (14 day old) daphnids at 1/10 LC_{50} in 800 mL COMBO media for 24 hours. Four replicates were conducted for each AgNW and for Ag^+ and COMBO control. Assays were conducted on daphnids grown in COMBO media only because the animals were not as fit in EPA media, as measured by fecundity. Animals were removed from exposure media and RNA was extracted immediately in Trizol reagent (Invitrogen) with a handheld homogenizer (Biospec Products Inc.). RNA was cleaned-up with an RNeasy kit (Qiagen) and quality was assessed via spectrometry and on an agarose gel. 300 ng total RNA was reverse-transcribed, amplified and hybridized onto a custom Agilent oligonucleotide DNA microarray (AMADID # 023710) with the Agilent Quick-Amp one-color array kit and protocol. The array was made from the best-responding probes on a 44,000 probe Agilent array, which was constructed from a *Daphnia magna* expressed sequence tag database.[78]

Arrays were scanned with a 16-bit GenePix 4000B microarray scanner with 5-micron resolution. Features were edited and fluorescent intensity regression analysis was done with GenePix Pro 6.0. Data were analyzed using a “Treatment vs. Control” design. Foreground intensities in each array were subtracted with local background. All negatives or flagged spots (using GenePix quality control flag system) were labeled as “NA”, i.e. treated as missing values. All positive values were log (base-2)-transformed. Relative intensity ratios were calculated (ratio= treatment sample /control) for the log-transformed values for each gene (cDNA). Relative intensity values (log2 ratios known as “M-values”) were corrected for non-linear trends (if any) with loess global normalization.[79] Differential gene expression was determined with an algorithm based on α-outlier detection procedures.[80] The further the outlier is the most likely it is a candidate gene. A local variance estimator based on loess was used to take heteroscedasticity (if any) into consideration.[80]

As a result, each gene in a given “Treatment vs. Control” pair was characterized by two values: the normalized log-transformed ratio (fold change value) and the corresponding q-value (derived from p-values, which were adjusted for multiplicity of comparisons).[81] The Fisher’s method of meta-analysis was applied to combine p-values (this approach is scale-free and, as a result, does not require the use of between-array normalization). The multiple slide procedure method was used to detect candidate genes (the same technique was applied to all microarrays based on all possible combinations of a given treatment and the corresponding control biological replicates). This technique was based on the number of biological replicates and treated the gene

expression outcomes as Bernoulli trials (independent binary outcomes). The Fisher's method-based p-values were adjusted with Bonferroni correction. A list of candidate genes was created for each treatment. Candidate genes were annotated using Blast2Go service.[82] Gene expression analysis and subsequent HOPACH analysis were done by Dr. Alex Loguinov at U.C. Berkeley.

Microarray data were confirmed with quantitative reverse transcription PCR. Seven genes were chosen based on q-value, degree of differential expression or potential mode of toxicity. RNA samples were extracted, cleaned up and quality assessed as for microarrays, above. 1 µg RNA was reverse transcribed with iScript cDNA synthesis kit (BioRad) on a Mycycler thermal cycler (Biorad). 25 primer sets were tested with SsoFast amplification kit (BioRad) on a melt curve from 55 to 65C and those with one qPCR product were used for subsequent analysis. qPCR amplification was performed on a BioRad C1000 Thermal Cycler with CFX96 R-T System. Probes were designed on the NCBI online primer-designing tool (http://www.ncbi.nlm.nih.gov/tools/primer-blast/) and ordered from Elim Biopharm. Each gene amplification was preformed in triplicate, or in duplicate if one reaction failed. Actin and GAPDH were used as housekeeping genes. Housekeeping cycle threshold (Ct) was subtracted from gene of interest Ct and values were $\log_2$ transformed. Significance between control and exposed was determined by Student's T-test in Excel (Microsoft) with two tails, assuming equal variance, $p<0.05$. Primer sequences are shown in **Table 5**.

To identify biological pathways affected by exposure to Ag^+ or to AgNW, each gene sequence represented on the microarray was subjected to a *Daphnia pulex* protein BLAST and sorted into Kyoto Encyclopedia of Genes and Genomes (KEGG) pathways (www.genome.jp/kegg). Pathways representing less than five genes in the array were removed, leaving 95 pathways and 1402 *Daphnia pulex* homologues with an expect (E) value less than or equal to 10^{-4}. Enrichment of significant pathways in each group of differentially expressed genes was calculated using a modified Fisher Exact Probability P-value.[83], [84] KEGG pathway analysis was done by Dr. Philipp Antczak at University of Birmingham, UK.

Gene expression data was further analyzed with Hierarchical Ordered Partitioning And Collapsing Hybrid (HOPACH) cluster analysis. HOPACH analysis clusters similar gene expression profiles by computationally generating plots of similar data into a hierarchical "tree of clusters" using statistical Euclidean distance matrices.[85] Similar gene expression profiles may have similar causal mechanisms or modes of toxicity. HOPACH statistically correlates and plots data in a colored heat map so relationships can be visualized. The R package *hopach* from Bioconductor.org was applied to the microarray gene expression data. All "NA" values were replaced with zeros. The method is a combination of divisive (top down) and agglomerative (bottom up) hierarchic clustering coupled with non-parametric bootstrap procedure to generate probability of cluster membership for each chemical. Cosine-angle (uncentered correlation) was applied as a measure of similarity.[85]

RESULTS

Physio-chemical characterizations

Assessment of AgNW stability in solution found that all AgNW were dispersed without aggregation in pure water. PVP AgNW were stable in both COMBO and EPA *Daphnia* growth media, but SiO_2 AgNWs aggregated in both media (**Figure 5**), although suspensions contained a non-aggregated fraction of AgNW even after 24 hours. All long NW settled at detectable rates. Only short NW that aggregated tended to settle. The maximum settling rate was for S-SiO_2 (**Figure 6**). The only wires that released detectable Ag^+ into media were S-SiO_2 in water, COMBO and EPA and S-PVP in EPA. **Figure 7** compares the rates of silver ion release at a total silver concentration of 12 mg/L over 24 hours following AgNW addition to deionized water, COMBO or EPA media. Silver speciation calculations of Ag^+ complexation by anions, principally Cl^- (**Table 4**), predicted a greater percentage of free Ag^+ in EPA (84%) than COMBO (41%).

Neither SEM nor TEM imaging revealed any morphological changes in PVP AgNW in conditions relevant to acute toxicity studies. However, morphological changes in SiO_2 coatings occurred within a few hours in EPA media. SiO_2 coated AgNW possessed enclosed voids at the tips, presumably formed by the etching away of metallic silver during an PVP/SiO_2 exchange process during manufacture (**Figure 2**). The morphology of the SiO_2 coatings was unchanged following a two-hour emersion in COMBO (**Figure 8a**). However, exposure to EPA media shows loss of these voids (**Figure 8b**). **Figure 8c** shows TEM and elemental imaging of a SiO_2 NW in EPA. The silica distribution shows evidence of a diffuse network extending out from the surface. The sodium distribution shows accumulation of Na^+ in a pattern that is consistent with diffusion into the silica and not Na^+ adsorption to the exterior of the silica surface.

Acute toxicity

The acute LC_{50} values for AgNW and Ag^+ after 24-hour exposures in COMBO or EPA media are reported in **Figures 9a** and **9b** and **Table 6**. LC_{50} values range from 3.6 to 522 micro-grams silver per liter media (μg/L). The log(LC_{50} ratio) to 0 was determined for each pair of LC_{50} values and confidence intervals to determine if AgNW LC_{50} values were significantly different.[86] The LC_{50} values for all samples were significantly different except for two cases: Ag^+ in COMBO versus Ag^+ in EPA and L-PVP in COMBO versus L-SiO_2 in EPA. The toxicity of ionic silver was greater than that of all AgNWs in both media and was not significantly affected by media composition. S-SiO_2 was the most toxic NW to *Daphnia* in both media and the most toxic exposure was S-SiO_2 in EPA. The amount of Ag^+ release into media (**Figure 7**) does not correlate with LC_{50} values.

Detection of AgNW in *Daphnia* hemolymph

Hemolymph from daphnids exposed to each of the AgNWs at the LD_{50} concentrations was imaged with the SEM. Every AgNWs was detected. Example SEM

images of internalized PVP and SiO_2 NWs are in **Figure 10**. The SiO_2 wire is completely bare, with no coating, while the PVP coating is intact and appears to have stringy attachments. At least one AgNW was observed in the hemolymph from all exposures, but the low absolute numbers preclude comparing uptake among the different AgNWs.

Single particle inductively coupled plasma mass spectrometry (spICP-MS) data on S-SiO_2 AgNW verified that the method could be used to detect and size AgNWs in hemolymph and that silver nanomaterials are inside the animals. It could simultaneously detect background Ag^+ and calculate dissolved Ag^+ concentrations in the hemolymph. **Figure 11** shows raw spICP-MS data and size distribution of S-SiO_2 from hemolymph. No pulses were detected in unexposed control hemolymph (**Figure 12**). Hemolymph from Ag^+-exposed daphnids resulted in the detection of nanomaterials, indicating silver precipitation or sorption to biomolecules (**Figure 13**). Fewer counts were seen in hemolymph from 1/10 LC_{50} exposures than from LC_{50} exposures, indicating a dose-response in absorption of Ag^+ or AgNW (**Figure 14**). Pulses were also seen in hemolymph post-depuration with and without feeding, indicating detection of AgNW in hemolymph was not due to contamination from gut contents (**Figure 15**).

In both COMBO and EPA media, the S-PVP AgNW appear to dissolve over a 48-hour time period (**Figure 16**). However, background signal (Ag^+) doesn't increase, indicating Ag^+ released by dissolution forms new particles or precipitates.

Unique gene expression profiles and potentially unique modes of toxicity

Each type of AgNW elicited a unique *Daphnia* gene expression profile compared to other NWs and to Ag^+ in COMBO media. The complete list of differentially expressed genes is available on Gene Expression Omnibus (https://www.ncbi.nlm.nih.gov/geo/). 2801 genes total were differentially expressed in all exposure conditions (**Table 7**). qPCR on seven genes (total of 12 qPCR reactions) had good correlation with microarray results, with the one exception of microarray gene probe 1395, a brix protein believed to be involved in ribosomal biogenesis (**Table 8**). KEGG pathway analysis found at least one pathway with significant enrichment in each exposure condition (**Table 9**). Analysis of silver exposure data resulted in the most highly significant KEGG pathways results; the oxidative phosphorylation and ribosomal pathways. qPCR of ribosomal 18S subunit verified an increase in ribosomal RNA expression.

HOPACH cluster analysis grouped the data into three distinct clusters or "centroids," named 1, 2, and 3 in **Figure 17**. HOPACH "cosangle" clustering of gene expression data generateed a plot based on similarity of gene expression profiles of each exposure. Samples in **Figure 17**, from left to right, are: L-SiO_2, L-PVP, S-SiO_2, Ag^+ and S-PVP. **Figure 18** is the same graph, labeled with sample names instead of centroid cluster number. L-SiO_2 and L-PVP caused unique gene expression profiles, while S-SiO_2, Ag^+ and S-PVP grouped together. Silver and S-SiO_2 were the most similar. L-PVP caused the most unique gene expression profile.

Venn diagrams were used to determine the number of differentially expressed genes (DEG) that were uniquely or commonly up- or down-regulated (**Figure 19**). Only seven genes total were differentially expressed in all five exposure conditions. Five (un-annotated) genes were differentially expressed in all AgNW conditions.

DISCUSSION

All silver nanowires (AgNWs) are classified by the EPA as highly toxic to aquatic organisms as they exhibit LC_{50} values lower than 1 mg/L (**Figure 9**, **Table 6)**.[87] However, the toxicity of all AgNWs was significantly less than that of Ag^+ ($AgNO_3$). AgNWs appear to exert less toxicity than Ag nanoparticles (AgNP). Poynton *et al.* studied the toxicity of 35-nm-diameter PVP-coated AgNP on 10-day old *Daphnia* in EPA media, finding LC_{50} values to be ~10 µg/L.[88] Only a single AgNW type (S-SiO_2 in EPA) was more toxic. The United States EPA recommends less than 3.2 µg/L silver in surface and fresh water, for human and ecological health.[89] Ag^+ is not usually found at high levels in the natural environment,[90] but in some locations downstream of wastewater effluent from, for example, industrial film production, Ag^+ can be as high as 16 g/L. [91] The LC_{50} values of AgNWs are higher than Ag^+ levels recommended by the EPA, but lower than possible output from industrial waste.

PVP suspensions contained 1.6% (S) and 0.8% (L) silver in the form of nanorod impurities while SiO_2 coated NW suspensions contained less than 0.1%. These ~100 x 500 nm nanorods could contribute to toxicity. However, the nanorods would have to be orders of magnitude more toxic than the AgNW (or 35-nm diameter nanoparticles[88]) to account for the observed LD_{50} values. Furthermore, the S-SiO_2 AgNW with no detectable nanorod contamination are much more toxic than PVP AgNW, which had the highest nanorod contamination. The nanorod impurities likely represent a minor contribution to toxicity.

Aggregation and settling behaviors of nanomaterials can affect toxicity.[92], [93], [94] However, S-SiO_2 were more toxic than S-PVP even though SiO_2 settled more rapidly and tended to aggregate more. Further, there was no statistical difference between LD_{50} values obtained with the *Daphnia* media shaken (to reduce NW settling) or still. Settling and aggregation were therefore not dominant determinants of the toxicity of AgNWs. This may in part be due to the behavior of the *Daphnia*, as they move from the top to the bottom of the water column and feed continuously.

The Ag^+ release rate into media between different AgNW (**Figure 7**) varied considerably; SiO_2-coated nanowires released the most Ag^+. This finding was surprising as the Al-doped SiO_2 coating was stable in the stock solution and was expected to completely encapsulate the silver.[95], [58] Comparison of Ag^+ release (**Figure 7)** with the LC_{50} data (**Figure 9)** shows that release of Ag^+ into media cannot explain the trends in toxicity because not enough Ag^+ is present in media to account for toxicity. Ag^+ release data were used to estimate the contribution of dissolved silver to AgNW toxicity. Because the release of silver in media is proportional to the concentration of AgNW, it is possible to predicted amounts of dissolved silver at the AgNW LD_{50} concentrations (**Table 10)**. At the LD_{50} for S-SiO_2 in COMBO (155 µg silver/L) the calculated Ag^+ concentration [Ag(*aq*)] = 0.115 µg/L. This value is the highest amount of calculated Ag^+ in media in any AgNW exposure and was only a fraction of the LD_{50} for $AgNO_3$ in COMBO (0.8 µg/L). All other AgNW-released Ag^+ concentrations were 10-1000 times less than the LD_{50} for $AgNO_3$. Thus, the AgNW were toxic to *Daphnia* through

mechanisms other than Ag^+ release into media, which is traditionally considered the toxic silver species to aquatic organisms.[96], [72], [90] Speciation calculations (**Table 4**) predict free Ag^+ concentration to be almost twice as high in EPA than COMBO (0.84 µg/L compared to 0.41 µg/L). This may contribute to the higher toxicity of most nanowires in EPA media, but cannot be a dominant effect because the LD_{50} values for $AgNO_3$ are not significantly different.

Chemical and physical processes occurring in the media cannot fully explain differences in AgNW toxicity. **Figures 10** to **15** provide evidence that AgNWs were absorbed into the daphnids, likely through the gut or gill epithelia, in contrast to carbon nanotubes (CNT), which are not always absorbed.[97], [98] The use of spICP-MS simultaneously detected particulate and dissolved Ag, which can be useful for detecting Ag^+ speciation trends in the organism and detecting type of silver exposure. Analysis to quantify the amounts of internal silver particle sizes and ions is ongoing.

Uptake of AgNW into the hemolymph could exacerbate silver ion toxicity by providing a higher internal dose of Ag^+ or by allowing silver ions to enter parts of the organism not typically accessed by dissolved external silver. Uptake could also lead to toxicity associated with direct interactions of the AgNW or coating within the daphnid. Silica NM can cause toxicity in human cell cultures by direct interactions[98], [99], [100]and by facilitating the transport of surface adsorbed molecular toxins. [101], [102] Nanoscale silica is toxic to gram negative and gram positive bacteria[103] and toxic to *Daphnia magna* and *Chironomus riparius* in 96-hour acute exposures.[104] However, silica coatings on metallic NM, including silver NP, typically reduce the toxicity relative to the bare NM.[58], [95] The apparent dissolution of the SiO_2 coating could, however, contribiute to toxicity. PVP is commonly used in pharmaceutical preparation and is found ubiquitously in the environment[105]. Excess toxicity specifically caused by the PVP coating material is unlikely.[106]

Microarray gene expression assays were used to investigate modes of toxicity of AgNW and Ag^+. The patterns of differential gene expression (DGE) were unique for each exposure condition, with relatively low levels of common DGE among the AgNW samples and between each AgNW and $AgNO_3$ (**Figure 19**). DGE patterns for genes encoding cellular transport Na^+/K^+ ATPase proteins were scrutinized because the toxicity of Ag^+ is caused by inhibition of a sodium-potassium adenosine triphosphatase (Na+/K+ ATPase) in the gill.[72], [73], [74] All exposures affected expression of at least one ion transporter; dissolved silver caused the strongest response. The expression of transporters was decreased in all exposures with one exception: L-SiO_2 caused an increase in an iron(III) dicitrate system. Silver significantly suppressed the expression of a calcium-transporting ATPase (with only 11% expression relative to control) and an ATPase binding cassette-related transporter (27%), although it is unknown whether these are also sodium transporters. Only S-PVP and S-SiO_2 affected transcription of known sodium transporter genes (**Table 11**).

KEGG pathway analysis performed on the gene expression data showed that each exposure significantly affected a different group of biological pathways. The most

statistically significant findings were in Ag^+ exposures, which caused enrichment of genes associated with the ribosome and with oxidative phosphorylation. The effects on oxidative phosphorylation is in agreement with studies that show both silver[107] and 40 and 80 nm sized uncoated silver nanoparticles[108] interfere with the oxidative phosphorylation coupling mechanism in rat liver mitochondria. qPCR of ribosomal 18S protein confirmed increased RNA expression. KEGG pathway analysis, however, was limited by the lack of annotation of the *Daphnia magna* microarray (only 50% of genes on the array have a known or hypothesized function).

Clustering analysis showed that the gene expression profiles from *Daphnia* exposed to Ag^+ was most similar to the S-SiO_2 AgNW. Because the SiO_2 AgNW coating dissolved inside the animals, it is possible the wires released more Ag^+ inside the animal, and therefore exert more ionic silver toxicity. However, the data from L-PVP, which generated the most unique gene expression profile, show that another toxicity is occurring – possibly by direct irritation of the AgNW, or some unknown mechanisms. This is the first study to show that silver nanomaterials likely cause toxicity by both internal silver dose and by an unknown, nanomaterial-related mechanism.

TABLES

Chemical Name	Chemical Class	Chemical Abbreviation
Long PVP-coated silver nanowire	Nanowire	L-PVP
Long silica-coated silver nanowire	Nanowire	L-SiO_2
Short PVP-coated silver nanowire	Nanowire	S-PVP
Short silica-coated silver nanowire	Nanowire	S-SiO_2
Ionic silver	Metal	Ag^+

Table 1. List of silver nanowires tested in this study.

Sample	% passed through 0.45 µm	% passed through 0.02 µm	Difference = % nanorod silver
S-PVP	2.2	0.6	1.6%
L-PVP	1.0	0.2	0.8%
S-SiO2	4.4	4.4	<0.1%
L-SiO2	0.5	0.4	<0.1%

Table 2. Estimates of the proportion of silver nanorods in silver nanowire suspensions. The filtered solutions were acidified with concentrated nitric acid and measured by ICP-MS for total silver. The 0.45 µm filter captured both AgNWs and NRs, while the 0.2 µm filter captured only NR.

COMBO			EPA	
Chemical	**Concentration (mg/L)**		**Chemical**	**Concentration (mg/L)**
$CaCl_2•2H_2O$	55		$NaHCO_3$	0.192
$MgSO_4•7H_2O$	55.5		$MgSO_4•7H_2O$	0.246
K_2HPO_4	4.36		$CaSO_4•2H_2O$	0.12
$NaNO_3$	42.5		KCl	0.008
$NaHCO_3$	50.5			
$Na_2SiO_3•9H_2O$	14.2			
H_3BO_3	12			

Table 3. Chemical composition of the two *Daphnia* growth medias.

COMBO		EPA	
Species	**Conc. in nM (µg/L)**	**Species**	**Conc. in nM (µg/L)**
$AgCl^0$	5.1 (0.55)	Ag^+	7.8 (0.84)
Ag^+	3.8 (0.41)	$AgCl^0$	1.4 (0.15)
$AgCl_2^-$	0.3 (0.037)	$AgSO_4^-$	0.1 (0.014)
$AgSO_4^-$	0.013 (0.0014)	$AgCl_2^-$	0.013 (0.0014)

Table 4. Calculated concentrations of aqueous species containing silver for the EPA and COMBO simulated growth media, ranked in order of decreasing concentration. The pH was fixed at 8 and the total silver concentration was 1µg/L.

Nickname	Reason	Protein	Changes	Direction	Sequence
7657	all affected	unknown	all down	Forward Reverse	GGGGTGGCCATCGCTGTTAGTC TCCATCGCGGCATCGTCCACT
7499	fold change	unknown	LP-, SP-	Forward Reverse	AACCTCTGCCAACCAGCCGTT CGCCGACGGCCTCCATGATT
2267	q-value	carbonic anhydrase	LP-	Forward Reverse	AGCAGCTCGAATCTTTCCGCGA TGCTCAACCGACAACGGTGGG
4057	fold change	conidiospore surface protein	LP+. SS-	Forward Reverse	CGGTGGCGATTACGTTCCTTCACC GCGCGAGGGTAATAGGGGGC
1395	mode of tox	ribosomal	LS+, SS+	Forward Reverse	TACGAGCTTCGGACGAGCCCT TCCCCGTGCAGCAAAGACAAGG
18S	mode of tox	ribosonal	Ag^{+} (?)	Forward Reverse	CGC TCT GAA TCA AGG GTG TT AAC CCC GAA GAG GAA GAA AA
GAPDH	house	GAPDH	n/a	Forward Reverse	GGGGACAGACGTTTCCTGTA AAGGGGTCATTGACAGCAAC
actin	house	actin	n/a	Forward Reverse	GGTATGTGCAAGGCTGGATT GGTGTGGTGCCAGATCTTTT

Table 5. List of gene primer sequences used in qPCR verification of microarray data.

Media	Treatment	LC_{50} µg/L	95% confidence interval
COMBO	PVP-S	421.0	322.2 - 602.6
COMBO	PVP-L	233.9	210.1 - 257.2
COMBO	SiO2-S	155.0	140.5 - 169.2
COMBO	SiO2-L	522.0	404 - 638.3
COMBO	AgNO3	0.8	0.4 - 1.3
EPA	PVP-S	260.7	139.5 - 319.6
EPA	PVP-L	415.4	297.8 - 563.4
EPA	SiO2-S	3.6	1.7 - 5.8
EPA	SiO2-L	226.5	28.0 - 382.4
EPA	AgNO3	0.6	0.28 - 1.2

Table 6. Acute 24-hour LC_{50} values for silver nanowires on *Daphnia magna.* Values were determined by probit statistical analyses. Each LC_{50} is representative of at least 12 replicates of six nanowire exposure concentrations containing five daphnids each.

Number of Differentially Expressed Genes per Exposure					
# DEG	**L-PVP**	**L-Silica**	**S-PVP**	**S-Silica**	**Silver**
Up	143	212	121	182	182
Down	134	307	502	381	510
Total	277	519	623	563	692

Table 7. Number of genes differentially expressed in each exposure condition.

Sample	GAPDH	4057/ fold	dCt	2^-dCt	Average	P-Value
con	23.720	33.740	10.020	0.001	0.001	
con	24.380	33.750	9.370	0.002		
con	24.620	33.720	9.100	0.002	Fold Change	
SS	22.740	32.560	9.820	0.001	0.772	0.097
SS	22.800	33.290	10.490	0.001	0.485	
SS	21.370	32.290	10.920	0.001	0.360	
Sample	GAPDH	7657/ all down	dCt	2^-dCt	Average	P-Value
con	23.720	25.010	1.290	0.409	0.378	
con	24.620	26.150	1.530	0.346	Fold Change	
Ag	23.270	24.700	1.430	0.371	0.983	0.588
Ag	22.780	24.340	1.560	0.339	0.898	
SS	22.740	24.700	1.960	0.257	0.681	0.072
SS	22.800	24.860	2.060	0.240	0.635	
SS	21.370	24.560	3.190	0.110	0.290	
LS	22.760	25.160	2.400	0.189	0.502	0.273
LS	22.720	24.310	1.590	0.332	0.880	
SP	22.050	28.420	6.370	0.012	0.032	0.002
SP	22.930	26.790	3.860	0.069	0.182	
SP	23.260	27.590	4.330	0.050	0.132	
Sample	actin	1395/ brix	dCt	2^-dCt	Average	P-Value
con	21.980	26.790	4.810	0.036	0.043	
con	22.540	26.830	4.290	0.051	Fold Change	
SS	21.110	25.120	4.010	0.062	1.431	0.580
SS	19.850	24.440	4.590	0.042	0.957	
LS	20.810	26.460	5.650	0.020	0.459	0.026
LS	20.420	26.280	5.860	0.017	0.397	
LS	20.890	26.540	5.650	0.020	0.459	
Sample	actin	18S ribosome	dCt	2^-dCt	Average	P-Value
con	21.980	12.730	-9.250	608.874	499.798	
con	22.540	13.930	-8.610	390.722	Fold Change	
Ag	22.060	12.070	-9.990	1016.927	2.035	0.442
Ag	21.980	12.990	-8.990	508.463	1.017	
Sample	actin	7499/ fold	dCt	2^-dCt	Average	P-Value
con	21.980	26.400	4.420	0.047	0.060	
con	22.540	26.300	3.760	0.074	Fold Change	
SP	19.430	27.690	8.260	0.003	0.054	0.068
SP	20.530	26.810	6.280	0.013	0.214	
LP	20.200	26.930	6.730	0.009	0.156	0.016
LP	20.920	27.440	6.520	0.011	0.181	
LP	21.700	28.430	6.730	0.009	0.156	
Sample	actin	2267/q-value	dCt	2^-dCt	Average	
con	21.980	23.920	1.940	0.261	0.398	P-Value
con	22.540	23.440	0.900	0.536	Fold Change	
LP	20.200	23.420	3.220	0.107	0.269	0.081
LP	20.920	23.640	2.720	0.152	0.381	
LP	21.700	24.690	2.990	0.126	0.316	
Sample	actin	4057/ fold	dct	2^-dct	Average	P-Value
con	24.320	35.790	11.470	0.000	0.001	
con	25.600	35.870	10.270	0.001		
con	25.160	35.580	10.420	0.001	Fold Change	
LP	24.380	23.430	-0.950	1.932	3062.721	0.161
LP	24.970	26.660	1.690	0.310	491.347	

Table 8. Results from RT-q-PCR analysis. Green highlights indicate agreement with microarray data, red indicates disagreement and blue indicates variation in results. All primers tested agreed with array data except for primer 1395, a protein associated with ribosomal biogenesis.

Affected Biological Pathway	L-PVP	L-SiO2	S-PVP	S-SiO2	Silver
Oxidative phosphorylation					5.28E-04
Spliceosome	0.02			0.08	
Pyrimidine metabolism					0.07
RNA polymerase					0.08
Peroxisome	0.09	0.02	0.09		
Lysosome		0.04			
Ribosome	0.01		0.01		1.80E-12
Progesterone-mediated oocyte maturation		0.01			
ECM-receptor interaction			0.09		
Ubiquitin mediated proteolysis		0.06			
Butanoate metabolism					0.07
Metabolism of xenobiotics by cytochrome P450		0.02			
Drug metabolism - cytochrome P450		0.03			
Retinol metabolism		0.05			

Table 9. KEGG pathways analysis of gene expression data from *Daphnia magna* exposed to AgNWs resulted in the enrichments of different biological pathways. P-values of 0.1 or less are considered significant.

	Abiotic Ag^+ release data						
Exposure	Ag added as NW (ug/L)	Ag^+ released (ug/L)	Fraction released	NW LD_{50} (ug/L)	Expected Ag^+ release at LD_{50}	Ag^+ LD_{50} (ug/L)	**$[Ag^+]$ / Ag^+ LD_{50}**
AgNW-S-SiO2 COMBO	12,000	8.9	0.00074	155	0.115	0.8	**0.14**
AgNW-S-SiO2 EPA	12,000	2.7	0.00022	3.6	0.00081	0.6	**0.0014**
AgNW-S-PVP EPA	12,000	1.6	0.00013	260.7	0.0347	0.6	**0.058**
AgNW-L-SiO2 EPA	12,000	0.3	0.000025	226.5	0.0056	0.6	**0.0094**

Table 10. Estimate of media Ag^+ contribution to AgNW toxicity. For each sample, the amount of Ag^+ released in abiotic trials at a concentration of 12 mg/L Ag was scaled proportionally to the LD_{50} concentrations of AgNW for the same sample and media. The last column reports the ratio between the LD_{50} for dissolved silver and the concentration of dissolved predicted released silver for each AgNW sample.

GeneID	Protein Function	L-PVP	L-SiO2	S-PVP	S-SiO2	Ag+
DM02485P1	**Solute Carrier**	-0.6				
DM05687P2	**ABC related**					-3.2
DM01730P3	**Calcium transporting ATPase**					-1.9
DM06992P4	**Iron(III) dicitrate permease protein fecC**		1.1			
DM06914P2	**Fe Transport**			-2.4	-1.4	
DM04501P3	**sodium-dependent phosphate transporter**			-0.2		
DM02022P2	**Na/K-transporting ATPase subunit alpha**			-1.1		
DM01589P2	**Na/K-transporting ATPase subunit alpha**				-0.7	
DM03514P2	**sodium/solute symporter**			-0.5		

Table 11. Probes identified by BLAST as transporter proteins that were differentially expressed in response to AgNW exposure. Red: sodium transporters; blue: other transporters

FIGURES

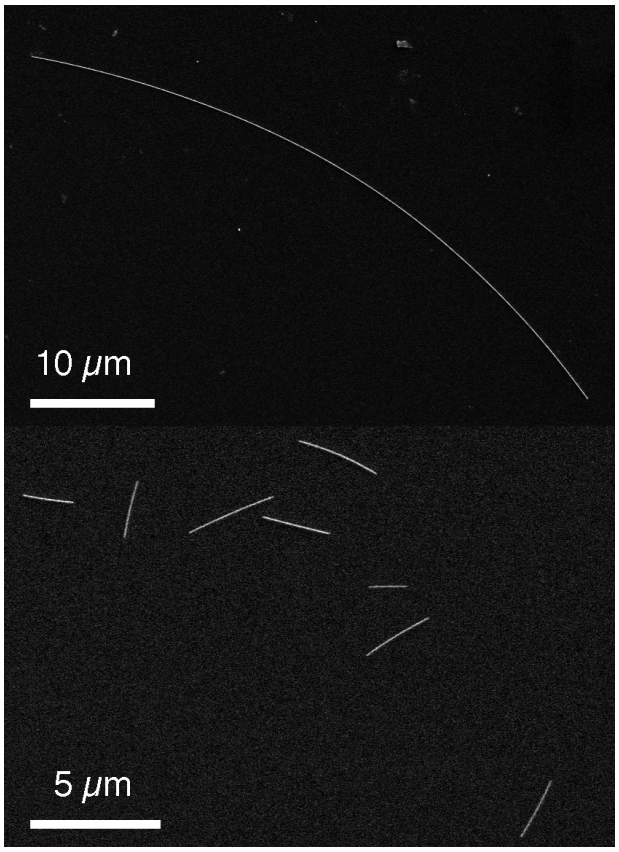

Figure 1. Long (top) and short silver nanowires (AgNWs). Image acquired with scanning electron microscope.

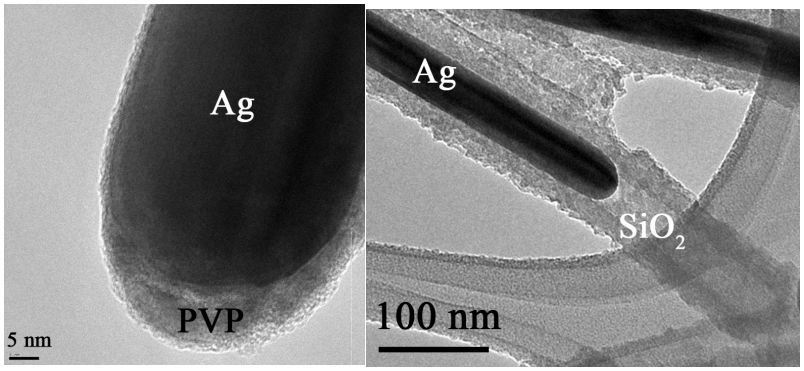

Figure 2. Transmission electron microscopy of silver nanowires from the stock solution. Left: polyvinylpyrrolidone (PVP) coating. Right: amorphous aluminum-doped silica (SiO_2) coating. All SiO_2-coated AgNW exhibited enclosed voids at the tips of the silver nanowires, introduced during manufacture.

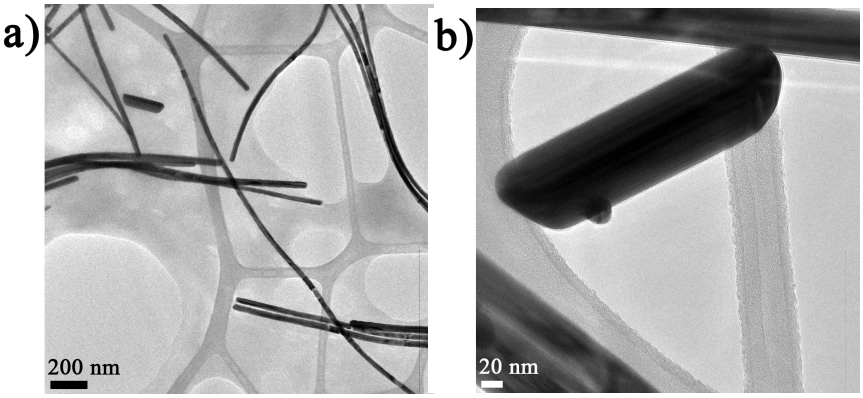

Figure 3. Transmission electron microscope images of PVP-coated AgNW nanorod impurities in the short PVP silver nanowire sample.

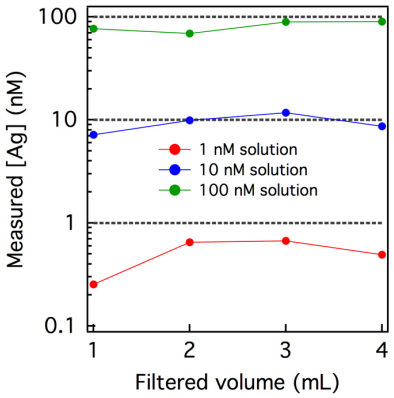

Figure 4. Tests of $Ag^{+}(aq)$ retention in the 0.2-µm filters used to remove AgNW from suspension prior to elemental analysis of dissolved silver. Four 1-mL aliquots of 1, 10 or 100 nM standard silver nitrate solutions were passed through a fresh filter and each aliquot was analyzed for total silver.

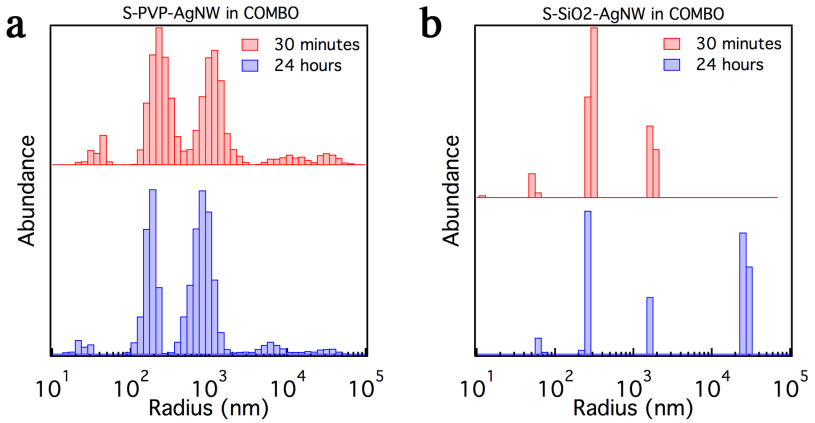

Figure 5. Dynamic light scattering observation of the stability of short (**a**) PVP and (**b**) SiO_2 coated silver nanowire in COMBO media. Initially, both samples contained a proportion of individual nanowires and small aggregates. After 24 hours, no change in aggregation state of S-PVP was observed. By contrast, micron-scale aggregates of S-SiO_2 AgNW appeareded after 24 hours.

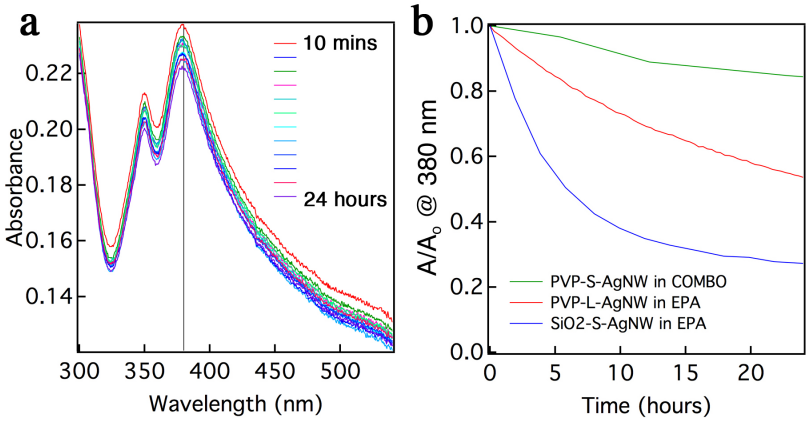

Figure 6. UV-vis determination of relative settling rates of AgNW in *Daphnia* growth media. (**a**) Series of optical absorption spectra acquired from unstirred suspension of L-PVP AgNW in COMBO media. The AgNW exhibited two characteristic surface plasmon resonance peaks. (**b**) Time dependent drop in absorbance (a) due to NW settling, monitored at 380 nm in a 1-cm pathlength cuvette with the beampath 1.5 cm beneath the solution meniscus.

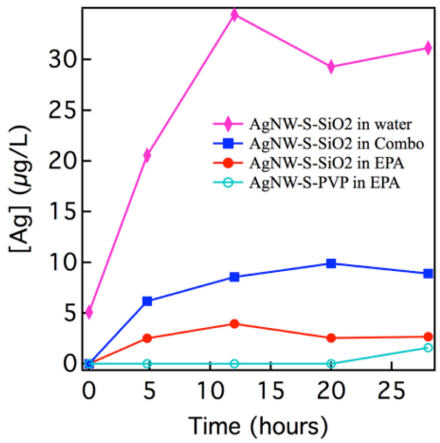

Figure 7. Determination of relative rates of release of dissolved silver by long (L) and short (S) AgNW at a silver concentration of 111 μM in water and in *Daphnia* media. Silver was undetectable for S-PVP in COMBO and all L-AgNW samples. AgNW samples not on the graph did not release detectable Ag^{+}.

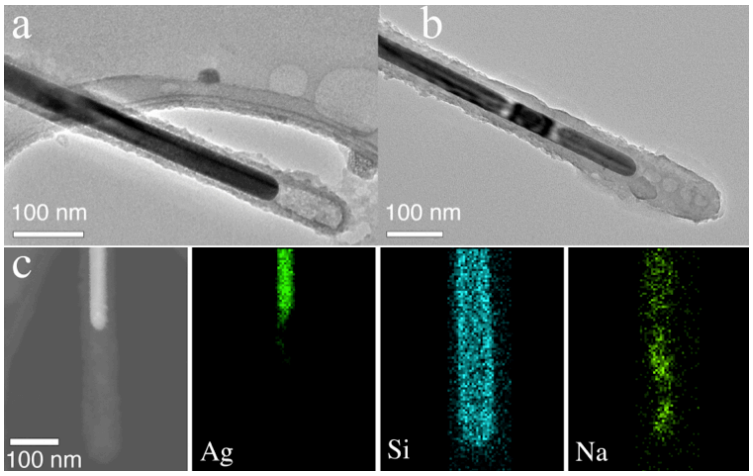

Figure 8. TEM study of the morphology of the aluminosilicate coating on short silver nanowire (S-SiO_2) following a two-hour exposure to **(a)** COMBO or **(b)** EPA media. **(c)** STEM image and a corresponding EDS map depicting the distribution of silver (Ag), silicone (Si) and sodium (Na) in coating.

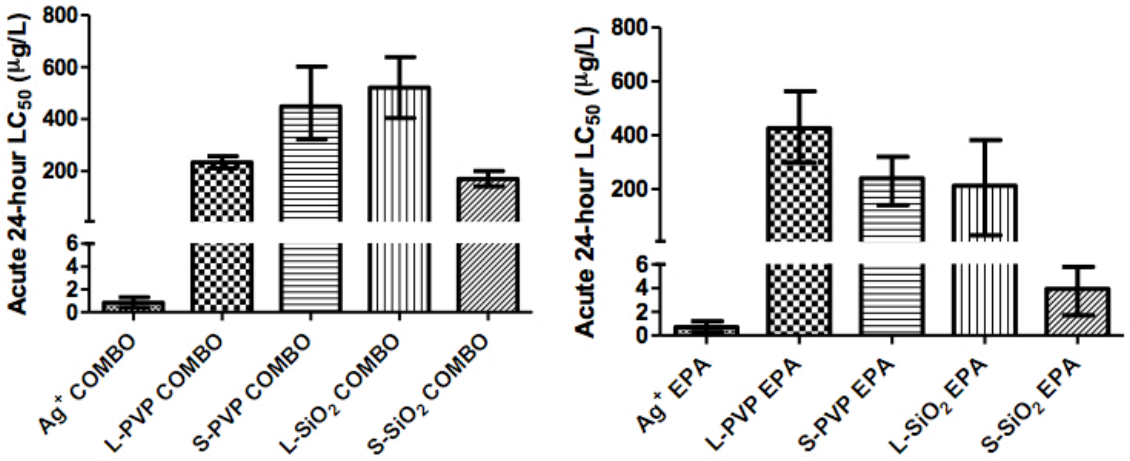

Figure 9. Acute 24-hour LC_{50} values for silver nanowire and ionic silver on *Daphnia magna* in **(a)** COMBO and **(b)** EPA media. LC_{50}s are measured in micro-grams silver per liter. Values and 95% confidence intervals were determined with probit analysis.

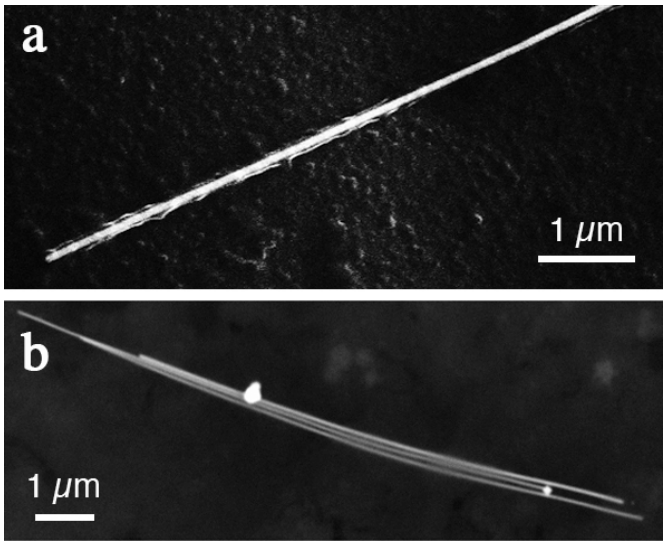

Figure 10. SEM imaging of silver nanowires extracted from the hemolymph of a daphnid exposed to (a) PVP-coated AgNW or (b) SiO_2-coated AgNW.

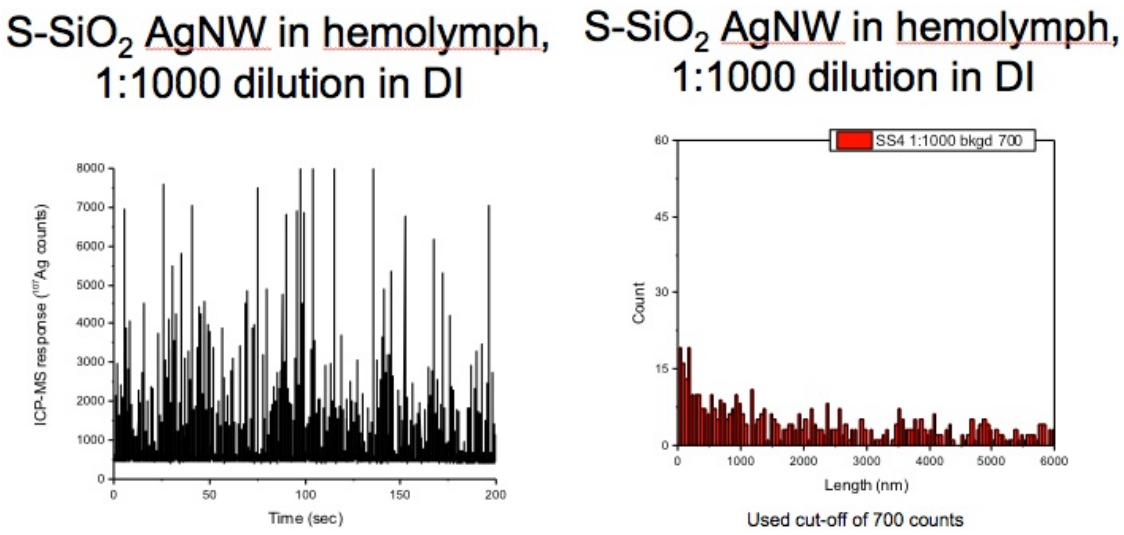

Figure 11. Raw spICP-MS data (left) of hemolymph extracted from *Daphnia* exposed to $S\text{-}SiO_2$. Exposure was 1/10 LC_{50}, and hemolymph was diluted before analysis 1:100 in deionized water. Binned spICP-MS data (right) shows size distribution of the wires inside the animal.

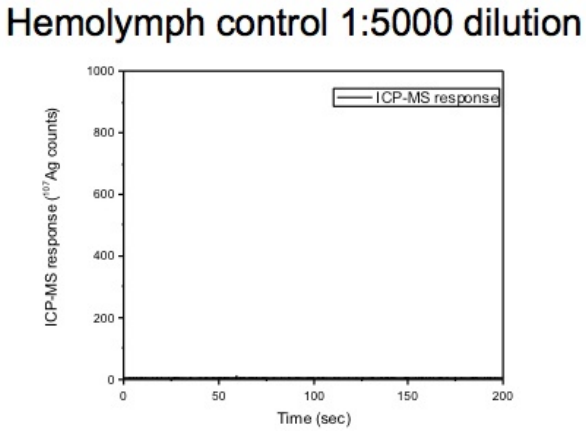

Figure 12. Hemolymph extracted from unexposed daphnids resulted in no "pulses" of detected silver nanomaterials when analyzed with spICP-MS.

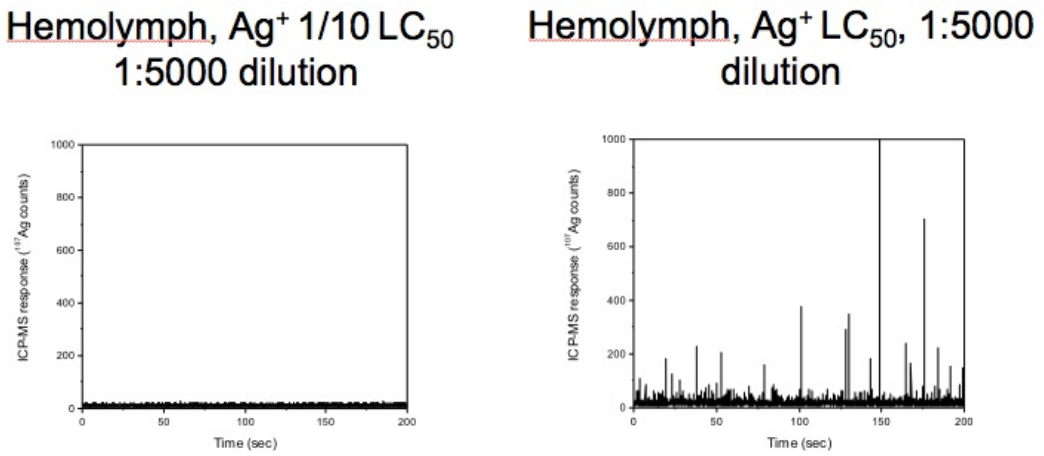

Figure 13. Exposure to Ag^{+} at both 1/10 LC_{50} (left) and at the LC_{50} (right) caused nanoparticles to form, which were detected with sp-ICP-MS. Newly formed silver particles may be precipitates or complexed with biological molecules. Detection of more pulses in the higher concentration alluded to a dose effect.

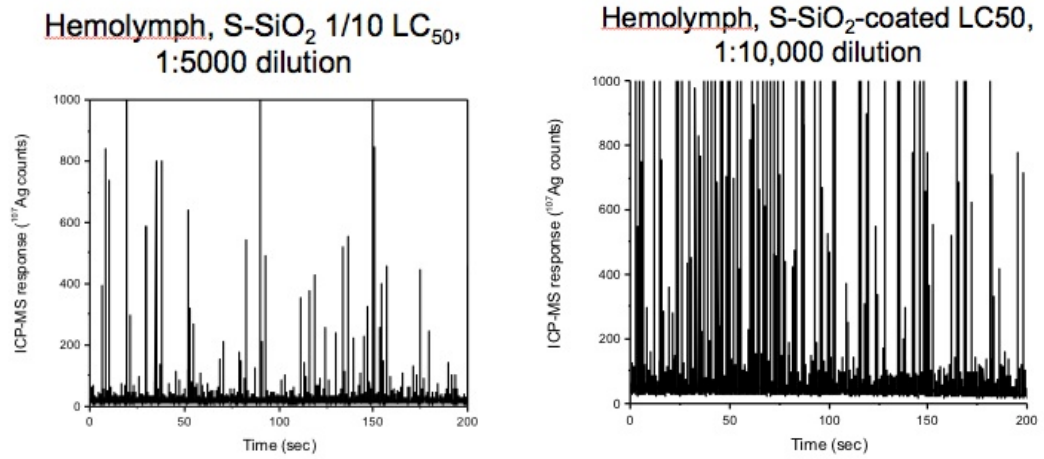

Figure 14. A dose-effect was also seen in hemolymph from daphnids exposed to silver nanowires. Left, 1/10 LC_{50} of S-SiO_2 AgNW. Right, LC_{50} of S-SiO_2. Analyzed with spICP-MS.

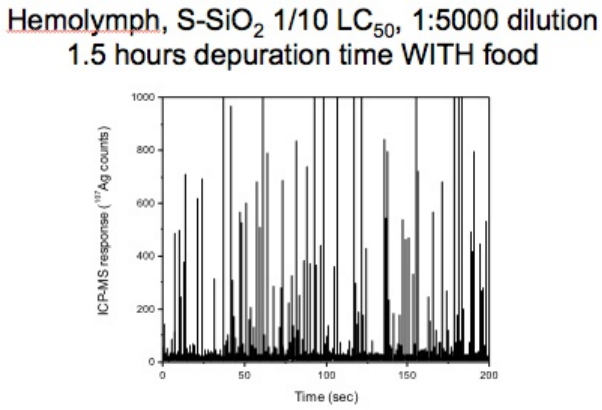

Figure 15. Hemolymph from *Daphnia* exposed to 1/10 LC_{50} with a 1.5-hour depuration period with feeding contained silver nanowires. This indicates the hemolymph is not contaminated with daphnid gut contents. Analyzed with spICP-MS. Depuration without food also resulted in detection of AgNW (data not shown).

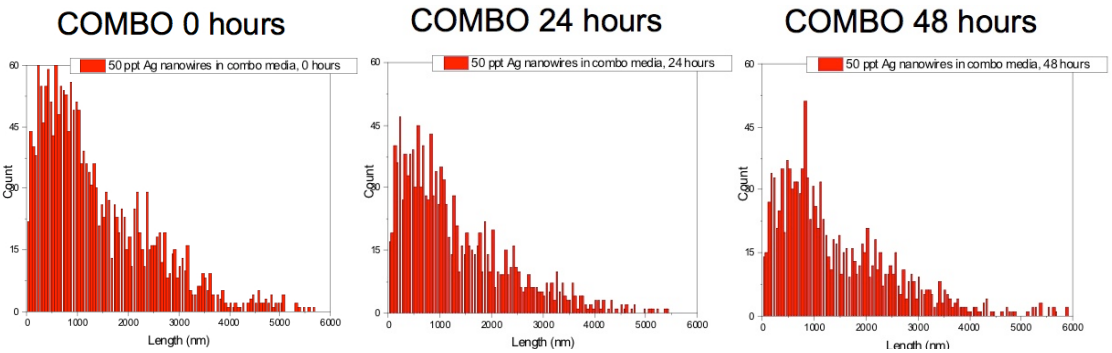

Figure 16. The size distribution of short silica nanowires (S-SiO_2 AgNW) in COMBO media changes over time, indicating dissolution and precipitation or aggregation of AgNW.

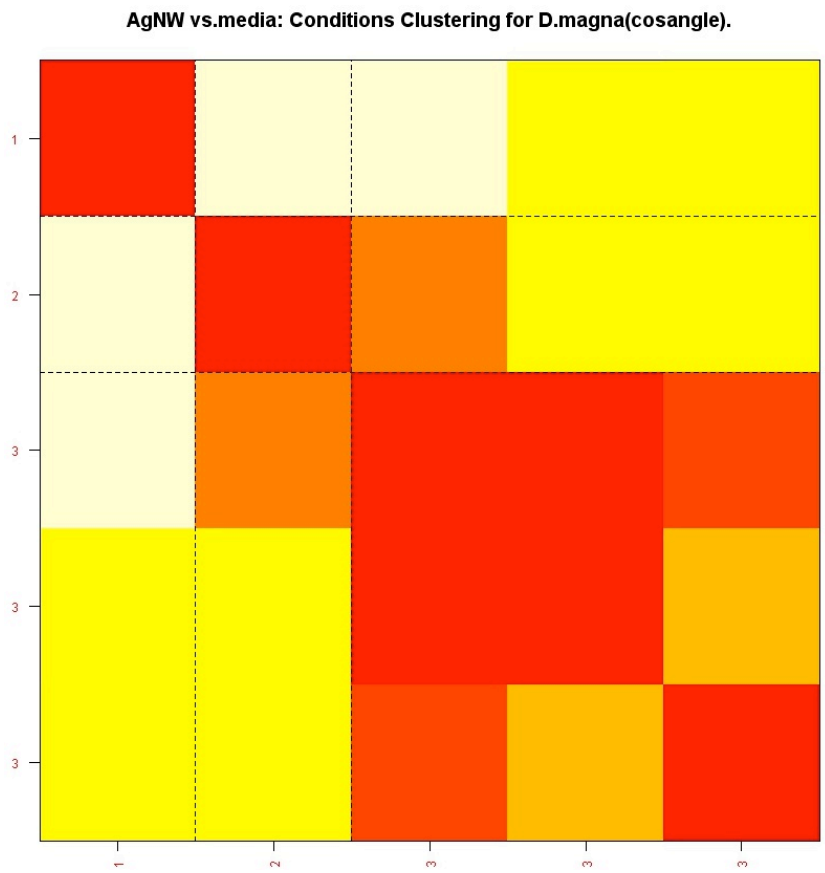

Figure 17. HOPACH "cosangle" clustering of gene expression data. This method generated a plot based on similarity of gene expression profiles between chemicals. Profiles that are more highly correlated (regardless of magnitude of correlation) are shown in red; color lightens from red to orange, yellow and white as similarity decreases. Samples, from left to right, are: L-SiO_2, L-PVP, S-SiO_2, Ag^+ and S-PVP. Each number represents a cluster or centroid. L-SiO_2 and L-PVP were unique, while S-SiO_2, Ag^+ and S-PVP grouped together.

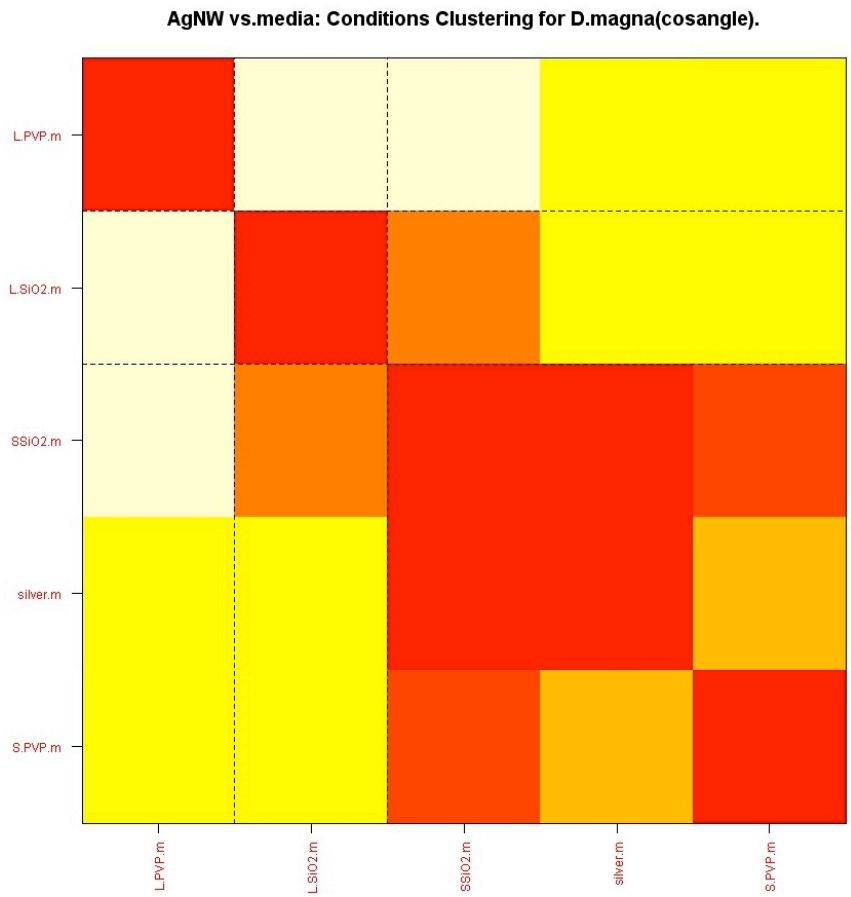

Figure 18. HOPACH "cosangle" clustering of gene expression data labeled by sample, instead of cluster group number. Profiles that are more highly correlated are shown in red; color lightens from red to orange, yellow and white as similarity decreases. Silver and S-SiO_2 are the most similar, followed by S-SiO_2 and S-PVP, L-SiO_2 and S-SiO_2, S-PVP and Ag^+. S-PVP and Ag^+ have less similarity with L-PVP and L-SiO_2. L-PVP caused the most unique gene expression profile.

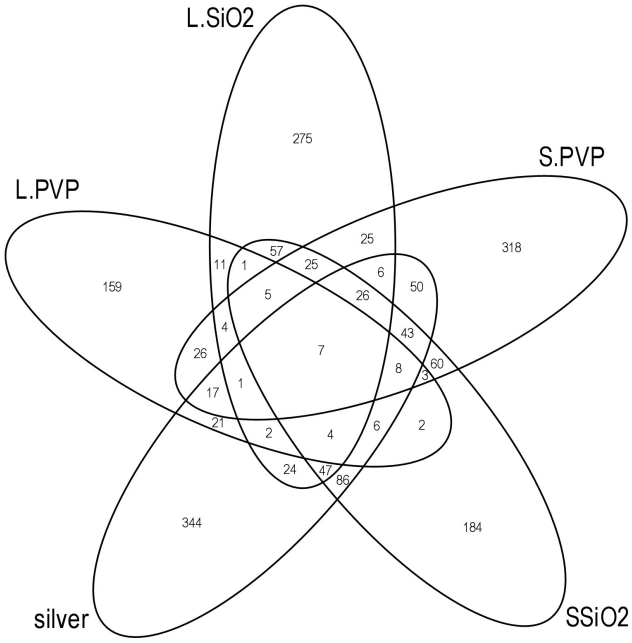

Figure 19. Venn diagram of differentially expressed genes in silver nanowire and ionic silver exposures as compared to the media-only control. Seven genes were differentially expressed in all conditions, while five genes were differentially expressed in all AgNW conditions. The five genes common to AgNW only may be useful as biomarkers of exposure.

Chapter 2.

Transcriptome Assembly from Short Read Sequencing

INTRODUCTION

The use of microarray gene expression analysis as a tool for assaying mode of toxicity is limited because microarrays, by design, contain only a portion of the animal's genome and therefore do not represent all possible genes or transcripts. Arrays have further technical limitations that make it difficult to obtain information on very highly- or lowly-expressed genes. This inhibits the effective analysis of mode of toxicity, especially in animals with no annotated reference genome and no comprehensive annotated expressed sequence tag (mRNA) database. In hopes of circumventing these issues, a transcriptome was assembled from and differential gene expression (DGE) was analyzed with high throughput short-read sequencing (SRS) data. The quality of the assembly was assessed and DGE results from SRS data were compared to results from microarray data.

SRS makes it possible to quickly and cost-effectively construct "transcriptomes" for and analyze differential gene expression in organisms with little or no previously existing genomic data. Quantitation of gene expression using SRS traditionally utilizes a sequenced, pre-existing genome[15], [109] or the genome of a closely related organism [110] as a scaffold on which SRS data is aligned and quantified. However, existing sequenced genomes are limited and are not always relevant to the organism under study – genomic data appropriate for use with environmentally relevant eco-indicator species are especially lacking.[111] Advances in sequencing technologies and in bioinformatics make it possible to assemble sequencing data into transcriptomes and quantify gene expression,[110], [112] identify new transcripts, [113] identify genes[114] or microRNAs[115] of biological interest, predict enzymatic activity, [116] and investigate toxicological responses[112], [117], [118] in a variety of biota including plants[119], [120], [121] and invertebrates. [122], [123], [124]

The utility of SRS and the advances in *de novo* transcriptome assembly made it an ideal tool for assessment of DGE in *Daphnia magna* exposed to silver nanowires (AgNWs) (**Table 1, Chapter 1**). As discussed in the previous chapter of this dissertation, gene expression analysis with microarrays showed unique differential gene expression in *Daphnia magna* exposed to four different AgNWs or to silver, which when analyzed with HOPACH clustering showed three distinct clusters of biological effect based on correlation of gene expression. However, specific mode of action determination was limited in part by lack of annotation of the microarray.

The construction of a *Daphnia magna* transcriptome has utility beyond the scope of this work. *D. magna* is an important freshwater crustacean that is used as an indicator of ecological health and to assess water quality. It is considered a keystone ecological species and is an accepted National Institute of Health model organism (www.nih.gov/science/models/daphnia/). However, the genome of *Daphnia magna* is not

available. The genome of *Daphnia pulex*, a close relation, is available, but is not appropriate for robust genomic studies. There are multiple cDNA and oligonucleotide microarrays for *D. magna*,[78], [125], created from expressed sequence tag (EST) databases. However, the arrays contain only some of the known *Daphnia* genes and therefore only a percentage of the animal's expressed genome.

A *D. magna* transcriptome will benefit the entire field of *Daphnia* ecotoxicogenomics in the following ways. First, it will identify more transcripts and more complete transcripts than are currently known. A larger number of known transcripts will allow more robust annotation of microarrays and gene expression assays and better mode of toxicity evaluation. Second, it will further develop the field of high-throughput SRS for quantitative assessment of mRNA expression in non-traditional model organisms. Many local organisms with no genomic data could similarly be used in molecular, ecological and toxicological assays. Third, a robust transcriptome could be used to generate more complete microarrays than are currently available. Microarrays are less expensive and easier to obtain than sequencing. An easy to generate and affordable transcriptome is highly valuable for scientists who work on organisms with no genomic data, but many scientists will benefit, for example, from a publically available, robust *D. magna* microarray.

Short-read sequencing is often based on a "shot-gun" sequencing approach, where RNA samples are fragmented into small pieces and converted into stable cDNA according to a sample preparation protocol. Small portions of the RNA are then sequenced in tandem. Results typically consist of several millions to hundreds of millions of 30-400 base pair-long "reads". In this study, SRS data was aligned with computational algorithms to generate a transcriptome. Numerous SRS data sets from different chemical exposures as well as the EST database the oligonucleotide microarray was constructed from were utilized in this study (**Table 2.1**). SRS data was then computationally aligned to the transcriptome to analyze DGE in *Daphnia* exposed to 1/10 LC_{50} AgNWs or 1/10 LC_{50} silver (Ag^{+}), as compared to control (**Table 2.2**). This work is the first comparison of SRS and microarray data in a toxicological study and is, to date, the most extensive analysis of the transcriptome of a ecological indicator in a toxicological study.

METHODS

Short read sequencing library sample preparation.

Daphnids were removed from growth media or from exposure conditions and RNA was extracted using Trizol reagent (Invitrogen) as per manufacturer's instructions with a handheld homogenizer (Biospec Products Inc.) or by grinding with mortar and pedestal. RNA quality was assessed with spectrometry and on an agarose gel. All sequencing was done at the Vincent J. Coates Genomics Sequencing Laboratory at U.C. Berkeley. Detailed methods for each library preparation follow.

EST database – 5000 randomly selected cDNA clones from the Daphnia Genome Consortium and 2681 cDNA clones enriched for genes affected by exposure to heavy metals and munitions chemicals were collected by for the creation of a cDNA *D. magna* microarray.[78]

35 and 45 base pair Illumina runs – To get the most diverse set of transcripts possible, equal masses of RNA from exposed and control female daphnids of different ages and from male daphnids were combined into one sample (**Table 2.4**). RNA was processed with the Illumina mRNA Seq V2 protocol. Briefly, mRNA was purified out of 10 μg total RNA with Dynal oligo(dT) magnetic beads (Invitrogen), randomly fragmented with 10X RNA Fragmentation Reagent (Ambion) and reverse transcribed with Random Hexamer Primers (Invitrogen) and SuperScript II reverse transcriptase (Invitrogen). Second strand cDNA was made with DNA Polymerase I (Invitrogen). The Illumina Genomic DNA Sample Prep Kit was used to repair cDNA ends, add a single A base and ligate sequencing adapters. cDNA templates were purified on a 2% agarose gel. Fragments in the ~200bp range were cut out and cleaned up in QIAquick gel extraction kit (Qiagen) and PCR enriched with Phusion Polymerase (New England Biolabs). Quality of sample was assessed with a Bioanalyzer 2100 on a DNA1000 LabChip (Agilent). The sample was sequenced on an Illumina Genome Analyzer II.

Control (con) and Copper (Cu) Illumina runs – These samples were prepared as above, but RNA was collected from adult (two week old) females exposed to 1/10 LC_{50} (6.15 μg/L) copper[5], [126]or to a media-only control. These samples were also sequenced on the Genome Analyzer II.

454 (2.TCA.454Reads.fasta) run – RNA used for this library was extracted from a variety of different exposure conditions (**Table 2.5**). Methods were adapted from The Joint Genome Institute cDNA Library Creation Protocol Version 1.[127] Briefly, mRNA was purified out of 60 μg total RNA with Dynal oligo(dT) magnetic beads (Invitrogen). mRNA was reverse transcribed with Superscript III reverse transcriptase (Invitrogen) and dT15VN2 (TTTTTTTTTTTTTTTVNN) primer. Second strand cDNA was made with *E. coli* DNA polymerase (Invitrogen) and purified with a QIAquick PCR purification column (Qiagen). mRNA was precipitated with phenol, chloroform, isoamyl alcohol mix and ethanol and was re-suspended in water. Samples were then processed for 454

sequencing using the GS FLX Titanium protocol and sequenced on one half of one sequencing plate.

Silver Nanowire (AgNW) Illunia TruSeq runs – These samples were prepared from adult daphnids exposed to 1/10 LC_{50} AgNWs, 1/10 LC_{50} silver (Ag^{+}) or media-only control. Samples used for transcriptome assembly include two biological replicates and one technical replicate for each AgNW, Ag^{+} and control (**Table 2.6**). These samples were prepared similarly to Illumina libraries, above, with the TruSeq RNA Sample Preparation Kits A and B (Illumina) via the low-throughput protocol. The biological replicates were paired-end sequenced on a High Seq 2000 (Illumina) at a length of 100 bases. The technical replicate was single-end sequenced at 100 nucleotides also on the High Seq 2000. All libraries were multiplexed six samples per lane. Two additional biological replicates of each condition were prepared in-house, as above, or on an Apollo robot (integenX) at the Functional Genomics Laboratory at U.C. Berkeley. The additional biological replicates were sequenced as single-end, 50-nucleotide reads, multiplexed nine samples per lane.

Assembly of transcriptome.

The large volume of sequencing data allowed for stringent quality control of short reads used for transcriptome assembly. All reads with any unknown bases (Ns) were removed using the fastq_quality_filter program from the Fastx toolkit (http://hannonlab.cshl.edu/fastx_toolkit/). A minimum base quality score of >= Q25 was also employed (99-99.9% accuracy). **Table 2.6** shows all samples used for transcriptome assembly. In **Figure 2.2**, a bar chart shows number of bases used. An initial assembly was performed using Oases[128] and Velvet[129] on the Illumina short read sequencing data. For the EST database and 454 RNAseq data, Newbler (GS assembler with -cdna option) was used. Both programs take the short-read data and align it into longer transcripts by matching pieces with sequence overlap. All Illumina data/ Velvet and Oases assemblies were performed in single end mode as all the paired end samples had overlapping mates. Reads from both mates that passed the quality step were combined into a single file. Each sample treatment group was assembled independently using different combinations of kmer settings. “k-mer” is the length of overlap between two different short-read sequences. Velvet and Oases are programs designed to use sequentially that work on very short-read data. Newbler is designed for longer (~400 base pair or longer) data.

35 and 45 base pair Illumina FASTA–Kmin 23, kmax 49 and Oases assembly merge with K = 24. Kmer steps were incremented at 6 base intervals.

AgNW LDS1 Illumina FASTQ – Kmin 51, kmax 100 and the Oases assembly merge with k = 55. The Kmer steps were at 2 base intervals.

AgNW LDS2 Illumina FASTQ – Kmin 51, kmax 100 and an Oases merge at k = 75bp; kmer intervals were set up at 6 base intervals.

AgNW Snafu FASTQ – Kmin 51, kmax 67 and an Oases merge at k = 51bp. This was performed using 4 base Kmer intervals.

454 and EST database –These databases were assembled separately using Newbler 2.6 with the -cDNA and adaptor trim options.

A final refinement of the assembly was performed using CD-HIT-EST and Minimus2 (http://sourceforge.net/apps/mediawiki/amos/index.php?title=Minimus2), based on the Laboratory of Genomics, Evolution and Development metagenomics guide (http://ged.msu.edu/angus/metag-assembly-2011/velvet-multik.html). The final merged transcriptome was annotated using blastall with Refseq and non-redundant (NR) protein databases. Assembly and gene expression analyses were done by Dr. John Herbert at the University of Birmingham, UK.

Differential gene expression analyses.

Differential gene expression (DGE) was first analyzed using four different methods: Limma (voom function),[130] Samseq,[131] edgeR[132] and DESeq.[133] After an initial evaluation, edgeR was chosen for this data set. It first estimated a common negative binomial dispersion parameter for the data set. Then, it estimated trended dispersion for negative binomial generalized linear model statistics (GLMs). Finally, it computed an empirical Bayes estimate of the negative binomial dispersion parameter for each transcript, with expression levels specified by a log-linear model. For all samples, a 10% false discovery rate (FDR) cut off was employed. **Table 2.2** lists samples used for DGE analysis.

Differential gene expression in all samples was first analyzed with a custom designed bowtie map (process by which short reads are aligned to the transcriptome) and with simple counting (described below). **Table 2.3** lists numbers of differentially expressed genes. Results from this analysis are preliminary. Next, samples were analyzed with four different map and count combinations, detailed below. This is a labor-intensive process, but is necessary to determine the best methods for analysis of the data set. S-PVP AgNW data are presented as a proof-of-concept analysis.

Reads were mapped onto the assembled transcriptome with Bowtie 0.12.8 in four combinations of count assignments and mapping method, listed below. “Custom” method was a stringent procedure that only mapped reads onto the transcriptome with less than four mismatches and not matching more than 30 distinct transcripts – no second best matches were counted. The protocol recommended by eXpress 1.2.1 software counted every alignment with less than four mismatches regardless of how many transcripts were matched. Method combinations were:

- Custom simple = custom bowtie map and simple counting
- Custom exp = custom bowtie map and eXpress counting
- Exp simple = eXpress bowtie mapping and simple counts
- Exp Exp = eXpress bowtie mapping and eXpress counts

Transcript counts were assigned using both simple Perl parsing "simple counting" and, as a comparison, with the eXpress software. (This program uses maximum likelihood statistics to assign transcript counts from BAM files, http://bio.math.berkeley.edu/eXpress/overview.html). Generalized linear model statistics (GLMs) from the Bioconductor edgeR package were employed to find differentially expressed genes. The DESeq package was used to generate variance stabilized counts for two-dimensional clustering and principle component analyses. Pruning of low quality reads was not done for differential expression analyses as the distribution of low quality reads across data sets may not be even. All mapping was done on all data, using all reads, with L1 and L2 reduced to 50bp, to be the same length as L3.

RESULTS

Sequencing runs resulted in different numbers of reads as sequencing technology advanced.

A large amount of sequencing data was gathered for assembly of the transcriptome. The earliest Illumina runs were 36 or 45 nucleotides long; later runs were as long as 100 nucleotides. **Table 2.5** lists all sequencing runs, lengths, numbers of reads and total bases sequenced that were used for transcriptome assembly (the only sequencing data not in this table are the shorter Illumina HiSeq 2000 runs). Only the highest quality reads were used for transcriptome assembly, as a very large volume of sequencing data was generated (**Figure 2.2**).

Transcriptome assembly was robust, and alternate splicing was detected.

Each sequencing database was assembled individually (**Figure 2.3**). The resultant contiguous sequences (contigs) were then aligned into a grand total of 103,231 sequences with an N50 of 1986 bases (**Figure 2.4**). In other words, the median size of assembled transcripts was 1986 bases long. The *Daphnia pulex* genome, which has been sequenced,[134] contains approximately 31,000 genes. The 103,231 transcripts assembled from SRS data therefore likely represent alternate splicing. Basic Local Alignment Search Tool (BLAST), a tool for identifying protein homologues from transcript sequence, was used to compare assembled transcripts to the *Daphnia pulex* genome. It resulted in 77,754 *Daphnia* protein hits (**Figure 2.5**); approximately 75% of aligned sequences have a protein homolog in *Daphnia pulex*. This new transcriptome represents 70 million bases of RNA sequence.

Differential gene expression analysis results from sequencing data are different than microarray results.

The numbers in Table 2.3 show that short-read sequencing and computational analysis of differential gene expression results were very different than results from microarray. Sequencing data resulted in the identification of ten times more differentially expressed genes than microarray data (30,785 DEG versus 2916 DEG). However, sequencing identified more DEG in only three out of the five conditions (L-PVP, L-SiO_2 and S-PVP). In Ag^+ and S-SiO_2, sequencing identified fewer DEG than microarray.

Short-read sequencing differential gene expression analysis was influenced by batch effects, read mapping parameters and transcript counting method.

Different parameters used for read mapping influenced the list of reported differentially expressed genes. The custom designed read-mapping method, mentioned above, only accepted reads that best mapped to no more than 30 different transcripts (potential isoforms of the same gene). In contrast, eXpress mapping parameters accepted any alignment with less than four mismatches, to any number of transcripts. **Table 2.7** illustrates how batch and analysis method affected the number of differentially expressed

genes for S-PVP versus control. Overlaps of genes can be seen in the Venn diagram, **Figure 2.6**, which further illustrates method affects. PCA analyses on the three sequencing datasets, L1, L2 and L3, showed strong batch effects. This is illustrated in **Figure 2.7** with S-PVP AgNW and control samples.

DISCUSSION

Transcript assembly was robust and will be used to generate a new microarray that contains more transcripts and better annotation. This in turn will aid in better toxicogenomic studies in *Daphnia magna*. Because the transcriptome was robust and the quality control was very rigid, the ~103,000 unique transcripts generated with *de novo* assembly likely represent alternate splicing.

BLAST results of the transcriptome to the *Daphnia pulex* genome resulted in 75% identification of protein homologues. This does not indicate poor transcriptome alignment. Rather, because *D. magna* and *D. pulex* contain different numbers of chromosomes in addition to being different species, it is logical that there would be some differences in the expressed genome. To identify protein homologues in other species, the transcriptome is currently being BLASTed to the non-redundant protein database, a collection of all known protein homologues. This will be a lengthy process, but will result in more transcripts with known identities, better pathway analysis and better mode of toxicity investigation.[111] The KEGG pathway database is in process of being updated with transcripts from the assembly (instead of transcripts from the microarray). Again, better annotation of the array will likely lead to more informative gene expression studies. Additionally, work is being done to identify how many proteins the 103,231 transcripts represent.

Differential gene expression analysis on sequencing data resulted in different numbers of identified genes than analysis with microarray. The samples are biological replicates, so it appears that SRS has different strengths or sensitivities than microarray techniques. SRS data is limited by transcripts expressed at time of extraction and not by transcripts represented on an array. It seems that over all, SRS will pick up more genes (ten times as many, on average). Further analysis is needed to determine which genes are in common and different between the different molecular techniques and to identify affected KEGG pathways and compare to KEGG results from microarray gene expression data.

Large differences in results with the four sequence-based gene expression analysis methods bring up a new avenue of investigation. It is not yet possible to say whether microarrays or sequencing is a better method for evaluation of gene expression. Microarray results were confirmed with qPCR, as described in Chapter 1 of this dissertation. Future studies will require qPCR confirmation of the different sequencing DEG analysis results to confirm which method is best for this data set. Within edgeR, model parameters can be specified that account for different batches. However, for safety, differential gene expression analysis was conducted on three combinations of batches: Just L1 and L2 together, L3 alone and L1, L2 and L3 together. L1 and L2 are probably the best combination, as PCA plots best separate the sample groups for these data, but further analysis are warranted. Furthermore, this work shows that variability is sample preparation leads to large variability in sequencing datasets.

Advances in sequencing technology make *de novo* transcriptome assembly possible and accurate.[135], [111] Until recently, long sequence read lengths, such as with 454, or genomes from related animals were needed for non-model organism transcriptome assembly.[136] Different assembly methods are known to produce different numbers of contigs generated and length of contigs.[135] This *Daphnia magna* transcriptome circumvented these assembly issues because it had an extraordinarily large amount of input data of varying lengths. Transcriptome assembly also utilized numerous "steps" in k-mer lengths, which is a modification of program instructions but which produces the best results.[128] Ultimately, the transcriptome will have far-reaching uses for toxicologists, biologists and ecologists that work with *Daphnia magna*.

Differential gene expression analysis from short-read sequencing is still in the developing phase. Specifically, interpreting RNA sequencing gene expression data faces serious challenges: reads contain errors, alternate splicing adds levels of complexity, and the current technological status needs improvement.[137] However, like sequencing technology and microarray technology before it, differential gene expression methods will continue to advance to better incorporate variation in datasets and produce more consistent results. For the present work, qPCR analysis of the different gene expression data sets should confirm which methods work best, which in turn may help other biologists assemble transcriptomes and analyze gene expression with RNA from non-traditional organisms.

TABLES

File name	Platform	Type	Length	Machine
EST database	Sanger	EST	varied	
2.TCA.454.Reads.fasta	454	single	~400	GS FLX
35bp_sequence.fasta	Illumina	single	36	GAII
45bp_sequence.fasta	Illumina	single	45	GAII
con.fasta	Illumina	single	36	GAII
cu.fasta	Illumina	single	36	GAII
LS001				
index 2 = L-PVP	Illumina	paired	100	HiSeq 2000
index 4 = Ag+	Illumina	paired	100	HiSeq 2000
index 5 = Control	Illumina	paired	100	HiSeq 2000
index 6 = L-SiO2	Illumina	paired	100	HiSeq 2000
index 7 = S-PVP	Illumina	paired	100	HiSeq 2000
index 12 = S-SiO2	Illumina	paired	100	HiSeq 2000
LS002				
index 2 = L-SiO2	Illumina	paired	100	HiSeq 2000
index 4 = S-SiO2	Illumina	paired	100	HiSeq 2000
index 5 = Control	Illumina	paired	100	HiSeq 2000
index 6 = Ag+	Illumina	paired	100	HiSeq 2000
index 7 = L-PVP	Illumina	paired	100	HiSeq 2000
index 12 = S-PVP	Illumina	paired	100	HiSeq 2000
LS002 snafu				
index 2 = L-SiO2	Illumina	single	100	HiSeq 2000
index 4 = S-SiO2	Illumina	single	100	HiSeq 2000
index 5 = Control	Illumina	single	100	HiSeq 2000
index 6 = Ag+	Illumina	single	100	HiSeq 2000
index 7 = L-PVP	Illumina	single	100	HiSeq 2000
index 12 = S-PVP	Illumina	single	100	HiSeq 2000
LS003				
index 1 = S-PVP	Illumina	single	50	HiSeq 2000
index 3 = L-PVP	Illumina	single	50	HiSeq 2000
index 6 = Control	Illumina	single	50	HiSeq 2000
index 7 = Control	Illumina	single	50	HiSeq 2000
index 8 = Ag+	Illumina	single	50	HiSeq 2000
index 9 = Ag+	Illumina	single	50	HiSeq 2000
index 10 = S-SiO2	Illumina	single	50	HiSeq 2000
index 11 = L-SiO2	Illumina	single	50	HiSeq 2000
index 2 = S-SiO2	Illumina	single	50	HiSeq 2000
index 2b = L-PVP	Illumina	single	50	HiSeq 2000
index 4b = S-PVP	Illumina	single	50	HiSeq 2000
index 5b = L-SiO2	Illumina	single	50	HiSeq 2000

Table 2.1. All sequencing samples used in this study. Platform: methodology; type: single or paired-end reads; length: average length reads.

File name	Platform	Type	Length	Machine
LS001				
index 2 = L-PVP	Illumina	paired	100	HiSeq 2000
index 4 = Ag+	Illumina	paired	100	HiSeq 2000
index 5 = Control	Illumina	paired	100	HiSeq 2000
index 6 = L-SiO2	Illumina	paired	100	HiSeq 2000
index 7 = S-PVP	Illumina	paired	100	HiSeq 2000
index 12 = S-SiO2	Illumina	paired	100	HiSeq 2000
LS002				
index 2 = L-SiO2	Illumina	paired	100	HiSeq 2000
index 4 = S-SiO2	Illumina	paired	100	HiSeq 2000
index 5 = Control	Illumina	paired	100	HiSeq 2000
index 6 = Ag+	Illumina	paired	100	HiSeq 2000
index 7 = L-PVP	Illumina	paired	100	HiSeq 2000
index 12 = S-PVP	Illumina	paired	100	HiSeq 2000
LS003				
index 1 = S-PVP	Illumina	single	50	HiSeq 2000
index 3 = L-PVP	Illumina	single	50	HiSeq 2000
index 6 = Control	Illumina	single	50	HiSeq 2000
index 7 = Control	Illumina	single	50	HiSeq 2000
index 8 = Ag+	Illumina	single	50	HiSeq 2000
index 9 = Ag+	Illumina	single	50	HiSeq 2000
index 10 = S-SiO2	Illumina	single	50	HiSeq 2000
index 11 = L-SiO2	Illumina	single	50	HiSeq 2000
index 2 = S-SiO2	Illumina	single	50	HiSeq 2000
index 2b = L-PVP	Illumina	single	50	HiSeq 2000
index 4b = S-PVP	Illumina	single	50	HiSeq 2000
index 5b = L-SiO2	Illumina	single	50	HiSeq 2000

Table 2.2. Short read sequencing data used to assay differential gene expression.

Exposure	Ag+	L-PVP	S-PVP	L-SiO2	S-SiO2	Total
# DEG seq	445	17,000	11,000	2230	110	30785
# DEG array	692	519	623	519	563	2916

Table 2.3. Numbers of differentially expressed genes determined by sequencing and microarray technology.

Condition	µg RNA
neonate control	2
2 week control	2
1 week control	2
1 week copper	2
2 week male control	2
2 week 1/10 LC_{50} copper	2
Total	12 µg

Table 2.4. *Daphnia magna* RNA samples from different aged daphnids and different exposure conditions used to generate the 36 base pair and 45 base pair sequencing samples.

Condition	µg RNA
2 week control	36
1 week control A	16
1 week control B	16
1 week 1/10 LC_{50} copper A	16
1 week 1/10 LC_{50} copper B	16
Total	100 µg

Table 2.5. *Daphnia magna* RNA samples used in 454 sequencing.

1	class	No. of seque	No. Mates	Sample name	No. of sequenc	QC	class	Platform	Type	Length	machine	Quality System
	public ncbi	15367		ncbi_ests	15367	15367		Sanger	single	400	Sanger	na
2	454	85138		2.TCA.454.Reads.fasta	85138	85138		454	single	400	Roche	SFF
3	35	7069526		35bp_sequence.fasta	7069526	6992976		Illumina	single	36	GAII	na
4	45	5505590		45bp_sequence.fasta	5505590	5390954		Illumina	single	45	GAII	na
5	con.fasta	18029836		con.fasta	18029836	17636574		Illumina	single	36	GAII	na
6	cu.fasta	15070902		cu.fasta	15070902	14690174		Illumina	single	36	GAII	na
7	LS001	12807766	12807766	index 2 = L-PVP	25615532	15417407	L-PVP	Illumina	paired	100	TruSeq	Sanger Q + 33
8	LS001	12927148	12927148	index 4 = Ag+	25854296	14866231	Ag+	Illumina	paired	100	TruSeq	Sanger Q + 33
9	LS001	17377482	17377482	index 5 = Control	34754964	20845952	Control	Illumina	paired	100	TruSeq	Sanger Q + 33
10	LS001	15103607	15103607	index 6 = L-SiO2	30207214	17420646	L-SiO2	Illumina	paired	100	TruSeq	Sanger Q + 33
11	LS001	12799073	12799073	index 7 = S-PVP	25598146	15365562	S-PVP	Illumina	paired	100	TruSeq	Sanger Q + 33
12	LS001	9686386	9686386	index 12 = S-SiO2	19372772	11441768	S-SiO2	Illumina	paired	100	TruSeq	Sanger Q + 33
13	LS002	27709448	27709448	index 2 = L-SiO2	55418896	23517018	L-SiO2	Illumina	paired	100	TruSeq	Sanger Q + 33
14	LS002	13598718	13598718	index 4 = S-SiO2	27197436	11598626	S-SiO2	Illumina	paired	100	TruSeq	Sanger Q + 33
15	LS002	27524721	27524721	index 5 = Control	55049442	24028830	Control	Illumina	paired	100	TruSeq	Sanger Q + 33
16	LS002	31409353	31409353	index 6 = Ag+	62818706	27037237	Ag+	Illumina	paired	100	TruSeq	Sanger Q + 33
17	LS002	20800196	20800196	index 7 = L-PVP	41600392	18047217	L-PVP	Illumina	paired	100	TruSeq	Sanger Q + 33
18	LS002	29074021	29074021	index 12 = S-PVP	58148042	25933074	S-PVP	Illumina	paired	100	TruSeq	Sanger Q + 33
19	LS002_snafu	17381442		index 2 = L-SiO2	17381442	7517096	L-SiO2	Illumina	single	100	TruSeq	Sanger Q + 33
20	LS002_snafu	8678775		index 4 = S-SiO2	8678775	3809154	S-SiO2	Illumina	single	100	TruSeq	Sanger Q + 33
21	LS002_snafu	17261945		index 5 = Control	17261945	7727734	Control	Illumina	single	100	TruSeq	Sanger Q + 33
22	LS002_snafu	20506572		index 6 = Ag+	20506572	8868426	Ag+	Illumina	single	100	TruSeq	Sanger Q + 33
23	LS002_snafu	13149350		index 7 = L-PVP	13149350	5891411	L-PVP	Illumina	single	100	TruSeq	Sanger Q + 33
24	LS002_snafu	18703730		index 12 = S-PVP	18703730	8655892	S-PVP	Illumina	single	100	TruSeq	Sanger Q + 33
					603,094,011	**312,800,464**						

Table 2.6. A tally of SRS data used in transcriptome assembly, which includes most of the SRS data. Describes the size of short-read produced and number of reads sequenced for each sample.

Condition	Custom, Simple	Custom, eXpress	eXpress, Simple	eXpress, eXpress
L1 L2	12272	4653	8618	4699
L3	166	2211	88	2540
L1, L2 + L3	1150	950	975	1062

Table 2.7. Counts of differentially expressed genes determined by four different analysis methods. Numbers are genes that were differentially expressed. S-PVP AgNW versus control.

.

FIGURES

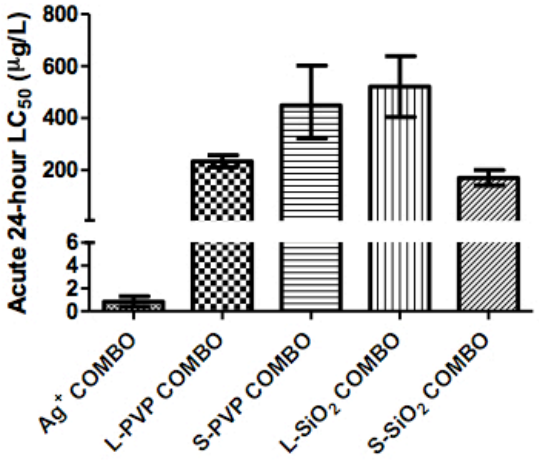

Figure 2.1. The Acute, 24-hour LC_{50} values for AgNW and Ag^{+} on *Daphnia magna*. Exposures for microarrays and for SRS gene expression analysis were conducted at 1/10 LC_{50}.

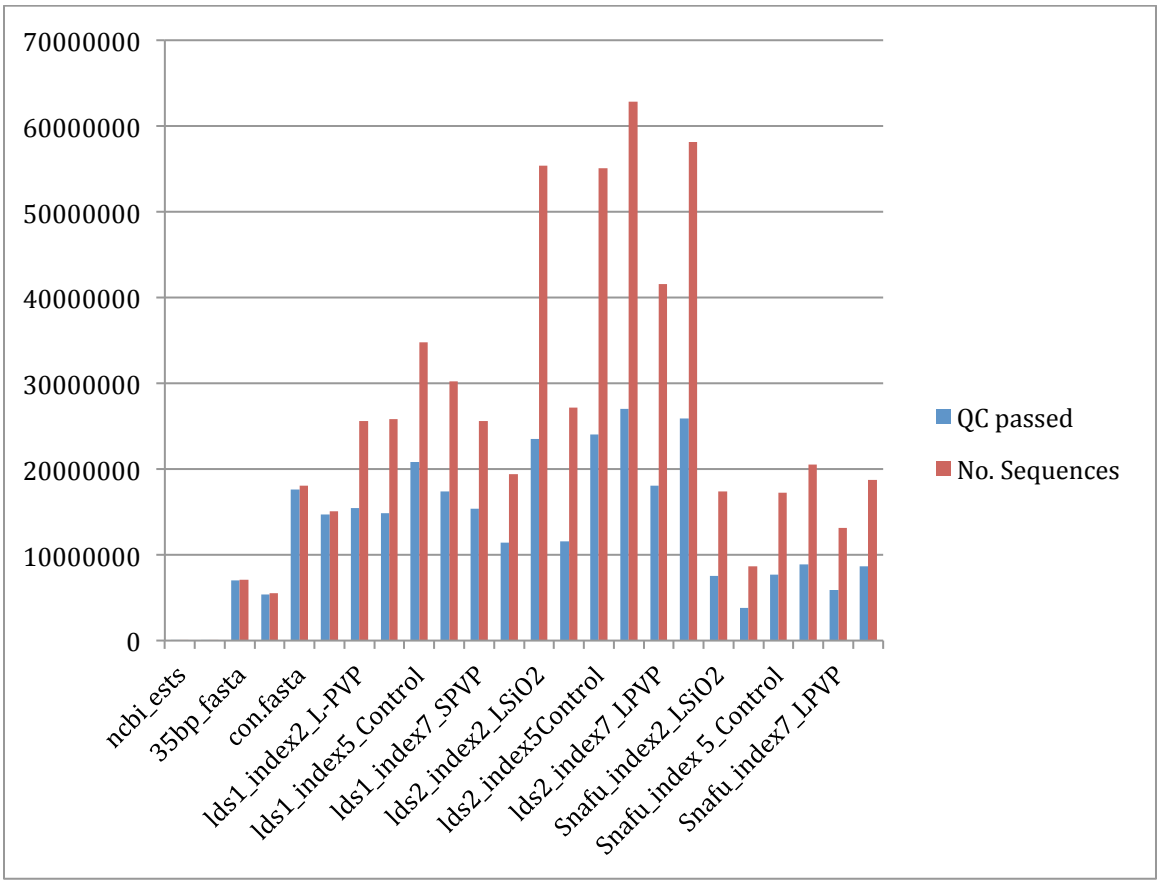

Figure 2.2. Because a very large volume of sequencing data was generated, only the highest quality reads were used for transcriptome assembly.

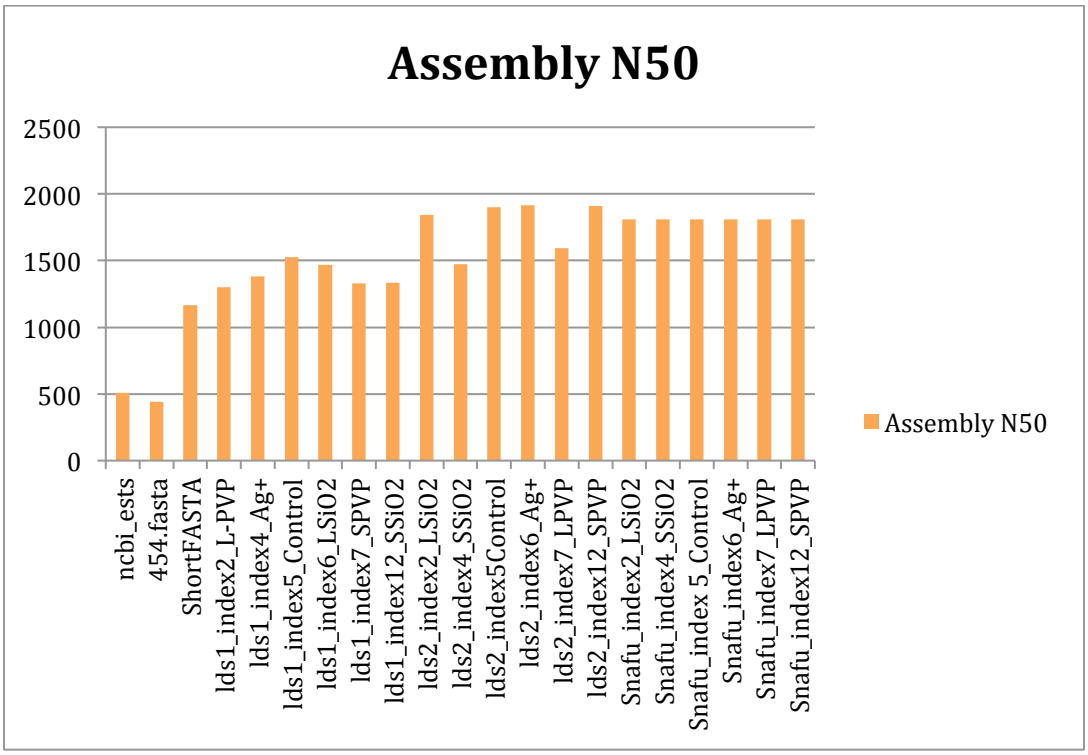

Figure 2.3. N50 is a metric in sequence assembly. Half of all bases in the sequence assemblies are less than N50. Each sequencing data file was assembled individually. Newer, longer sequencing files resulted in larger N50s, and therefore the assembled databases contain more, longer transcripts.

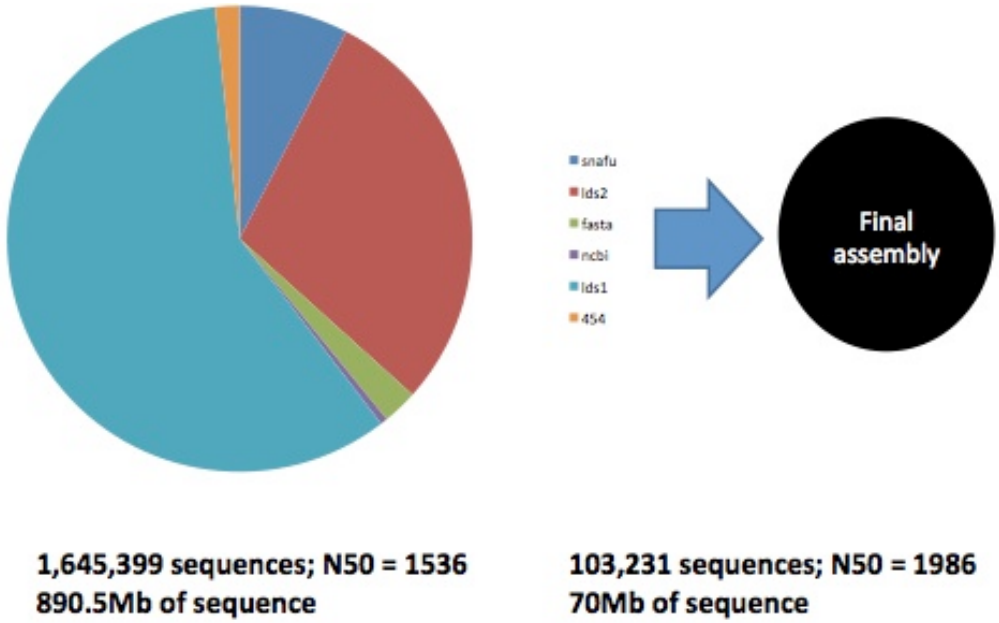

Figure 2.4. The pie chart to the left shows the transcript assemblies from the different data sets. Each SRS dataset was aligned, and resultant files were then merged into the final transcriptome.

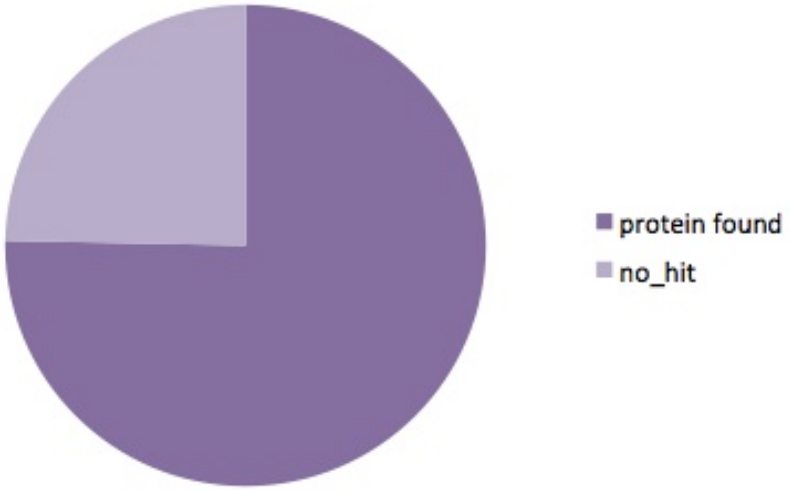

77,754 hit a daphnia protein, 25,477 don't (e-value = 1e-9)
NR blast still ongoing

Figure 2.5. Percent of sequences that had homologous proteins in BLAST analysis.

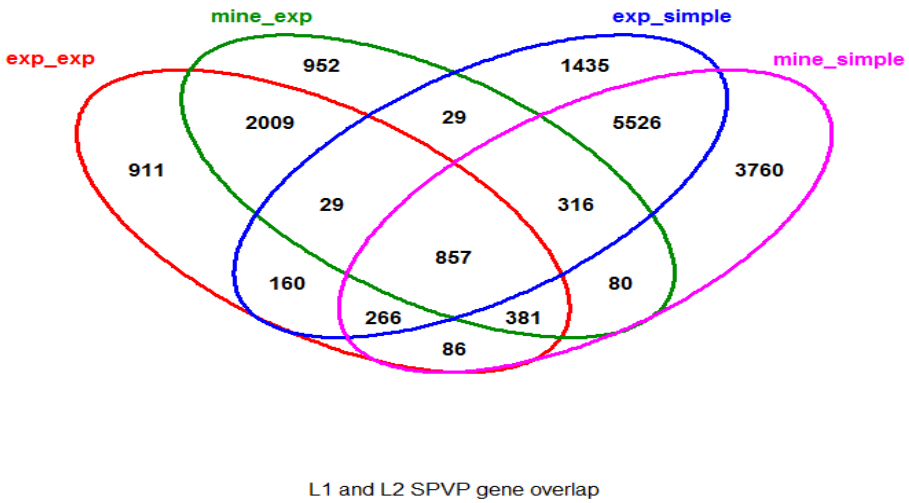

Figure 2.6. Venn diagram of differentially expressed gene analysis on S-PVP vs. control. This portrays how the different mapping reads and transcript assignment counting methods affected the number of differentially expressed genes reported. Exp_exp = eXpress bowtie parameters and eXpress counting. mine_exp = Stringent bowtie parameters and eXpress counting. exp_simple = eXpress bowtie mapping and simple counting. mine_simple = Stringent bowtie parameters and simple counting.

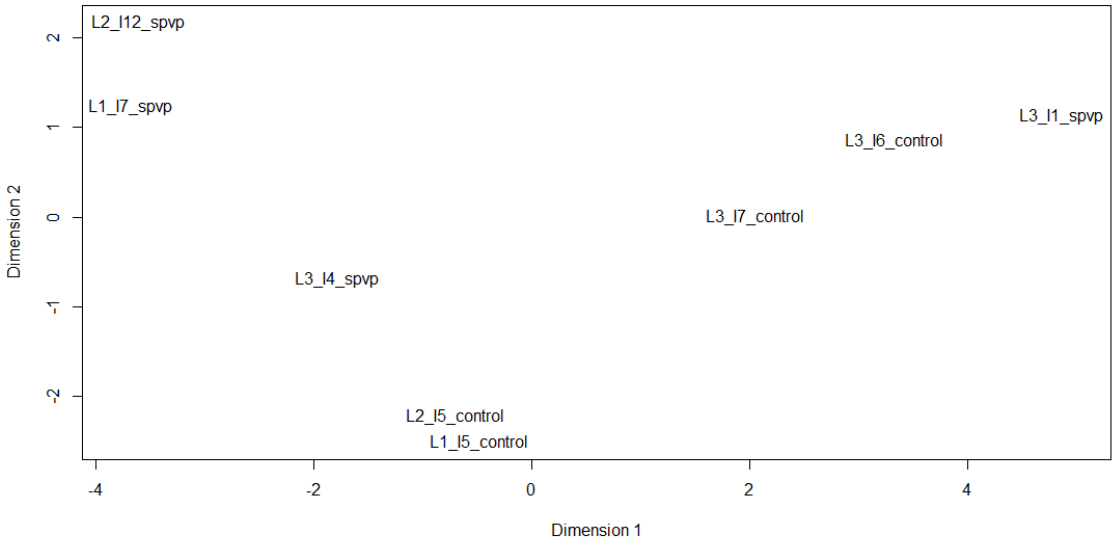

Figure 2.7. PCA plot shows sequencing sample variation. Control and S-PVP exposed samples do not cluster into their respective groups. L1 and L2 batches cluster into separate groups but this is confounded when L3 is added.

Chapter 3.

Toxicity of chemical flame-retardants on *Daphnia magna*

INTRODUCTION

Chemical flame-retardants (FR) have been used extensively in California since the 1970s. One FR, pentabromodiphenyl ether (pentaBDE) was banned in the European Union and restricted in the United States due to persistence, accumulation and toxicity. Other FRs are used in its place and are largely untested for toxicity. In this work, freshwater crustacean *Daphnia magna* was exposed to commonly used FRs including pentaBDE and octaBDE technical mixtures, pentaBDE's replacement Firemaster® 550 (FM550) and FM550's chemical components. The PBDE technical mixtures are more ecologically relevant than single PBDE congeners as they contain numerous PBDE congeners, as in global ecosystems. This work investigates whether the chemical FRs cause toxicity to *Daphnia*, whether each hydrophobic chemical elicits a unique response instead of a nonspecific narcotic effect and if chemicals with similar structures cause similar toxicities. Microarray gene expression technique was used to help understand biological effect.

Although chemical FRs often have low water solubility, daphnids will be exposed to FRs in the environment because, as filter feeders, they ingest particles such as sediment or suspended solids they come into contact with. PBDEs accumulate in marine copepods,[138], [139] and brominated FRs biomagnify in aquatic food chains,[140] indicating exposure potential. Daphnids are commonly used to evaluate invertebrate response to pollutants,[20],[19] are important in fresh water ecology and, because they reproduce parthenogenically, are a good model for gene expression assays. Their unique biology, ecological importance and method of feeding makes *Daphnia magna* an ideal organism for assessing toxicological effects of FRs.

The toxicity of PBDEs is well studied, but exact molecular mechanisms behind toxicity are still unknown. Structure-activity relationships suggest that PBDE acute toxicity results from a receptor-mediated effect.[141] PentaBDE elicits numerous effects, including hyperactivity in mice and rats [142], [143], impaired spermatogenesis (reduced sperm and spermatid counts) in rats[143] and changes in retinoid status in zebrafish.[144] It is a potential thyroid modulator, although reports are conflicted.[145], [146], [147] PBDEs can be photochemically converted to dioxin, a potent carcinogen,[148], [149] but they do not act via the same AhR mechanism.[150] PBDE congeners with less bromine atoms are usually more toxic.[141] They are found in solid effluent from sewage treatment facilities that is reused for agriculture, landscape, sport-field and industrial purposes[37] and is considered a source of exposure for humans and animals alike.

The effects of pentaBDE replacement FM550 are less characterized. FM550 consists of two brominated compounds, tetrabromo phthalate (TBPH) and tetrabromo benzoate (TBB), and two organophosphate compounds, triphenyl phosphate (TPP) and

isopropylated triaryl phosphate (ITP). Very few toxicity studies on the brominated compounds exist. Accumulation and DNA damage studies of TBB and TBPH in fathead minnow showed a significant increase in DNA strand breaks in liver cells during exposure but not after a recovery period.[56] *In vitro* hepatic metabolism of TBB and TBPH in fathead minnow, carp, mouse and snapping turtle showed a "metabolic loss" of TBPH in all species and TBB loss in all except the turtle.[57] Metabolism of TBB and TBPH in human and rat liver microsomes and in purified porcine carboxylesterase resulted in phase I cleavage metabolites, but no phase II sulfation, glucuronidation or glutathione conjugate metabolites.[151] A study done on pregnant rats with mono-(2-ethyhexyl) tetrabromophthalate, a potentially toxic metabolite of TBPH, showed maternal hypothyroidism and decreased serum T3, hepatotoxicity, and increased multinucleated germ cells in fetal testes. The metabolite inhibited deiodinase activity *in vitro*, induced adipocyte differentiation and activated PPARα and γ-mediated gene transcription.[152] A recent study on the effects of FM550 on female rats and their pups showed a significant increase in adiposity in the offspring after an environmentally relevant exposure (100 or 1000 μg/day) during gestation and lactation and a significant increase in total serum thyroxine (T4) levels in the high-dose exposed dams compared to control.[153]

FM550 component triphenyl phosphate (TPP) has been studied more thoroughly than FM550.[154] TPP is a EU high-production volume plasticizer and flame-retardant that enters the environment by diffusive volatilization, leaching and abrasion.[155] It has been detected in sewage treatment plant influent and effluent [156] and in air, water and sediment, but data on TPP occurrence in biota and mode of toxicity are limited.[157]. TPP increased 17β-estradiol and testosterone concentrations in human adrenal corticocarcinoma cells and in zebrafish[158] It has a high LC_{50} in rats (5000-20,000 mg/kg), but causes sporadic visceral hemorrhages after exposure. It is not genotoxic. LC_{50}s in different fish species range from 0.7-300 mg/L.[154] EPA-reported LC_{50}s for TPP in *Daphnia* range from 1 to 1.35 mg/L, while Lin *et al* found 24-hour and 48-hour LC_{50} values of 0.51 and 0.089 mg/L.[158] Mechanisms of toxicity and molecular effects of TPP to mammals or other organisms are largely unknown.

In this work, the acute 48-hour toxicity of pentaBDE, octaBDE, FM550, TBPH, TPP, Firemaster® BZ-54 (BZ54), which consists of TBPH and TBB, and plasticizer di(2-ethylhexyl) phthalate (DEHP, the non-brominated TBPH analog) were evaluated on *Daphnia magna*. Differential gene expression was then analyzed between control daphnids and those treated at 1/10 LC_{50} for each chemical. Gene ontology pathway analysis was employed to determine potential modes of toxicity. HOPACH clustering was also done on the gene expression data to determine if biological effects were similar or unique. Accumulation was assayed in *Daphnia* exposed to FM550, and metabolome changes and lipidome changes were measured in *Daphnia* exposed to FM550 and pentaBDE. Gene expression data was also used to test whether chemicals with similar structures cause similar genomic responses in *Daphnia magna*.

METHODS

Daphnia magna culture.

Daphnia magna originally obtained from Aquatic Research Organisms (Hampton, NH) were cultured asexually in a Conviron (Pembina, ND) growth chamber at 21±1C with 16 hours of light and eight hours of dark per day in COMBO[75] media. They were fed *Pseudokirchneriella subcapitata* (formerly *Selenastrum capricornutum)* and yeast cereal-leaf and trout chow mix three times per week following renewal of media. Media was aerated overnight to increase dissolved oxygen levels. Media pH was maintained at pH 7.4-7.8. The chemical composition of COMBO media is described in **Table 4**, **Chapter 1**.

Toxicity assays.

Acute toxicity assays were similar to the U.S. EPA Whole Effluent Toxicity (WET) protocol.[76] Chemical FRs were dissolved in polar solvent dimethyl sulfoxide (DMSO) (EMD Chemicals, Inc). Five first instar (<24 hours old) daphnids were added to glass beakers containing 35 ml aliquots of COMBO media. FRs in up to 0.05% DMSO were added to make five different concentrations of FR. Typically, four replicates of five daphnids were exposed to five different concentrations of FR and a solvent and media-only control at one time. Animals were fed algae after 24 hours, and lethality was measured after 48 hours. At least three sets of four replicates were conducted per FR, with the exception of BZ54, for which a LC_{50} was determined after fewer exposures. Acute LC_{50}s were determined using probit[76] or Spearman-Karber[159] statistical programs. Attempts at determining an LC_{50} for decaBDE failed, as it was too insoluble in aqueous media. Chemical manufacturers: FM550 and BZ54 (Chemtura), TBPH (Unitex), TPP (Aldrich), pentaBDE (Larodan Chemicals), octa and decaBDE (Bromine Compounds Ltd), DEHP (Aldrich). The molecular structures of chemicals used in this study are in **Figure 3.1**.

Gene expression microarrays.

Differential gene expression was analyzed between control and FR-exposed animals with microarray technology. 15-20 adult (14 day old) daphnids were exposed at 1/10 FR LC_{50} in 800 ml COMBO media, except for FM550 48.6 243 µg/L and 48.6 ng/L exposures, which were done with ~100 animals in 4 liters media (see accumulation methods, below). Further FM550 exposures were done at ½ LC_{50} (243 µg/L) and at 1/2000 LC_{50} (243 ng/L) to investigate dose effects. Animals were fed after 24 hours and after 48 hours RNA was extracted in Trizol reagent (Invitrogen) with a handheld homogenizer (Biospec Products Inc.). RNA quality was assessed with spectrometry and via agarose gel electrophoresis. RNA was then reverse-transcribed, amplified and hybridized onto a custom Agilent oligonucleotide DNA microarray (AMADID # 023710) with the Agilent Low-input Quick-Amp one-color array kit and protocol (Santa Clara, CA). 200 nanograms total RNA was used as starting material. Four exposed and four control arrays were done per chemical and chemical concentration. However, one TPP

control, one FM550 control and two of the FM550 48.6 µg/L and 243 µg/L were compromised during processing, which resulted in fewer biological replicated for those comparison groups. Arrays were processed and analyzed as described in **Chapter 1**. HOPACH cluster analysis was performed on gene expression data, as outlined in **Chapter 1**.

Quantitative reverse transcription PCR.

To independently verify microarray results, the expression of eight genes in nine conditions was analyzed with qPCR. Genes were verified because of q-value, degree of differential expression or potential mode of toxicity. RNA used for qPCR was extracted and quality controlled as for microarrays. 1 µg RNA was reverse transcribed with iScript cDNA synthesis kit (BioRad, CA) on a Mycycler thermal cycler (Biorad). 12 primer sets were tested with the SsoFast (BioRad) amplification kit with a melt curve from 55 to 65C on a BioRad C1000 Thermal Cycler with CFX96 R-T System. Primers with only one qPCR product were used for subsequent analysis, also with SsoFast amplification kit. Probes were designed on the NCBI online primer-designing tool (http://www.ncbi.nlm.nih.gov/tools/primer-blast/) and ordered from Elim Biopharm. Each gene amplification was preformed in duplicate or triplicate in both the control and treated RNA samples. Actin and GAPDH were used as housekeeping genes. Housekeeping Ct was subtracted from gene of interest Ct and values were $\log_2$ transformed. Significance between control and exposed was determined by Student's T-test with $p<0.05$. Primer sequences are shown in **Table 3.1**.

Gene ontology and pathway enrichment.

To further elucidate modes of toxicity and identify biological pathways affected by FR exposure, Kyoto Encyclopedia of Genes and Genomes (KEGG) analysis was used on the differentially expressed gene (DEG) dataset. The *Daphnia magna* array as annotated with a protein blast to identify 4958 *Daphnia pulex* homologues with an expect (E) value less than or equal to 10^{-4}. The list was matched with the available KEGG database annotation (www.genome.jp/kegg) and genes were sorted into their respective pathways. Of these, 1425 genes mapped onto 114 *Daphnia pulex* KEGG pathways. Pathways representing less than five genes in the array were removed, leaving 95 pathways and 1402 genes total in an unbiased sample of the original 371 KEGG pathways. Enrichment of significant differentially expressed genes in KEGG pathways was calculated using a modified Fisher Exact Probability P-value.[83], [84]

Metabolomics of FM550 and pentaBDE-exposed *Daphnia*.

Daphnia hemolymph was extracted and used to assess how endogenous metabolite levels changed in exposed compared to control animals. Hemolymph from unexposed adult (14 day old) daphnids was first collected to optimize instrumentation. Animals exposed to 800 mL COMBO media were fed algae after 24 hours, and after 48 hours hemolymph was extracted by piercing the carapace with a needle and aspirating hemolymph with a small pipette[77] For metabolomics analysis, adult daphnids were

similarly exposed to 1/10 LC_{50} FM550, 1/10 LC_{50} pentaBDE or to DMSO control. They were fed after 24 hours and after 48 hours were frozen on dry ice and stored at -80C until analysis by Dr. Quincy Teng at the US EPA.

Samples of 20 daphnids were extracted using a dual phase extraction procedure.[160] Briefly, a mixture of methanol, chloroform and water in the volume ratio of 4:4:2.85 was used to generate a two-phase extract. Only the aqueous phases were used for the present study. Prior to NMR analysis, extraction solvents were completely removed using a vacuum concentrator (Thermo Electron, Waltham, MA, USA). Each polar sample was then reconstituted in 220 mL of 0.1M sodium phosphate buffered deuterium oxide (pH 7.4) containing 20 mM 2,2-dimethyl-2-silapentane-5-sulfonate sodium salt (DSS), vortexed briefly, and centrifuged at 10,000 x g for 15 minutes at 4 ºC to remove any insoluble components. The resulting supernatant was pipetted into a 3 mm NMR tube (Wilmad LabGlass, Buena, NJ, USA) for NMR analysis.

All NMR spectra were acquired at 20 ºC on an Agilent Inova 600 MHz NMR spectrometer with a cryogenic triple-resonance flow probe using direct-injection NMR analysis.[161] ^{1}H chemical shifts were referenced internally to DSS. One-dimensional (1D) NOESY spectra were collected using 1024 transients, 7,200-Hz spectral width, 50-ms mixing time and 2-s acquisition time. Two dimensional (2D) TOCSY[162] experiment was performed to confirm metabolite identities. All NMR spectra were processed using Mnova (Mestrelab Research, Santiago de Compostela, Spain). 1D ^{1}H NOESY spectra were processed with 0.3-Hz apodization followed by zero-filling to 128 k points. Residual solvent regions were filtered, and spectra were aligned and normalized to unit total intensity. Spectra with a range of 0.50 – 9.50 ppm were segmented into 0.005 ppm bins. Two-dimensional spectra were processed using line broadening of 0.5 Hz and 60º-shifted squared sine bell functions for both F1 and F2 dimensions. Linear prediction was used to double the data points for the F1 dimension.[163]

For data analysis, a text file of binned spectra was imported into SIMCA-P+ (Umetrics Inc., Umea, Sweden) for multivariate data analysis. Principal components analysis (PCA) and partial least squares discriminant analysis (PLS-DA) were conducted for the entire dataset using mean-centered and Pareto-scaled bins. All samples (N = 7) were observed to fall inside of the Hotelling's T^2 ellipse at the 95% confidence interval in scores plots. The relative impact of a given chemical exposure was assessed, in part, by comparing score values for different treatment classes within a given PLS-DA model. All PLS-DA models are validated with 100 permutations. In addition, univariate analysis of the binned spectra was conducted using Excel. First, an "average class spectrum" was calculated by averaging the binned spectra across all class members, where class was defined by exposure level (including controls) and duration. Next, a difference spectrum was generated by subtracting the averaged bins of the relevant control class from those of each exposed class. Then, a Student's t-test was conducted on each bin using a p-value < 0.05. As described previously,[164] to greatly reduce the rate of false positives, any single isolated bin that passed the t-test (without an adjacent bin also passing) was replaced with a zero (i.e., it was rejected), because legitimate metabolite peaks span more than one bin at this bin size. The result was a "t-test filtered difference spectrum" for

each exposed class. Positive peaks in these difference spectra correspond to metabolites that increase (with statistical significance) upon treatment, whereas negative peaks represent metabolites that decrease.

Lipidome of FM550 and pentaBDE-exposed *Daphnia*.

To investigate changes in hydrophobic endogenous metabolites, daphnids were exposed to 1/10 LC_{50} FM550, 1/10 LC_{50} pentaBDE or DMSO control, as for gene expression and metabolomic studies, above. They were removed from culture, flash-frozen on dry ice, ground in 1.6 ml ultra pure water with a handheld homogenizer (Biospec Products Inc.) and frozen at -80C until analysis. Lipids were extracted and analyzed by the Kansas State University Lipidomics Research Center. Data acquisition, analysis, and lipid quantification in comparison to internal standards was done with an automated electrospray ionization-tandem mass spectrometry approach as previously described by Sparkes *et al.*, 2010,[165] except that an aliquot of 80 µl of extract in chloroform was used for analysis, and free fatty acids and acyl product ions were not analyzed. The molar results were normalized to the sample analyzed and to the number of daphnids to produce data in nano-moles of each lipid per daphnid (nanomol/daphnid). More details on methodology can be found at http://www.k-state.edu/lipid/lipidomics/profiling.htm. Five replicated of 10-11 animals each were collected for each exposure condition. The five biological replicates were averaged and statistical significance was determined with a two-tailed Student's t-test function in Excel (Microsoft). Samples with p-value <0.05 were considered significantly different from the control.

Accumulation of FM550.

Approximately 100 adult daphnids were exposed in 4 liters COMBO media to 1/10 $LC_{50,}$ 1/10000 LC_{50} or to a DMSO control. Animals were fed algae after 24 hours, removed from exposure media at 48 hours and put in clean, chemical-free media for a 24-hour depuration with feeding before removal from media and freezing at -80C. Animals used for RNA extraction and subsequent microarray analysis were removed from exposure media and RNA was extracted immediately, as per methods outlines above, with no gut-clearance in clean media. Exposures were repeated until a total of four biological replicates of 300-400 daphnids were collected per concentration for analytical analysis. *Daphnia* samples were analyzed for TBB and TBPH using gas chromatography mass spectrometry operated in negative chemical ionization mode (GC/ECNI-MS). Samples were extracted in a 50:50 mixture of dichloromethane:hexane and extracts were further cleaned using Florisil solid phase extraction cartridges. GC/ECNI-MS conditions are reported in Stapleton *et al.* 2008.[52] Results are reported in nanogram TB or TBPH per gram daphnid, dry weight (ng/g). Biological replicates were averaged and statistical significance was determined with a two-tailed Student's t-test function in Excel (Microsoft). Samples with p-value <0.05 were considered significantly different from the control. Analysis was done by Dr. Heather Stapleton at Duke University.

RESULTS

Flame-retardants cause toxicity to *Daphnia magna*.

All flame-retardants except insoluble decaBDE caused toxicity to *Daphnia magna* after 48 hours (**Figure 3.2** and **Table 3.2**). LC_{50}s are reported as milligrams FR per liter COMBO media (mg/L). These values represent the mass of FR chemical added to each system, and do not necessarily represent the amount of chemical dissolved in media, or the amount that is biologically available to the daphnids. PentaBDE (LC_{50} = 58 µg/L) was the most toxic FR, while octaBDE and DEHP were the least toxic (3.96 and 3.31 mg/L). FM550, TBPH and BZ54 had similar levels of toxicity (0.486, 0.5 and 0.53 mg/L), while TPP was slightly less toxic (0.91 mg/L). Plasticizer DEHP was significantly less toxic than TBPH (3.31 mg/L). The numbers of DEG can be found in **Table 3.3**.

Differential gene expression patterns are unique for each chemical.

Gene expression profiles generated in this study were unique to each compound. Venn diagrams generated from the gene expression data show numbers of genes that were similarly expressed in response to different exposure conditions (**Figure 3.3**). KEGG pathway analysis resulted in distinct biological processes affected by exposure to FM550, pentaBDE or TBPH; analyses for the other chemicals were not significant (**Table 3.4**). Results with a p-value < 0.1 were considered significant; results with a p-value < 0.2 were included as potentially significant, as limited annotation on the *Daphnia magna* microarray and transcriptome reduce the power of pathway analysis. qPCR verified microarray results in nine out of nine experiments. qPCR experiment results are detailed in **Table 3.5**.

Different concentrations of FM550 elicited different responses in *D. magna*.

Microarrays performed with RNA from daphnids exposed to 243 µg/L, 48.6 µg/L (1/10 LC_{50}), 243 ng/L or 48.6 ng/L FM550 caused unique differential gene expression profiles. Exposure in the ng/L range, or 1/10,000 LC_{50}, caused more differentially expressed genes (DEG) than at the 1/10 LC_{50}. The no-observed transcriptional effect level was not reached. **Table 3.6** lists numbers of differentially expressed genes in each exposure. KEGG pathway analysis resulted in similarity in affected pathways (tyrosine metabolism and the Jak-STAT signaling pathway), but with different degrees of significance (**Table 3.7**). HOPACH clustering of gene expression based on Euclidian distance, which is based on gene correlation and magnitude of correlation, show that octaBDE, pentaBDE and TPP grouped together as a "centroid" (**Figure 3.4**). Cosangle HOPACH clustering, based on correlation of gene expression only, groups the chemicals into three centroids (**Figure 3.5**).

FM550 metabolite profiles are distinguishable from control, while pentaBDE profiles are not.

To complement transcriptomic data, metabolomics assays were conducted on the pentaBDE and on FM550. Hemolymph extracted from animals exposed to 1/10 LC50 FM550, pentaBDE or the control were analyzed with ^{1}H-NMR. A representative ^{1}H one-dimensional NOESY NMR spectrum is shown in **Figure 3.6**. After 48 hours, exposure to 1/10 LC_{50} showed a change in gene expression in animals exposed to pentaBDE, but there was no significant difference in metabolite profile. This is illustrated in PLS-DA score plots (**Figures 3.7 and 3.8**). Data were t-test filtered and difference spectra were generated showing comparisons between exposed and treated groups (**Figure 3.9**).

Changes in endogenous lipid levels were detected in FM550 and in pentaBDE-exposed daphnids.

Because KEGG pathway analysis pointed to steroid effects in pentaBDE-exposed animals and glycerophospholipid effects in TBPH-exposed animals, lipidomics was performed on both pentaBDE and on TBPH-containing FM550. Both pentaBDE and FM550 exposures significantly changed four fatty metabolite levels of the 352 tested, as determined by Student's t-test in Excel, p-value < 0.05. One of the metabolites, phosphatidylcholine (42:7) was affected by both exposures. **Table 3.8** shows a list of affected lipids, while **Figure 3.10** shows fold-change of lipid relative to control. FM550 affected three phosphatidylcholines and a lysophosphatidylcholine while pentaBDE affected two phosphatidylcholines, a phosphatidylinositol and an ether-linked phosphatidylserine.

FM550 accumulates in *Daphnia magna* after 48 hours.

Daphnids exposed to 1/10 LC_{50} FM550 (48.6 μg/L) for 48 hours showed a significant increase in levels of FM550 components TBB and TBPH, while daphnids exposed to 1/10,000 LC_{50} (48.6 ng/L) did not. **Figure 3.11** shows average TBB levels and **Figure 3.12** shows average TBPH levels detected in nmol/g dry weight of daphnid tissue. TBB and TBPH were present in the unexposed controls at very low levels, which may indicate laboratory or atmospheric contamination.

DISCUSSION

The chemical FRs used in this study were toxic to *Daphnia magna*. PentaBDE was the most toxic FR. PentaBDE's LC_{50} value was one to two orders of magnitude more toxic than any other FR, including octaBDE, which was the least toxic chemical tested. A phenomenon of increased toxicity with lower-brominated PBDEs has been seen in other organisms,[166], [167], [141] but the trend is not always true in *Daphnia magna*.[168] With the phthalate molecules, the LC_{50} of DEHP is significantly higher than its brominate-analogue TBPH (**Figure 3.2**). All FM550 compounds had similar levels of toxicity. The statistically determined acute LC_{50} values represent nominal LC_{50} values, not dissolved or biologically available chemical concentrations, and may underestimate toxicity of FRs to *Daphnia magna*. The levels tested in this work are higher than those detected in the environment.[169] [170] However, the no-observed-effect-level has not yet been reached, so lower exposure concentrations at real-world exposure concentrations over the lifetime of the animal may cause detrimental effects.

Hydrophobic molecules such as these FRs could cause toxicity via narcosis, a nonspecific mechanism that results from disruption of lipid-based cellular membranes.[171], [172] Narcotic molecules should cause similar gene expression profiles.[173] Exposures done at sub-acute chemical concentrations elicited unique gene expression profiles and therefore appear to cause unique biological effects. Some chemicals caused more similar transcriptomic responses, as can be seen in the HOPACH clustering analysis (**Figure 3.4** and **3.5**). When analyzed with HOPACH Euclidian distances, which is based on gene correlation and magnitude of correlation,[85] OctaBDE, pentaBDE and TPP grouped together but all other FRs and the different FM550 concentrations were different (**Figure 3.4**). There is some similarity between the TBPH and BZ54 samples, but not enough to group as a centroid. When grouped only by gene correlations, three centroids were formed: 1) FM550n exposures, pentaBDE and octaBDE. 2) BZ54 and TBPH. 3) FM550μ exposures, TPP and BEPH. BZ54 is composed of TBB and TBPH, so this cluster is not surprising. The other clusters, however, do not have any clear patterns. All FM550 exposures were done with equal stock volume to media ratios, so clustering is not an artifact of exposure volume. PentaBDE and FM550n exposures have the smallest amount of molecules added, by mass, to each system; however octaBDE has the largest. The limited number of replicates for some of the FM550 exposures may contributes to this effect, as the use of different numbers of biological replicates can affect statistical significance of results by not having the power to identify candidate differentially expressed genes. While some of the FR chemicals may have similar modes of toxicity (TBPH and BZ54), or may have similar gene expression profiles when clustered with HOPACH, it is clear that not all of the FR chemicals tested in this study act in the same way.

This is also illustrated in Venn diagrams of gene expression. PentaBDE and octaBDE caused the differential expression of 18 genes in common out of 107 (octaBDE) or 292 (pentaBDE) genes total. This represents 17.3% and 6.2% of the octaBDE and pentaBDE expression profiles (**Figure 3.3A**), indicating little similarity in biological response (**Figure 3.4**). The in-common DEG may be useful as biomarkers of PBDE

exposure. DEHP and TBPH shared four genes in common, 2.6% of the DEHP and 0.08% of the TBPH profiles (**Figure 3.3C**). The different FM550 concentrations had similarities but did not cause the differential gene expression of any genes in common in all exposure concentrations (**Figure 3.3B**). These results indicate a concentration effect to toxicity. Future studies will employ additional microarray replicates as well as annotation from the transcriptome, and may find genes common to all exposure concentrations, which could then be used as biomarkers of exposure. No genes were differentially expressed in common between pentaBDE, TPP, TBPH, FM550 and BZ54 exposures (**Figure 3.3D**).

KEGG pathway analysis further illustrates differences in the daphnids response to different flame-retardant chemicals. At the 1/10 LC_{50}, pentaBDE affected steroid biosynthesis and pyrimidine metabolism biological pathways, FM550 affected peroxisome, ribosome and glycolysis pathways, and TBPH affected proteins involved in glycerphospholipid metabolism. This analysis is limited, as it is based on the *Daphnia magna* array, and therefore does not represent all *Daphnia* genes. It is further limited by the lack of functional annotation of *Daphnia* genes. Further work to investigate toxic mechanisms of these flame-retardant chemicals is to group gene expression data with a gene ontology computation program that looks at classes of proteins affected, instead of biological pathways.

FM550 elicited different effects at different exposure concentrations. This shows a concentration-dependent effect to toxicity that is ignored in the 1/10 LC_{50} analysis discussed above. **Table 3.7** shows KEGG pathway analysis of all different FM550 concentrations. A trend that stands out is the effects of FM550 on biological pathways involved in RNA transcription and translation to protein. Splicesome, RNA polymerase, ribosome and JAK-STAT signaling pathways are all affected by at least one FM550 concentration. Splicesome, RNA polymerase and ribosome involvement in transcription and translation are well characterized. The signal transducer and activator of transcription (STAT) protein is a signaling-protein family that regulates transcription. It is conserved in eukaryotic organisms including slime molds, worms, flies, and vertebrates [174] and it has a putative immune defense mechanism in the giant tiger prawn crustacean (*Penaeus monodon*).[175] STAT works in tandem with Janus kinase (JAK), a protein that binds to the intracellular domains of cytokine signaling receptors and catalyzes phosphorylation as part of a signal transduction that targets gene promoters and changes transcriptional activity of target genes.[174] None of these pathways are associated with exposure to phthalates or brominated compounds. The flame-retardant mixture may affect this pathway specifically, such as through receptor-mediated binding, or it may affect other systems that then affect this pathway.

Metabolomics data further indicate different responses in daphnids exposed to different chemicals. PentaBDE had little difference from control in detected metabolites (sugars, amino acids, etc), whereas FM550 elicited numerous differences from control. It will take further analysis to determine the fold-change from control of each metabolite, and to compare data to gene expression data. It is possible that pentaBDE works via a slower acting mode of action than FM550, or that the 1/10 LC50 elicits a more general stress response. It would be interesting to repeat the transcriptomic and metabolimic data

with different concentrations of pentaBDE, or at different time courses, to see how the pentaBDE-exposed *Daphnia* metabolome changes. Although the concentration of chemicals is very different (FM550 = 48.6 μg/L, pentaBDE is 5.8 μg/L), the level of toxicity of the chemicals is similar (1/10 LC_{50}). These exposure conditions were done with equal-volumes of chemical stock solution or DMSO in each exposure replicate, so effects are from the added flame-retardants and are not a product of experimental design. Further work is needed to determine fold-change of exposed compared to control for each metabolite.

Lipidomic data detected differences in daphnids exposed to FM550 and to pentaBDE as compared to control. Lipids are important in many biological processes, and investigation of the disruption of lipid function could help determine modes of toxicity. The lipidomic data to date is anonymous – four lipids were increased in each exposure, with one lipid on common: PC(42:7), a phosphatidylcholine phospholipid with a total of 42 carbons and seven double bonds in the two fatty acid tails. Further analytical investigations are needed to determine exactly what these lipids are and to assign biological function.

Because the FM550 predecessor pentaBDE is found ubiquitously in the environment, accumulates in biological tissues and moves up food chains,[33] and because FM550 components have been found in marine mammals[40] and accumulate in fathead minnows,[56] the potential for FM550 to accumulation in *Daphnia magna* was investigated. After 48 hours, FM550 did accumulate, but at a higher concentration (48.6 μg/L) is than is biologically relevant. The lower concentration tested, 48.6 ng/L, did not accumulate after 48 hours. However, differential gene expression occurred at this dose, which is closer to levels collected from sewage treatment plant solids.[170] Whether FM550 has the potential to accumulate in *Daphnia magna* at environmentally relevant concentrations is unknown. If it does accumulate, it might have potential for trophic transfer in freshwater food webs.

TABLES

Gene ID	Forward	Reverse	Notes
DM00871	GATTGTGGCAACTGGTGTCTG	TCCACCACCTTCATGACCAAG	low fold change
DM00174	GCACGGAAGCAACCAAAGTT	GCCACTCCAGTAACGGTTGA	low fold change
DM00594	ATTACGAGTCAACGGCTCCC	TGATACGTTGCGGAGTCAGG	higher fold
DM00141	ATTTTTCGCCATCGTCCAGC	GTGTGGCTTCCCAAGTCAGT	less significant q-value
DM14209	GAGGAAGAATGGGGAAGAAGTGA	TCTAACCGCACTTACGCCAT	less significant q-value
DM06382	TTCAACTCCGTGACGCACAT	CCTTGGTTGAGGGAAACCCA	highly significant q-value
DM07860	AATAATTACCGTCCGGCGCA	CAGTTCGCACCCATGAAAGC	highly significant q-value
DM00376	CGTTCGGGCAAAATGTGTCA	TCCATCCGAAGTGGAGGGAT	mode of toxicity TBPH
DM03384	ACATAGCCGGCGTTTCAGTT	CGCCACAAAGCCCATAACAG	mode of toxicity TBPH
DM05899	TTGCTCCAGCTCCCGTTATC	GAAACCTGGAACACCGCTGA	mode of toxicity pentaBDE
DM11506	CAATTGCCGTGGTTTCCGTC	GTCCGTCCCGATAAGCCAAT	mode of toxicity pentaBDE
DM00972	CGAATCGGGACCTATCGTCG	CGCCGTTTGAACCATTCCTC	Lowest FM550 affected
DM01631	AAGTCGTTGAGGGCATGGAG	GTCGACGATCTTAACGGGCT	only PBDE affected

Table 3.1. Primer sequences used for qPCR verification of microarray data. Gene ID is the identifier for a specific probe that was differentially expressed in *Daphnia manga* in response to flame-retardant exposure.

Chemical	LC_{50} (mg/L)	Statistical Method	95% confidence interval
FM550	0.486	Spearman-Karber	0.357-0.661
TBPH	0.91	Spearman-Karber	0.83-0.99
BZ54	0.5	Spearman-Karber	0.4 - 0.62
TPP	0.53	Spearman-Karber	0.48 - 0.58
PentaBDE	0.058	probit	0.0456 - 0.070
OctaBDE	3.96	probit	1.629-5.963
DEHP	3.311	probit	1.928-4.930

Table 3.2. Acute (48-hour) LC_{50} values of different chemical flame-retardant formulations and related chemicals on freshwater crustacean, *Daphnia magna*.

	FM550	octaBDE	pentaBDE	BZ54	TBPH	TPP	DEHP
Down	193	97	218	187	687	121	117
Up	452	10	74	228	499	44	36
Total	645	107	292	415	1187	165	153

Table 3.3. Numbers of genes differentially expressed in *Daphnia magna* after a 48-hour exposure to 1/10 LC_{50} of chemical flame-retardants.

Affected Biological Pathway	FM550	pentaBDE	TBPH
Steroid biosynthesis		0.04	
Pyrimidine metabolism		0.13	
Peroxisome	0.174		
Ribosome	1.3E-11		
Glycerophospholipid metabolism			0.17
Glycolysis / Gluconeogenesis	0.174		

Table 3.4. KEGG pathway analysis of microarray gene expression results shows FM550, pentaBDE and TBPH affected different biological pathways in *Daphnia magna*. Numbers in this graph represent the p-value of each analysis. P-values of 0.1 or less are considered significant. Values of 0.2 or less are included as potentially significant.

	141	actin	dct	2^-(dct)	average	
BZ54 con	28.77	22.52	6.25	0.013139006	0.01458683	
BZ54 con	28.52	22.08	6.44	0.011517728		
BZ54 con	27.82	22.11	5.71	0.019103754	Fold Change	p-value
BZ54	28.95	22.56	6.39	0.0119239	0.817442863	0.227009605
BZ54	28.95	22.44	6.51	0.010972226	0.752200827	
BZ54	27.97	21.45	6.52	0.010896435	0.747004997	
	6382	actin	dct		average	
TPP con	27.65	19.92	7.73	0.004710187	0.004607051	
TPP con	28.17	21.12	7.05	0.007546378		
TPP con	29.7	20.38	9.32	0.00156459	Fold Change	p-value
TPP	29.09	20.22	8.87	0.002137292	0.463917674	0.270446334
TPP	31.57	22.28	9.29	0.001597465	0.346743493	
TPP	29.63	21.35	8.28	0.003217152	0.69831057	
	375	actin			average	
TBPH con	27.64	20.26	7.38	0.006003419	0.00593582	
TBPH con	30.57	23.2	7.37	0.006045176		
TBPH con	29.35	21.91	7.44	0.005758864	Fold Change	p-value
TBPH	31.28	23.49	7.79	0.004518313	0.761194446	0.203389543
TBPH	27.86	20.47	7.39	0.00596195	1.004402094	
TBPH	29.99	20.96	9.03	0.00191293	0.322268915	
	1631	GAPDH	dct	2^-(dct)	average	
octa con	23.9	30.79	-6.89	118.6032719	40.06648328	
octa con	24.04	24.22	-0.18	1.132883885		
octa con	23.51	22.4	1.11	0.463294031	Fold Change	p-value
octa	23.51	24.64	-1.13	2.188587403	0.054623896	0.505275806
octa	22.31	22.82	-0.51	1.424050196	0.035542181	
	1631	GAPDH	dct	2^-(dct)	average	
penta con	21.63	25.04	-3.41	10.62948651	4.977739154	
penta con	22.07	23.34	-1.27	2.411615655		
penta con	22.51	23.43	-0.92	1.892115293	Fold Change	p-value
penta	22.13	23.79	-1.66	3.160165247	0.634859552	0.565024294
penta	22.44	24.1	-1.66	3.160165247	0.634859552	
penta	22.47	24.19	-1.72	3.294364069	0.661819346	
	871	GAPDH	dct	2^-(dct)	average	
BEPH con	27.53	24.54	2.99	0.125869444	0.120017243	
BEPH con	26.42	23.55	2.87	0.136786713		
BEPH con	26.14	22.78	3.36	0.097395572	Fold Change	p-value
BEPH	26.27	23.42	2.85	0.138696184	1.155635478	0.556365813
BEPH	27.81	24.33	3.48	0.089622203	0.746744391	
BEPH	26.13	22.72	3.41	0.094077922	0.783870045	
	11506	GAPDH	dct	2^-(dct)	average	
penta con	26.37	25.04	1.33	0.397768242	0.177211187	
penta con	27.41	23.34	4.07	0.059539875		
penta con	27.18	23.43	3.75	0.074325445	Fold Change	p-value
penta	26.45	23.79	2.66	0.158219574	0.892830622	0.648557969
penta	27.29	24.1	3.19	0.109575715	0.618334074	
penta	27.53	24.19	3.34	0.098755164	0.55727387	
	5899	GAPDH	dct	2^-(dct)	average	
penta con	26	25.04	0.96	0.514056913	0.255315667	
penta con	26.28	23.34	2.94	0.13030822		
penta con	26.47	23.43	3.04	0.121581868	Fold Change	p-value
penta	26.12	23.79	2.33	0.198884121	0.77897343	0.67848558
penta	26.34	24.1	2.24	0.211686328	0.829116092	
penta	26.65	24.19	2.46	0.181746565	0.71185042	

	174	GAPDH	dct	2^-(dct)	average	
BEPH con	27.18	24.54	2.64	0.160428237	0.143403739	
BEPH con	26.22	23.55	2.67	0.157126672		
BEPH con	25.93	22.78	3.15	0.112656308	Fold Change	p-value
BEPH	26.1	23.42	2.68	0.156041319	1.088125872	0.258093698
BEPH	27.84	24.33	3.51	0.087777805	0.612102623	
BEPH	27.31	22.72	4.59	0.041521432	0.289542183	

Table 3.5. Quantitative polymerase chain reaction (qPCR) results on genes of interest, confirming microarray data are consistent with microarray results. Three samples in red are the only samples out of 53 reactions that did not agree with array data.

FM550.48.6nano	FM550.243nano	FM550.48.6micro	FM550.243micro
1079	522	645	111

Table 3.6. Exposure of chemical flame-retardant Firemaster®550 (FM550) caused differential gene expression as compared to control in all concentrations tested (243 and 48.6 micro-grams and nano-grams per liter). The lowest concentration, 48.6 ng/L, caused the most differentially expressed genes.

Affected Biological Pathway	FM550.nano	FM550.243nano	FM550.micro
Oxidative phosphorylation		0.175	
Purine metabolism	0.063		
Wnt signaling pathway	0.174		
Spliceosome		0.186	
RNA polymerase		0.049	
Peroxisome			0.174
Lysosome		0.077	
Ribosome	0.004	0.122	1.3E-11
Endocytosis	0.129		
Jak-STAT signaling pathway		0.067	
Glycolysis / Gluconeogenesis			0.174
Proteasome	0.076		

Table 3.7. KEGG pathways analysis of gene expression data from *Daphnia magna* exposed to different concentrations of FM550 (48.6 micro-grams or nano-grams per liter) resulted in similar and different biological effects. Differences allude to a concentration effect. P-values of 0.1 or less are considered significant. Because annotation of the *Daphnia magna* microarray and transcriptome is limited, values of 0.2 or less are included as potentially significant.

Lipid	Fold Change	St. Dev	p-value
LPC(20:0)	5.4762	0.0003	0.0256
PC(42:9)	1.9309	0.0004	0.0181
PC(42:7)	21.9091	0.0003	0.0019
PC(44:12)	2.7770	0.0004	0.0139
PC(44:12)	14.2727	0.0002	0.0064
PC(44:9)	2.1789	0.0002	0.0366
PI(42:3)	2.3846	0.0001	0.0483
ePS(40:4)	0.1852	0.0001	0.0034

Table 3.8. Fold-change difference from control in abundance of lipids measured with mass spectrometry. Orange cells represent 1/10 LC_{50} FM550 exposure; blue cells represent 1/10 LC_{50} pentaBDE exposures. P-values determined with t-test in Excel.

FIGURES

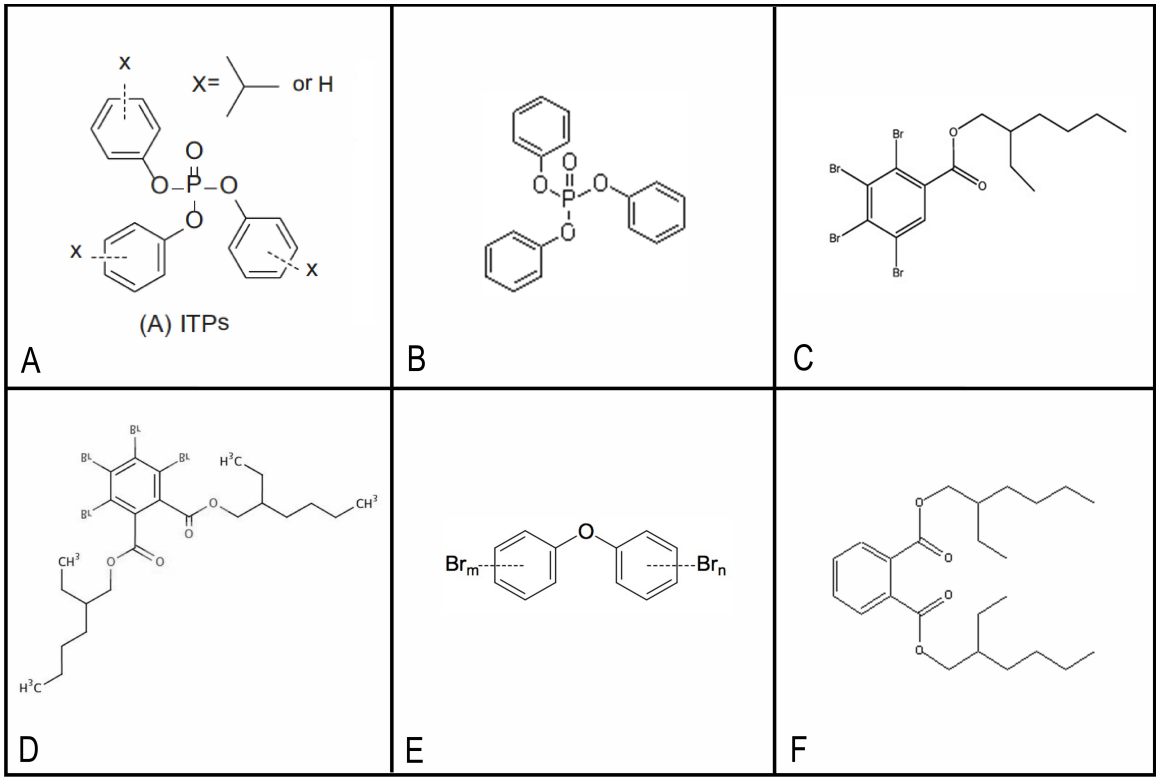

Figure 3.1. Molecular structures of flame-retardant chemicals under study. A. Isopropylated triaryl phosphate. B. Triphenyl phosphate. C. Tetrabromo benzoate. D. Tetrabromo phthalate. E. Polybrominated diphenyl ether. F. Di(2-ethylhexyl) phthalate (DEHP). A-D are components of Firemaster®550. C and D are components of Firemaster® BZ-54.

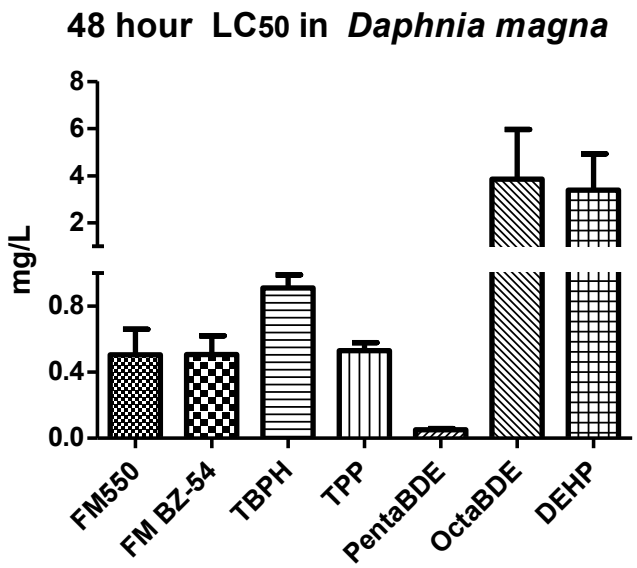

Figure 3.2. Acute, 48-hour LC_{50} values for chemical flame-retardants on *Daphnia magna*.

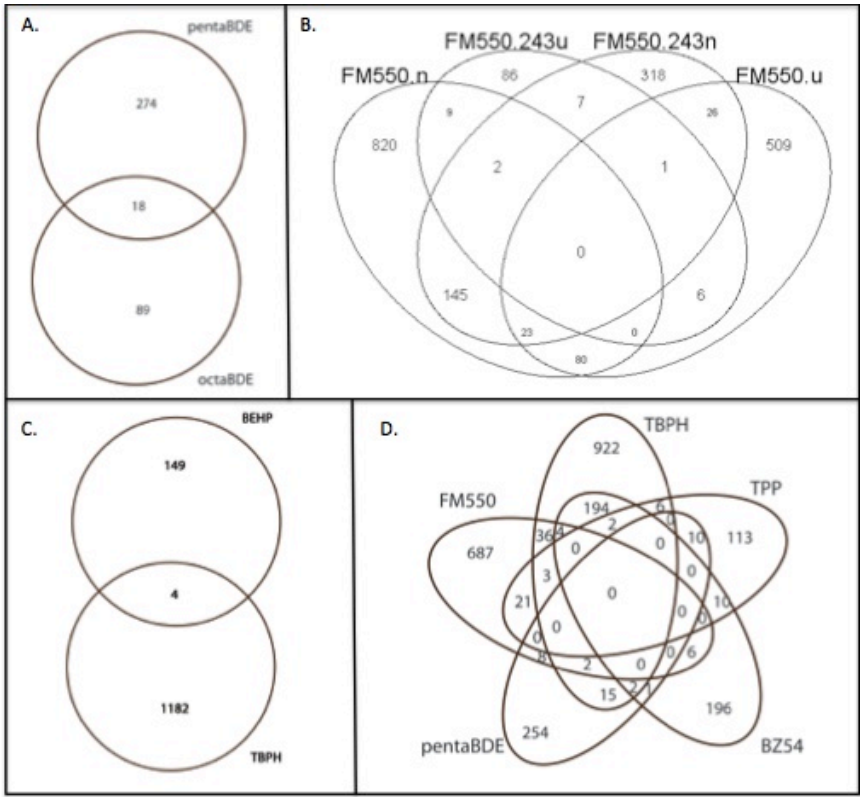

Figure 3.3. Venn diagrams show the similarities and differences between different exposure conditions. Numerical values represent the number of differentially expressed genes (up- and down-regulated) in single or multiple conditions. A. PBDEs. B. Different FM550 concentrations. C. DEHP and TBPH. D. Numerous chemicals.

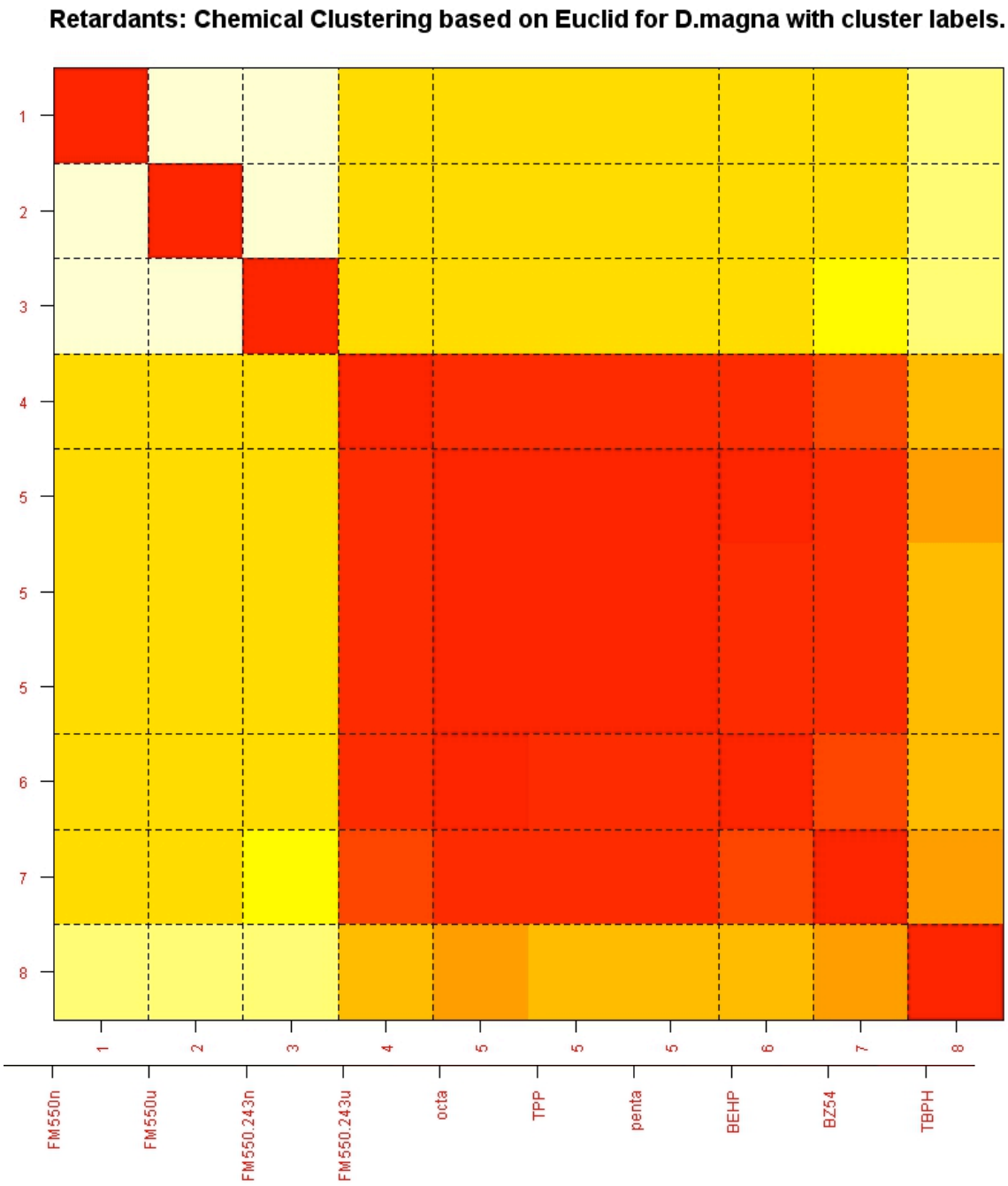

Figure 3.4. HOPACH clustering of gene expression data shows similarity between different gene expression profiles by color coordination and by physical distance. Red is more similar than yellow. The Euclidian distance analysis is based on gene correlation and magnitude of correlation. The labels at the bottom identify which chemical is in which group. OctaBDE, pentaBDE and TPP grouped together. There is some similarity between the TBPH and BZ54 samples, but not enough to group as a centroid.

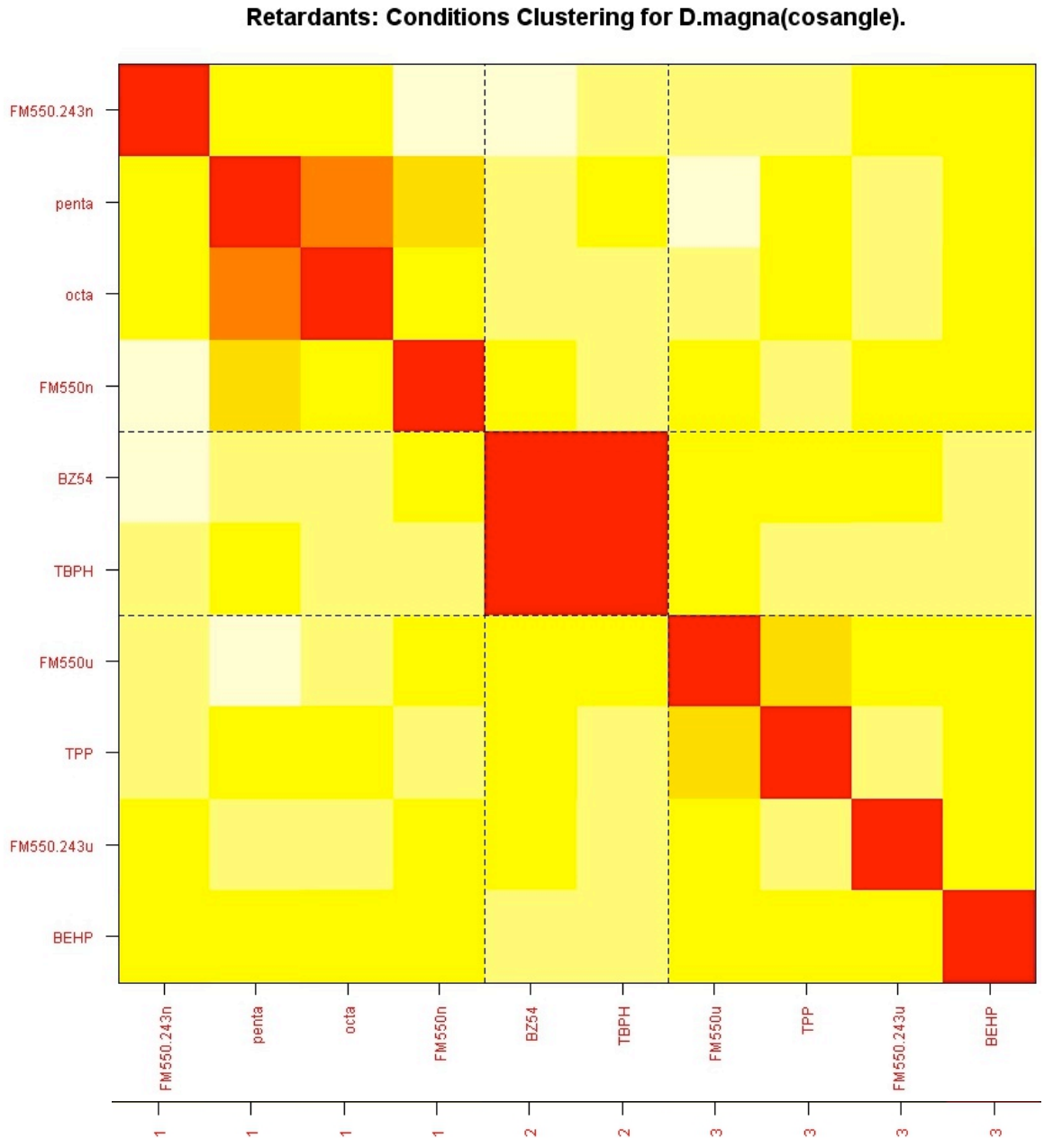

Figure 3.5. When grouped using cosangle metrics, the gene expression data falls into three centroids based on correlation of gene expression only. 1) FM550 243ng/L, FM550 48.6ng/L, pentaBDE and octaBDe. 2) TBPH and BZ54. 3) FM550 48.6 µg/L, FM550 243 µg/L, TPP and BEPH. Within these groups, there is little similarity, however, except between the PBDEs and between TBPH and BZ54.

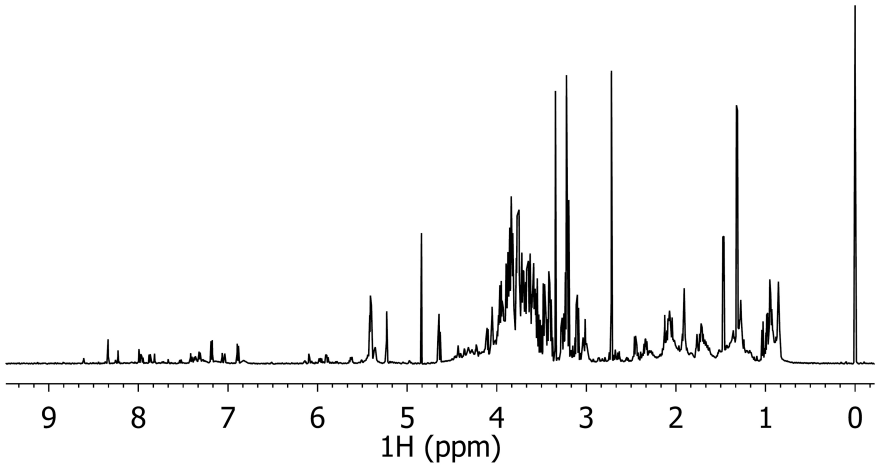

Figure 3.6. A representative ^{1}H one-dimensional NOESY NMR spectrum of daphnia polar extracts. The chemical shifts were referenced to DSS at 0.0 ppm. The half-height linewidth of DSS is less than 1.2 Hz. The insert is the spectral region with 10 times of Y scale.

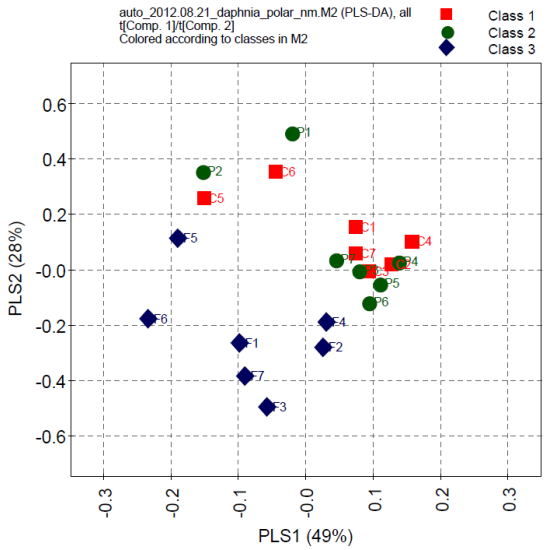

Figure 3.7. Scores plots of PLS-DA models of treated (1/10 LC_{50} FM550 or 1/10 LC_{50} pentaBDE) and control daphnia extracts. PLS-DA model for all classes (red squares: controls, green circles: pentaBDE, and blue diamonds: FM550) shows separation between FM550-treated and control groups, but no difference between pentaBDE-treated and controls.

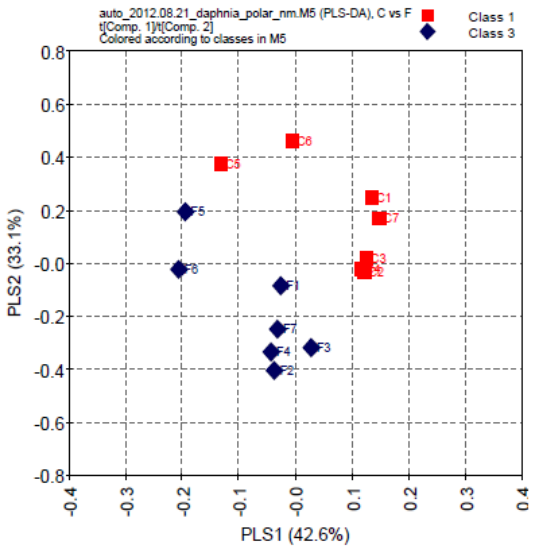

Figure 3.8. Validated PLS-DA model for FM550-treated (blue diamonds) and controls (red squares). The class separation is on both components (PLS1 and PLS2).

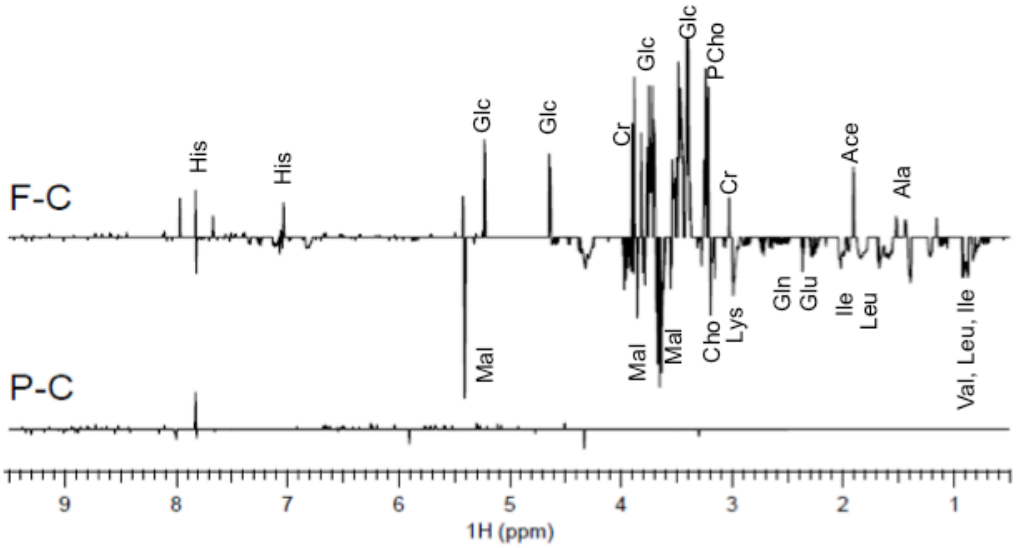

Figure 3.9. T-test filtered difference spectra generated from untreated and control groups. The peaks with positive intensity correspond to metabolites that increase (with statistical significance) upon treatment, whereas negative peaks represent metabolites that decreased. Identified metabolites are labeled on the t-test difference spectra. A p-value of 0.05 was used for the t-test filter.

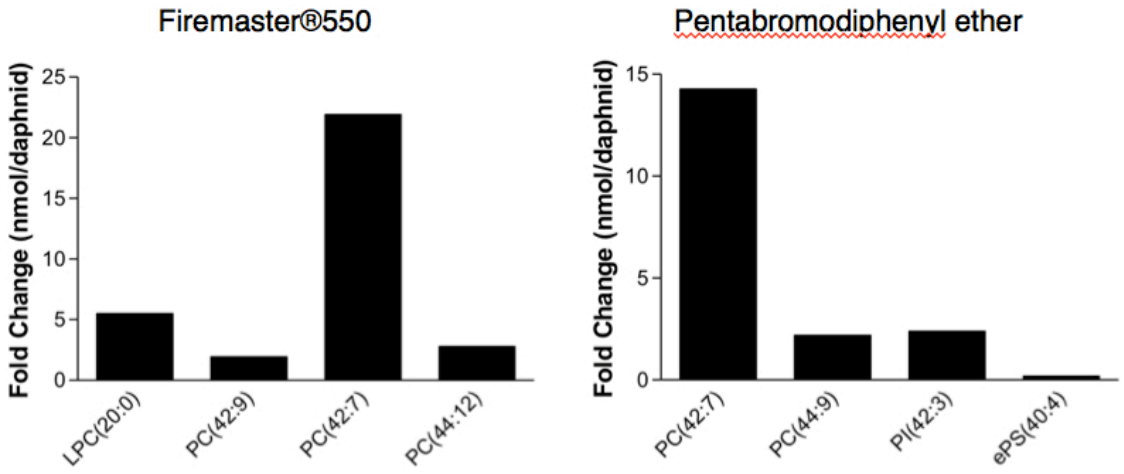

Figure 3.10. Lipidomics fold change on lipids with changed abundance in exposed conditions as compared to control. T-test with p-value <0.05 was used as the significance cut-off.

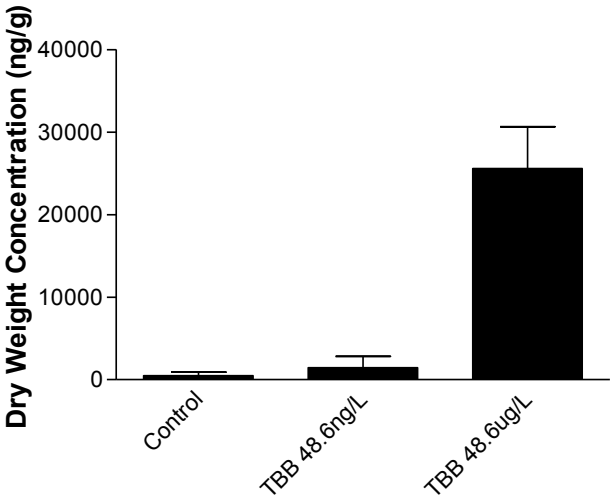

Figure 3.11. Tetrabromobenzoate (TBB) is one component in FM550. This figures shows accumulation of TBB after a 48-hour exposure to 1/10 LC_{50} 48.6 µg/L or 48.6 ng/L in *Daphnia*. The plots represent an average of five biological replicates of ~400 animals each. The 48.6 µg/L exposure is statistically significant from control, as determined by student's t-test, p-value = 0.0026.

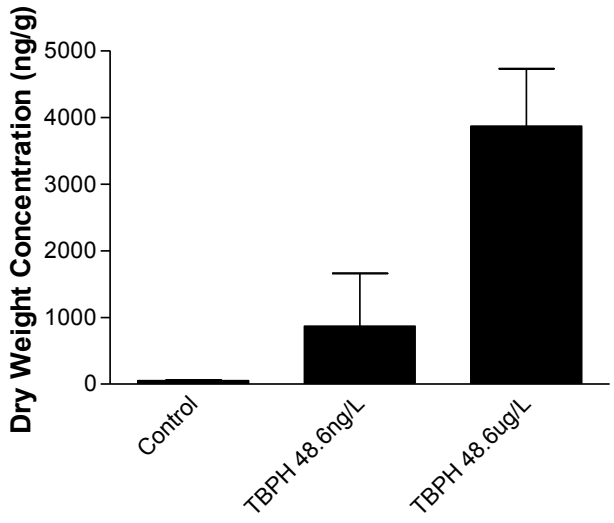

Figure 3.12. Tetrabromophthalate (TBPH) is one component in FM550. This figures shows accumulation of TBPH after a 48-hour exposure to 1/10 LC_{50} 48.6 µg/L or 48.6 ng/L in *Daphnia*. The plots represent an average of five biological replicates of ~400 animals each. The 48.6 µg/L exposure is statistically significant from control, as determined by student's t-test, p-value = 0.0043.

CONCLUSIONS

This work contributes to scientific knowledge on the effects of the emerging environmental contaminants silver nanowires and chemical flame-retardants. This was done through the establishment of LC_{50} values, the generation of gene expression profiles and the use of other toxicological assays. Acute toxicity testing to establish the lethal concentration that kills fifty percent of organisms tested (LC_{50}) is commonly used as a parameter to compare effects of different chemical exposures to the same species, or to compare effects of the same chemical on different species. Current literature on emerging contaminants such as silver nanowires or flame-retardant Firemaster®550 lack acute toxicity data. This work therefore fills a gap in the sphere of knowledge about these contaminants. Current analytical methods for detection of environmental contaminants require *a priori* knowledge for chemical detection. Gene expression profiles and subsequent biomarker of exposure discovery can aid in the detection of contaminant without analytical techniques. The biomarker of exposure process is used in biological studies from environmental toxicology to pharmacology and exposure assessment.[78], [176], [177]

It is important to note that the LC_{50} values established in this work for chemical flame-retardants are nominal values – they likely underestimate the toxicity of the flame-retardants. These chemicals are hydrophobic and may stick to the exposure vessels. Even with the use of a solvent (DMSO), the chemicals still have limited solubility in aqueous environments. Therefore, a smaller fraction of chemical is available to the *Daphnia* than was added to the system. It is also important to note that molecular effects occurred after exposure to lower doses of FM550, in the ng/L range, which is a more ecologically relevant concentration. The no-observed-transcriptional-effect level, or low concentration at which no transcriptional effect is seen in the organism, was not reached.

This is the first study to show that dissolved ionic silver in aqueous solution is not the dominating factor in toxicity of silver nanowires. An ongoing debate exists in this field about whether toxicity from silver nanoparticles is caused by ionic silver release or by the particle itself.[178], [179] The use of genomics in this study illuminated the separate effects of particle (wire) and silver. This can be seen in HOPACH clustering **Figures 17** and **18** in **Chapter 1**. No other group has studied the toxicity of silver nanowires, established LC_{50} values or looked at gene expression profiles in any model system caused by exposure to nanowires. Additionally, this work is the first to show the likely uptake of silver nanowires into the *Daphnia* (**Figure 10**), either through the gut lumen or gills. The use of spICP-MS for detection of particles *in vivo* to analyze internal concentration and changes in particle size over time may revolutionize the field of metal nanoparticle toxicity. It will likely have impacts on the development of environmental monitoring techniques for nanoparticles, which do not yet exist.

The gene expression data is limited, however, by the constraints of the *Daphnia magna* microarray. This array consists of 15,000 unique expressed sequence tags – cDNAs made from RNAs isolated from *Daphnia*. It is by no means a comprehensive list

of the animal's genome. The array contains enough genomic information to do gene ontology KEGG pathway analysis and HOPACH clustering, which were informative methods of data analysis. However, because the *Daphnia magna* genome is not available, there is no way to know what exactly is missing from the array or how complete it is. The *Daphnia magna* transcriptome construction therefore contributes significantly to genomic tool box for *Daphnia magna*. It is now possible to generate a microarray with many more sequences than were previously known. It is also possible to look at chemical effects on alternately spliced genes. This work aimed to use short-read sequencing data to analyze differential gene expression and then compare results to microarray results. here is not yet a clear consensus on what the best methods are for analysis. Further verification of results is underway.

Chemical flame-retardant LC_{50} values generated in this work were similar to those that exist in literature for PBDEs and TPP.[168], [154] This is, however, the first study to explore the effects of emerging flame-retardant contaminant FM550 on freshwater crustacean *Daphnia magna*. It is also the first study that looks at FM550, it's predecessor pentaBDE and five other related flame-retardant mixtures and compounds. It represents a broad study of great importance in California and the world: Chemical flame-retardants are used at astonishingly high rates in consumer products. It has been shown that chemical flame-retardants do not prevent injury or death from fire,[180] but they do accumulate and cause toxicity.[153], [56], [141] Toxicity of FRs to *Daphnia magna* varied greatly, and both KEGG pathway analysis and HOPACH cluster analysis indicated different biological effects for the majority of the compounds tested. All compounds were highly toxic to *Daphnia* except for octaBDE and DEHP. Gene expression data identified potential biomarkers of exposure for PBDEs, and lipidomic and metabolomics data indicate FM550 caused different effects than pentaBDE.

This is the first study to show accumulation of FM550 in a lower-trophic organism. The study was short-term, and results with the lower concentration exposure were not significant. It is possible that accumulation could occur in a long-term, chronic exposure at a lower concentration. It is also possible that the FM550 components could get transferred up the food chain, as happens with PBDEs.[42] The brominated compounds in this mixture are already detected in numerous higher-level species including humans, who are exposed in their homes,[181] and animals, who are exposed through environmental contamination.[40]

The use of transcriptomic techniques is both a starting place for and an informative method in modern toxicological studies. The assays are not yet used alone as they alone do not result in definitive answers about modes of toxicity. However, they do illuminate possible molecular reactions in response to toxicity and they can be used to determine biomarkers of exposure,[176], [126] especially in better-characterized systems or in combination with other omics techniques.[173] Other molecular techniques for *Daphnia magna* are only now being developed: a technique for RNAi exists,[182] but there are no stable cell lines, which greatly limits molecular techniques for determining specific modes of toxicity. The difficulty of understanding mechanisms on *Daphnia* is further exacerbated by lack of characterization of the *Daphnia magna* genome and

proteins – although 75% of transcripts in the *Daphnia magna* transcriptome BLAST to the *Daphnia pulex* genome, the gene and protein function of many of those proteins is unknown. *Daphnia* biology will become better characterized over time, as with models such as yeast and mice. Transcriptomic and other molecular omics techniques will evolve over time, too, and will enable scientists to watch a system change in real-time, with thousands of endpoints measured at once.

This work outlines the beginning of understanding about toxicity of silver nanowires and chemical flame-retardants on *Daphnia magna*. It is the basis of continuing investigations into absorption of nanowires into *Daphnia* and human, rat and fish cell culture. It also inspired new *Daphnia magna* microarray design and work on the effects of TPP and other organophosphate related flame-retardants in the mouse brain. While further studies will be necessary to elucidate the specific molecular phenomena behind toxicity, and to investigate effects are ecologically relevant concentrations, this work has significant findings on the effects of silver nanowires and on chemical flame-retardants to freshwater crustacean *Daphnia magna*.

REFERENCES

1. Wilson, M.P., D.A. Chia, and B.C. Ehlers, *Green Chemistry in California: A Framework for Leadership in Chemicals Policy and Innovation*, 2006, California Policy Research Center: Berkeley, CA.
2. Massachusetts Department of Environmental Protection, *Emerging Contaminants Fact Sheet & Overview*: Boston, Masachusetts.
3. United States Geological Survey, *Emerging Contaminants In the Environment*, 2012.
4. Gewurtz, S.B., et al., *Contaminant biomonitoring programs in the Great Lakes region: Review of approaches and critical factors.* Environmental Reviews, 2011. **19**: p. 162-184.
5. Poynton, H.C., et al., *Gene expression profiling in Daphnia magna part I: concentration-dependent profiles provide support for the No Observed Transcriptional Effect Level.* Environmental science & technology, 2008. **42**(16): p. 6250-6256.
6. Snape, J.R., et al., *Ecotoxicogenomics: the challenge of integrating genomics into aquatic and terrestrial ecotoxicology.* Aquatic Toxicology (Amsterdam, Netherlands), 2004. **67**(2): p. 143-154.
7. Nuwaysir, E.F., et al., *Microarrays and toxicology: the advent of toxicogenomics.* Mol Carcinog, 1999. **24**(3): p. 153-9.
8. Poynton, H.C., et al., *Daphnia magna ecotoxicogenomics provides mechanistic insights into metal toxicity.* Environmental science & technology, 2007. **41**(3): p. 1044-1050.
9. Fielden, M.R. and T.R. Zacharewski, *Challenges and limitations of gene expression profiling in mechanistic and predictive toxicology.* Toxicol Sci, 2001. **60**(1): p. 6-10.
10. Garcia-Reyero, N., et al., *Gene expression responses in male fathead minnows exposed to binary mixtures of an estrogen and antiestrogen.* BMC genomics, 2009. **10**: p. 308.
11. Miracle, A.L. and G.T. Ankley, *Ecotoxicogenomics: linkages between exposure and effects in assessing risks of aquatic contaminants to fish.* Reprod Toxicol, 2005. **19**(3): p. 321-6.
12. Bartlett, J.M. and D. Stirling, *A short history of the polymerase chain reaction.* Methods Mol Biol, 2003. **226**: p. 3-6.
13. Velculescu, V.E., et al., *Serial analysis of gene expression.* Science (New York, N.Y.), 1995. **270**(5235): p. 484-487.
14. Solexa, I., ,, *Protocol for Whole Genome Sequencing using Solexa Technology.* BioTechniques® Protocol Guide 2007, 2006(Journal Article): p. 29.
15. Mortazavi, A., et al., *Mapping and quantifying mammalian transcriptomes by RNA-Seq.* Nature methods, 2008(Journal Article).
16. Wintz, H., et al., *Gene expression profiles in fathead minnow exposed to 2,4-DNT: correlation with toxicity in mammals.* Toxicological sciences : an official journal of the Society of Toxicology, 2006. **94**(1): p. 71-82.
17. Ludwig, S., et al., *Potential new targets involved in 1,3-dinitrobenzene induced testicular toxicity.* Toxicology letters, 2012. **213**(2): p. 275-284.

18. Poynton, H.C., et al., *Metabolomics of microliter hemolymph samples enables an improved understanding of the combined metabolic and transcriptional responses of Daphnia magna to cadmium.* Environmental science & technology, 2011. **45**(8): p. 3710-3717.
19. Seda, J., A. Petrusek, and F. Sehnal, *Daphnia as a model organism in limnology and aquatic biology: some aspects of its reproduction and development PREFACE.* Journal of Limnology, 2011. **70**(2): p. 336-336.
20. Watanabe, H., et al., *Transcriptome profiling in crustaceans as a tool for ecotoxicogenomics: Daphnia magna DNA microarray.* Cell Biol Toxicol, 2008. **24**(6): p. 641-7.
21. Harris, K.D., N.J. Bartlett, and V.K. Lloyd, *Daphnia as an emerging epigenetic model organism.* Genet Res Int, 2012. **2012**: p. 147892.
22. Blaser, S.A., et al., *Estimation of cumulative aquatic exposure and risk due to silver: contribution of nano-functionalized plastics and textiles.* The Science of the total environment, 2008. **390**(2-3): p. 396-409.
23. The Project on Emerging Nanotechnologies. *Consumer Products Inventory*. 2012 [cited 2012 January 12]; Available from: http://www.nanotechproject.org/inventories/consumer/.
24. Lieber, C.M. and Z.L. Wang, *Functional Nanowires.* Mrs Bulletin, 2007. **32**(2): p. 99-108.
25. Kelly, K.L., Coronado, E., Zhao, L.L., Schatz, G.C., *The Optical Properties of Metal Nanoparticles: The Influence of Size, Shape and Dielectric Environment.* J. Phys. Chem B, 2003. **107**(3): p. 668-677.
26. Hu, J., et al., *Fringing field effects on electrical resistivity of semiconductor nanowire-metal contacts.* Applied Physics Letters, 2008. **92**(8).
27. Law, M., et al., *Nanowire dye-sensitized solar cells.* Nature materials, 2005. **4**(6): p. 455-459.
28. Agency, U.S.E.P., *Nanotechnology White Paper*. Vol. EPA100/B-07/001. 2007, Washington, D.C.: U.S. EPA.
29. Maynard, A.D., et al., *Safe Handling of Nanotechnology.* Nature, 2006. **444**(Journal Article): p. 267-269.
30. Kim, B., et al., *Discovery and characterization of silver sulfide nanoparticles in final sewage sludge products.* Environmental science & technology, 2010. **44**(19): p. 7509-7514.
31. Philbrick, M. and M. Taylor. *The Curiously Understudied Toxicity of "Nanofibers": A Risk-Benefit Approach*. in *Society for Risk Analysis*. 2011. Charleston, S.C.
32. California Department of Consumer Affairs, *EXEMPTION OF JUVENILE PRODUCTS FROM REQUIREMENTS OF TECHNICAL BULLETIN 117. INITIAL STATEMENT OF REASONS*, Bureau of Electronic and Appliance Repair, Home Furnishings and and Thermal Insulation, Editors. 2012.
33. Stockholm Convention, *Decision POPRC-1/3: Pentabromodiphenyl ether*, Stockholm Convention on persistent organic pollutants (POPs), Editor 2011.
34. The European Parliment, *Directive 2002/95/EC of the European Parliment and of the Council of 27 January 2003 on the restriction of the use of certain hazardous substances in electrical and electrical equipment*, 2003.

35. Kimbrough, K.L., et al., *An Assessment of Polybrominated Diphenyl Ethers (PBDEs) in Sediments and Bivalves of the U.S. Costal Zone*, N.T. Memorandum, Editor 2009: Silver Spring, MD. p. 87.
36. Gao, S., et al., *Polybrominated diphenyl ethers in surface soils from e-waste recycling areas and industrial areas in South China: Concentration levels, congener profile, and inventory.* Environmental toxicology and chemistry / SETAC, 2011(Journal Article).
37. Daso, A.P., et al., *Occurrence of Selected Polybrominated Diphenyl Ethers and 2,2',4,4',5,5'-Hexabromobiphenyl (BB-153) in Sewage Sludge and Effluent Samples of a Wastewater-Treatment Plant in Cape Town, South Africa.* Archives of Environmental Contamination and Toxicology, 2011(Journal Article).
38. Alava, J.J., et al., *Geographical variation of persistent organic pollutants in eggs of threatened loggerhead sea turtles (Caretta caretta) from southeastern United States.* Environmental toxicology and chemistry / SETAC, 2011. **30**(7): p. 1677-1688.
39. Mora, M.A., et al., *PBDEs, PCBs, and DDE in eggs and their impacts on aplomado falcons (Falco femoralis) from Chihuahua and Veracruz, Mexico.* Environmental pollution (Barking, Essex : 1987), 2011. **159**(12): p. 3433-3438.
40. Lam, J.C., et al., *Temporal trends of hexabromocyclododecanes (HBCDs) and polyrominated diphenyl ethers (PBDEs) and detection of two novel flame retardants in marine mammals from Hong Kong, South China.* Environmental science & technology, 2009. **43**(18): p. 6944-6949.
41. Kuo, Y.M., et al., *Bioaccumulation and biomagnification of polybrominated diphenyl ethers in a food web of Lake Michigan.* Ecotoxicology (London, England), 2010. **19**(4): p. 623-634.
42. Liu, P.Y., et al., *Bioaccumulation, maternal transfer and elimination of polybrominated diphenyl ethers in wild frogs.* Chemosphere, 2011. **84**(7): p. 972-978.
43. Chao, H.R., et al., *Levels of polybrominated diphenyl ethers (PBDEs) in breast milk from central Taiwan and their relation to infant birth outcome and maternal menstruation effects.* Environment international, 2007. **33**(2): p. 239-245.
44. Koh, T.W., et al., *Breast-milk levels of polybrominated diphenyl ether flame retardants in relation to women's age and pre-pregnant body mass index.* International journal of hygiene and environmental health, 2009(Journal Article).
45. Main, K.M., et al., *Flame retardants in placenta and breast milk and cryptorchidism in newborn boys.* Environmental health perspectives, 2007. **115**(10): p. 1519-1526.
46. Meironyte, D., K. Noren, and A. Bergman, *Analysis of polybrominated diphenyl ethers in Swedish human milk. A time-related trend study, 1972-1997.* Journal of toxicology and environmental health.Part A, 1999. **58**(6): p. 329-341.
47. Allen, J.G., et al., *Linking PBDEs in house dust to consumer products using X-ray fluorescence.* Environmental science & technology, 2008. **42**(11): p. 4222-4228.
48. Birgul, A., et al., *Atmospheric polybrominated diphenyl ethers (PBDEs) in the United Kingdom.* Environmental Pollution, 2012. **169**: p. 105-111.

49. de Wit, C.A., D. Herzke, and K. Vorkamp, *Brominated flame retardants in the Arctic environment - trends and new candidates.* The Science of the total environment, 2009(Journal Article).
50. Huwe, J.K. and M. West, *Polybrominated diphenyl ethers in U.S. Meat and poultry from two statistically designed surveys showing trends and levels from 2002 to 2008.* Journal of Agricultural and Food Chemistry, 2011. **59**(10): p. 5428-5434.
51. Chemtura USA Corporation, *MATERIAL SAFETY DATA SHEET: Firemaster® 550*, 2006.
52. Stapleton, H.M., et al., *Alternate and new brominated flame retardants detected in U.S. house dust.* Environmental science & technology, 2008. **42**(18): p. 6910-6916.
53. Stapleton, H.M., et al., *Detection of Organophosphate Flame Retardants in Furniture Foam and US House Dust.* Environmental science & technology, 2009. **43**(19): p. 7490-7495.
54. Verslycke, T.A., et al., *Flame retardants, surfactants and organotins in sediment and mysid shrimp of the Scheldt estuary (The Netherlands).* Environmental pollution (Barking, Essex : 1987), 2005. **136**(1): p. 19-31.
55. Stapleton, H.M., et al., *Identification of flame retardants in polyurethane foam collected from baby products.* Environmental science & technology, 2011. **45**(12): p. 5323-5331.
56. Bearr, J.S., H.M. Stapleton, and C.L. Mitchelmore, *Accumulation and DNA damage in fathead minnows (Pimephales promelas) exposed to 2 brominated flame-retardant mixtures, Firemaster 550 and Firemaster BZ-54.* Environ Toxicol Chem, 2010. **29**(3): p. 722-9.
57. Bearr, J.S., et al., *Species specific differences in the in vitro metabolism of the flame retardant mixture, Firemaster((R)) BZ-54.* Aquat Toxicol, 2012. **124-125C**: p. 41-47.
58. Fuertes, G., et al., *Switchable Bactericidal Effects from Novel Silica-Coated Silver Nanoparticles Mediated by Light Irradiation.* Langmuir : the ACS journal of surfaces and colloids, 2011(Journal Article).
59. Baber, O., et al., *Amorphous silica coatings on magnetic nanoparticles enhance stability and reduce toxicity to in vitro BEAS-2B cells.* Inhalation toxicology, 2011. **23**(9): p. 532-543.
60. Jeon, I.T., et al., *Ni-Au core-shell nanowires: synthesis, microstructures, biofunctionalization, and the toxicological effects on pancreatic cancer cells.* Journal of Materials Chemistry, 2011. **21**(32): p. 12089-12095.
61. Kopwitthaya, A., et al., *Biocompatible PEGylated gold nanorods as colored contrast agents for targeted in vivo cancer applications.* Nanotechnology, 2010. **21**(31): p. 315101-315101.
62. Chen, F., et al., *The photoluminescence, drug delivery and imaging properties of multifunctional Eu3+/Gd3+ dual-doped hydroxyapatite nanorods.* Biomaterials, 2011. **32**(34): p. 9031-9039.
63. Ahamed, M., et al., *ZnO nanorod-induced apoptosis in human alveolar adenocarcinoma cells via p53, survivin and bax/bcl-2 pathways: role of oxidative*

stress. Nanomedicine-Nanotechnology Biology and Medicine, 2011. **7**(6): p. 904-913.
64. Begum, P. and B. Fugetsu, *Phytotoxicity of multiwalled carbon nanotubes on red spinach and role of ascorbic acid.* Toxicology letters, 2012. **211**(Journal Article).
65. Larue, C., et al., *Quantitative evaluation of multi-walled carbon nanotube uptake in wheat and rapeseed.* Journal of hazardous materials, 2012. **227**(Journal Article).
66. Li, M. and C.P. Huang, *The responses of Ceriodaphnia dubia toward multi-walled carbon nanotubes: Effect of physical-chemical treatment.* Carbon, 2011. **49**(5): p. 1672-1679.
67. Naya, M., et al., *In vivo lung comet assay of SWCNTs following intratracheal instillation to rats.* Toxicology letters, 2012. **211**(Journal Article).
68. Ge, C., et al., *Acute pulmonary and moderate cardiovascular responses of spontaneously hypertensive rats after exposure to single-wall carbon nanotubes.* Nanotoxicology, 2012. **6**(5).
69. Pichardo, S., et al., *Oxidative stress responses to carboxylic acid functionalized single wall carbon nanotubes on the human intestinal cell line Caco-2.* Toxicology in Vitro, 2012. **26**(5).
70. Wood, C.M., et al., *Biological Effects of Silver*, in *Silver in the Evinronment: Transport, Fate and Effects*, A.W. Andren and T.W. Bober, Editors. 2002, Society of Environmental Toxicology and Chemistry (SETAC): Pensacola, FL. p. 27-63.
71. Brunner, T.J., et al., *In vitro cytotoxicity of oxide nanoparticles: comparison to asbestos, silica, and the effect of particle solubility.* Environmental science & technology, 2006. **40**(14): p. 4374-4381.
72. Bianchini, A. and C.M. Wood, *Mechanism of acute silver toxicity in Daphnia magna.* Environmental toxicology and chemistry / SETAC, 2003. **22**(6): p. 1361-1367.
73. Ferguson, E.A., D.A. Leach, and C. Hogstrand. *Metallothionein protects against silver blockage of Na+/K+ ATPase.* in *4th International Conference on Transport, Fate and Effects of Silver in the Environment*. 1996. Madison, WI.
74. Péqueux, A., *Osmotic regulation in crustaceans.* Journal of Crustacean Biology, 1995. **15**(1): p. 1-60.
75. Kilham, S.S., et al., *COMBO: a defined freshwater culture medium for algae and zooplankton.* Hydrobiologia, 1998. **377**(Journal Article): p. 147-159.
76. Agency, U.S.E.P., *Methods for Measuring the Acute Toxicity of Effluents and Receiving Waters to Freshwater and Marine Organisms. Fifth Edition*, 2002, U.S. Environmental Protection Agency, Office of Water: Washington, D.C.
77. Mucklow, P.T., et al., *Variation in phenoloxidase activity and its relation to parasite resistance within and between populations of Daphnia magna.* Proceedings.Biological sciences / The Royal Society, 2004. **271**(1544): p. 1175-1183.
78. Garcia-Reyero, N., et al., *Biomarker discovery and transcriptomic responses in Daphnia magna exposed to munitions constituents.* Environmental science & technology, 2009. **43**(11): p. 4188-4193.

79. Yang, Y.H., et al., *Normalization for cDNA microarray data: a robust composite method addressing single and multiple slide systematic variation.* Nucleic Acids Res, 2002. **30**(4): p. e15.
80. Loguinov, A.V., I.S. Mian, and C.D. Vulpe, *Exploratory differential gene expression analysis in microarray experiments with no or limited replication.* Genome biology, 2004. **5**(3): p. R18.
81. Storey, J.D. and R. Tibshirani, *Statistical significance for genomewide studies.* Proceedings of the National Academy of Sciences of the United States of America, 2003. **100**(16): p. 9440-9445.
82. Conesa, A., et al., *Blast2GO: a universal tool for annotation, visualization and analysis in functional genomics research.* Bioinformatics (Oxford, England), 2005. **21**(18): p. 3674-3676.
83. Huang da, W., B.T. Sherman, and R.A. Lempicki, *Systematic and integrative analysis of large gene lists using DAVID bioinformatics resources.* Nature protocols, 2009. **4**(1): p. 44-57.
84. Huang da, W., B.T. Sherman, and R.A. Lempicki, *Bioinformatics enrichment tools: paths toward the comprehensive functional analysis of large gene lists.* Nucleic acids research, 2009. **37**(1): p. 1-13.
85. van der Laan, M.J. and K.S. Pollard, *A new algorithm for hybrid hierarchical clustering with visualization and the bootstrap.* Journal of Statistical Planning and Inference, 2003. **117**(2): p. 275-303.
86. Wheeler, M.W., R.M. Park, and A.J. Bailer, *Comparing median lethal concentration values using confidence interval overlap or ratio tests.* Environmental toxicology and chemistry / SETAC, 2006. **25**(5): p. 1441-1444.
87. United States Environmental Protection Agency. *Technical Overview of Ecological Risk Assessment*. Ecotoxicity Categories for Terrestrial and Aquatic Organisms 2012 [cited 2012 December 10]; Available from: http://www.epa.gov/oppefed1/ecorisk_ders/toera_analysis_eco.htm.
88. Poynton, H.C., et al., *Toxicogenomic Responses of Nanotoxicity in Daphnia magna Exposed to Silver Nitrate and Coated Silver Nanoparticles.* Environmental science & technology, 2012(Journal Article).
89. United States Environmental Protection Agency. *National Recommended Water Quality Criteria*. 2012 [cited 2012 December 10]; Aquatic Life Criteria Table]. Available from: http://water.epa.gov/scitech/swguidance/standards/criteria/current/index.cfm - D.
90. Andren, A.W. and T.W. Bober, *Silver in the Environment: Transport, fate and effects*2002, Pensacola, FL, USA: Society of Environmental Toxicology and Chemistry (SETAC).
91. Grigoletto, J.C., et al., *Silver discharged in effluents from image-processing services: a risk to human and environmental health.* Biol Trace Elem Res, 2011. **144**(1-3): p. 316-26.
92. Zhou, D. and A.A. Keller, *Role of morphology in the aggregation kinetics of ZnO nanoparticles.* Water research, 2010. **44**(9): p. 2948-2956.
93. Levard C Fau - Hotze, E.M., et al., *Environmental transformations of silver nanoparticles: impact on stability and toxicity.* (1520-5851 (Electronic)).

94. Romer, I., et al., *Aggregation and dispersion of silver nanoparticles in exposure media for aquatic toxicity tests.* Journal of chromatography.A, 2011. **1218**(27): p. 4226-4233.
95. Jeon, H.J., S.C. Yi, and S.G. Oh, *Preparation and antibacterial effects of Ag-SiO2 thin films by sol-gel method.* Biomaterials, 2003. **24**(27): p. 4921-4928.
96. Bianchini, A. and C.M. Wood, *Physiological effects of chronic silver exposure in Daphnia magna.* Comparative biochemistry and physiology.Toxicology & pharmacology : CBP, 2002. **133**(1-2): p. 137-145.
97. Ke, P.C., *Fiddling the string of carbon nanotubes with amphiphiles.* Physical chemistry chemical physics : PCCP, 2007. **9**(4): p. 439-447.
98. Julien, D.C., et al., *In vitro proliferating cell models to study cytotoxicity of silica nanowires.* Nanomedicine : nanotechnology, biology, and medicine, 2010. **6**(1): p. 84-92.
99. Tao, Z., et al., *Mesoporosity and functional group dependent endocytosis and cytotoxicity of silica nanomaterials.* Chemical research in toxicology, 2009. **22**(11): p. 1869-1880.
100. Park, M.V., et al., *In vitro developmental toxicity test detects inhibition of stem cell differentiation by silica nanoparticles.* Toxicology and applied pharmacology, 2009. **240**(1): p. 108-116.
101. Kwon, N.H., et al., *Nanowire-based delivery of Escherichia coli O157 shiga toxin 1 A subunit into human and bovine cells.* Nano letters, 2007. **7**(9): p. 2718-2723.
102. Beaux, M.F., 2nd, et al., *Fibronectin bonding to nanowires and their internalization by epithelial cells.* Journal of Biomedical Nanotechnology, 2006. **2**(Journal Article): p. 1-6.
103. Adams, L.K., et al., *Comparative toxicity of nano-scale TiO2, SiO2 and ZnO water suspensions.* Water science and technology : a journal of the International Association on Water Pollution Research, 2006. **54**(11-12): p. 327-334.
104. Lee, S.W., S.M. Kim, and J. Choi, *Genotoxicity and ecotoxicity assays using the freshwater crustacean Daphnia magna and the larva of the aquatic midge Chironomus riparius to screen the ecological risks of nanoparticle exposure.* Environmental toxicology and pharmacology, 2009. **28**(1): p. 86-91.
105. Bühler, V., *Excipients for Pharmaceuticals - Povidone, Crospovidone and Copovidone*2005, Berlin Heidelberg New York: Springer.
106. Bilberg, K., et al., *In Vivo Toxicity of Silver Nanoparticles and Silver Ions in Zebrafish (Danio rerio).* Journal of toxicology, 2012. **2012**(Journal Article): p. 293784.
107. Hollunger, G., *The effect of trivalent thallium on oxidative phosphorylation.* Acta Pharmacologica et Toxicologica, 1960. **16**(Journal Article): p. 347-356.
108. Teodoro, J.S., et al., *Assessment of the toxicity of silver nanoparticles in vitro: a mitochondrial perspective.* Toxicology in vitro : an international journal published in association with BIBRA, 2011. **25**(3): p. 664-670.
109. Sharma, C.M., et al., *The primary transcriptome of the major human pathogen Helicobacter pylori.* Nature, 2010. **464**(7286): p. 250-255.
110. Hornett, E.A. and C.W. Wheat, *Quantitative RNA-Seq analysis in non-model species: assessing transcriptome assemblies as a scaffold and the utility of*

evolutionary divergent genomic reference species. BMC genomics, 2012. **13**(1): p. 361.
111. Mehinto, A.C., et al., *Applications for next-generation sequencing in fish ecotoxicogenomics.* Frontiers in genetics, 2012. **3**(Journal Article): p. 62.
112. Zhang, J.J., et al., *Molecular dissection of atrazine-responsive transcriptome and gene networks in rice by high-throughput sequencing.* Journal of hazardous materials, 2012. **219-220**(Journal Article): p. 57-68.
113. Sadamoto, H., et al., *De Novo Sequencing and Transcriptome Analysis of the Central Nervous System of Mollusc Lymnaea stagnalis by Deep RNA Sequencing.* PLoS ONE, 2012. **7**(8): p. e42546.
114. Sun, X., et al., *De novo assembly and characterization of the garlic (Allium sativum) bud transcriptome by Illumina sequencing.* Plant Cell Reports, 2012(Journal Article).
115. McDaneld, T.G., et al., *Next-Generation Sequencing of the Porcine Skeletal Muscle Transcriptome for Computational Prediction of MicroRNA Gene Targets.* PLoS ONE, 2012. **7**(7): p. e42039.
116. Hsu, J.C., et al., *Discovery of Genes Related to Insecticide Resistance in Bactrocera dorsalis by Functional Genomic Analysis of a De Novo Assembled Transcriptome.* PLoS ONE, 2012. **7**(8): p. e40950.
117. Huang, Q., et al., *Deep sequencing-based transcriptome profiling analysis of Oryzias melastigma exposed to PFOS.* Aquatic Toxicology (Amsterdam, Netherlands), 2012. **120-121**(Journal Article): p. 54-58.
118. Zhou, Z.S., J.B. Song, and Z.M. Yang, *Genome-wide identification of Brassica napus microRNAs and their targets in response to cadmium.* Journal of experimental botany, 2012. **63**(12): p. 4597-4613.
119. Chen, H., et al., *Basic leucine zipper transcription factor OsbZIP16 positively regulates drought resistance in rice.* Plant science : an international journal of experimental plant biology, 2012. **193-194**(Journal Article): p. 8-17.
120. Gruenheit, N., et al., *Cutoffs and k-mers: implications from a transcriptome study in allopolyploid plants.* BMC genomics, 2012. **13**(Journal Article): p. 92.
121. Tao, X., et al., *Digital gene expression analysis based on integrated de novo transcriptome assembly of sweet potato [Ipomoea batatas (L.) Lam.* PLoS ONE, 2012. **7**(4): p. e36234.
122. Ghiselli, F., et al., *De Novo assembly of the Manila clam Ruditapes philippinarum transcriptome provides new insights into expression bias, mitochondrial doubly uniparental inheritance and sex determination.* Molecular biology and evolution, 2012. **29**(2): p. 771-786.
123. Kawahara-Miki, R., et al., *Expression profiling without genome sequence information in a non-model species, Pandalid shrimp (Pandalus latirostris), by next-generation sequencing.* PLoS ONE, 2011. **6**(10): p. e26043.
124. Zeng, V., et al., *De novo assembly and characterization of a maternal and developmental transcriptome for the emerging model crustacean Parhyale hawaiensis.* BMC genomics, 2011. **12**(Journal Article): p. 581.
125. Watanabe, H., et al., *Development of a Daphnia magna DNA microarray for evaluating the toxicity of environmental chemicals.* Environmental toxicology and chemistry / SETAC, 2007. **26**(4): p. 669-676.

126. Poynton, H.C., et al., *Gene expression profiling in Daphnia magna, part II: validation of a copper specific gene expression signature with effluent from two copper mines in California.* Environmental science & technology, 2008. **42**(16): p. 6257-6263.
127. Zhao, Z. and D. Ng. *cDNA Library Creation Protocol*. 2007 [cited 2009 June 6]; Available from: http://my.jgi.doe.gov/general/protocols/SOP_DRAFT_cDNA_library_creation_454.doc.
128. Schulz, M.H., et al., *Oases: robust de novo RNA-seq assembly across the dynamic range of expression levels.* Bioinformatics (Oxford, England), 2012. **28**(8): p. 1086-1092.
129. Zerbino, D.R. and E. Birney, *Velvet: algorithms for de novo short read assembly using de Bruijn graphs.* Genome research, 2008. **18**(5): p. 821-829.
130. Smyth, G.K., *Limma: Linear models for microarray data*. Statistics for Biology and Health, ed. R. Gentalman, et al.2005: Springer, 233 Spring Street, New York, Ny 10013, United States. 397-420.
131. Tusher, V.G., R. Tibshirani, and G. Chu, *Significance analysis of microarrays applied to the ionizing radiation response.* Proceedings of the National Academy of Sciences of the United States of America, 2001. **98**(9): p. 5116-5121.
132. Robinson, M.D., D.J. McCarthy, and G.K. Smyth, *edgeR: a Bioconductor package for differential expression analysis of digital gene expression data.* Bioinformatics, 2010. **26**(1): p. 139-40.
133. Anders, S. and W. Huber, *Differential expression analysis for sequence count data.* Genome Biol, 2010. **11**(10): p. R106.
134. Colbourne, J.K., et al., *The ecoresponsive genome of Daphnia pulex.* Science, 2011. **331**(6017): p. 555-61.
135. Feldmeyer, B., et al., *Short read Illumina data for the de novo assembly of a non-model snail species transcriptome (Radix balthica, Basommatophora, Pulmonata), and a comparison of assembler performance.* BMC genomics, 2011. **12**: p. 317.
136. Rawat, A., et al., *CAPRG: sequence assembling pipeline for next generation sequencing of non-model organisms.* PloS one, 2012. **7**(2): p. e30370.
137. Chen, G., C. Wang, and T. Shi, *Overview of available methods for diverse RNA-Seq data analyses.* Sci China Life Sci, 2011. **54**(12): p. 1121-8.
138. Magnusson, K. and P. Tiselius, *The importance of uptake from food for the bioaccumulation of PCB and PBDE in the marine planktonic copepod Acartia clausi.* Aquatic Toxicology (Amsterdam, Netherlands), 2010. **98**(4): p. 374-380.
139. Magnusson, K., et al., *Bioaccumulation of 14C-PCB 101 and 14C-PBDE 99 in the marine planktonic copepod Calanus finmarchicus under different food regimes.* Marine environmental research, 2007. **63**(1): p. 67-81.
140. Losada, S., et al., *Biomagnification of anthropogenic and naturally-produced organobrominated compounds in a marine food web from Sydney Harbour, Australia.* Environment international, 2009. **35**(8): p. 1142-1149.
141. Usenko, C.Y., et al., *PBDE DEVELOPMENTAL EFFECTS ON EMBRYONIC ZEBRAFISH.* Environmental Toxicology and Chemistry, 2011. **30**(8): p. 1865-1872.

142. Viberg, H., A. Fredriksson, and P. Eriksson, *Investigations of strain and/or gender differences in developmental neurotoxic effects of polybrominated diphenyl ethers in mice.* Toxicol Sci, 2004. **81**(2): p. 344-53.
143. Kuriyama, S.N., et al., *Developmental exposure to low dose PBDE 99: effects on male fertility and neurobehavior in rat offspring.* Environ Health Perspect, 2005. **113**(2): p. 149-54.
144. Chen, L., et al., *Alterations in retinoid status after long-term exposure to PBDEs in zebrafish (Danio rerio).* Aquatic Toxicology, 2012. **120**: p. 11-18.
145. Zoeller, R.T., *Environmental chemicals impacting the thyroid: targets and consequences.* Thyroid : official journal of the American Thyroid Association, 2007. **17**(9): p. 811-817.
146. Chevrier, J., et al., *Prenatal Exposure to Polybrominated Diphenyl Ether Flame Retardants and Neonatal Thyroid-Stimulating Hormone Levels in the CHAMACOS Study.* American Journal of Epidemiology, 2011(Journal Article).
147. Siddiqi, M.A., R.H. Laessig, and K.D. Reed, *Polybrominated diphenyl ethers (PBDEs): new pollutants-old diseases.* Clin Med Res, 2003. **1**(4): p. 281-90.
148. Erickson, P.R., et al., *Photochemical formation of brominated dioxins and other products of concern from hydroxylated polybrominated diphenyl ethers (OH-PBDEs).* Environ Sci Technol, 2012. **46**(15): p. 8174-80.
149. Steen, P.O., et al., *Photochemical formation of halogenated dioxins from hydroxylated polybrominated diphenyl ethers (OH-PBDEs) and chlorinated derivatives (OH-PBCDEs).* Environ Sci Technol, 2009. **43**(12): p. 4405-11.
150. Wahl, M., et al., *Polybrominated diphenyl ethers and arylhydrocarbon receptor agonists: Different toxicity and target gene expression.* Toxicol Lett, 2010. **198**(2): p. 119-26.
151. Roberts, S.C., L.J. Macaulay, and H.M. Stapleton, *In vitro metabolism of the brominated flame retardants 2-ethylhexyl-2,3,4,5-tetrabromobenzoate (TBB) and bis(2-ethylhexyl) 2,3,4,5-tetrabromophthalate (TBPH) in human and rat tissues.* Chem Res Toxicol, 2012. **25**(7): p. 1435-41.
152. Springer, C., et al., *Rodent Thyroid, Liver, and Fetal Testis Toxicity of the Monoester Metabolite of Bis-(2-ethylhexyl) Tetrabromophthalate (TBPH), a Novel Brominated Flame Retardant Present in Indoor Dust.* Environ Health Perspect, 2012.
153. Patisaul, H.B., et al., *Accumulation and Endocrine Disrupting Effects of the Flame Retardant Mixture Firemaster((R)) 550 in Rats: An Exploratory Assessment.* J Biochem Mol Toxicol, 2012.
154. United States Environmental Protection Agency, *Furniture flame retardancy partnership environmental profiles of chemical Flame-Retardant Alternatives for Low-Desnisty Polyuretane Foam*. Flame Retardant Alternatives: Triphenyl Phosphate Hazard Review. Vol. 2. 2005, Cincinnati, OH.
155. Lin, K., *Joint acute toxicity of tributyl phosphate and triphenyl phosphate to Daphnia magna.* Environmental Chemistry Letters, 2009. **7**(4): p. 309-312.
156. Marklund, A., B. Andersson, and P. Haglund, *Organophosphorus flame retardants and plasticizers in Swedish sewage treatment plants.* Environ Sci Technol, 2005. **39**(19): p. 7423-9.

157. van der Veen, I. and J. de Boer, *Phosphorus flame retardants: properties, production, environmental occurrence, toxicity and analysis.* Chemosphere, 2012. **88**(10): p. 1119-53.
158. Liu, X., K. Ji, and K. Choi, *Endocrine disruption potentials of organophosphate flame retardants and related mechanisms in H295R and MVLN cell lines and in zebrafish.* Aquat Toxicol, 2012. **114-115**: p. 173-81.
159. Hamilton, M.A., R.C. Russo, and R.V. Thurston, *TRIMMED SPEARMAN-KARBER METHOD FOR ESTIMATING MEDIAN LETHAL CONCENTRATIONS IN TOXICITY BIOASSAYS.* Environmental science & technology, 1977. **11**(7): p. 714-719.
160. Viant, M.R., *Revealing the metabolome of animal tissues using 1H nuclear magnetic resonance spectroscopy.* Methods Mol Biol, 2007. **358**: p. 229-46.
161. Teng, Q., et al., *Push-through direct injection NMR: an optimized automation method applied to metabolomics.* Analyst, 2012. **137**(9): p. 2226-32.
162. Bax, A. and D.G. Davis, *MLEV-17-BASED TWO-DIMENSIONAL HOMONUCLEAR MAGNETIZATION TRANSFER SPECTROSCOPY.* Journal of Magnetic Resonance, 1985. **65**(2): p. 355-360.
163. Guang, Z. and A. Bax, *Two-dimensional linear prediction for signals truncated in both dimensions.* Journal of Magnetic Resonance, 1992. **98**(1): p. 192-199199.
164. Collette, T.W., et al., *Impacts of an anti-androgen and an androgen/anti-androgen mixture on the metabolite profile of male fathead minnow urine.* Environ Sci Technol, 2010. **44**(17): p. 6881-6.
165. Sparkes, B.L., et al., *Intestinal lipid alterations occur prior to antibody-induced prostaglandin E2 production in a mouse model of ischemia/reperfusion.* Biochim Biophys Acta, 2010. **1801**(4): p. 517-25.
166. Mhadhbi, L., J. Fumega, and R. Beiras, *Toxicological Effects of Three Polybromodiphenyl Ethers (BDE-47, BDE-99 and BDE-154) on Growth of Marine Algae Isochrysis galbana.* Water Air and Soil Pollution, 2012. **223**(7): p. 4007-4016.
167. Pellacani, C., et al., *Evaluation of DNA Damage Induced by 2 Polybrominated Diphenyl Ether Flame Retardants (BDE-47 and BDE-209) in SK-N-MC Cells.* International journal of toxicology, 2012. **31**(4): p. 372-379.
168. Davies, R. and E. Zou, *Polybrominated diphenyl ethers disrupt molting in neonatal Daphnia magna.* Ecotoxicology, 2012. **21**(5): p. 1371-1380.
169. Klosterhaus, S.L., et al., *Brominated and chlorinated flame retardants in San Francisco Bay sediments and wildlife.* Environment international, 2012. **47**: p. 56-65.
170. Davis, E.F., S.L. Klosterhaus, and H.M. Stapleton, *Measurement of flame retardants and triclosan in municipal sewage sludge and biosolids.* Environ Int, 2012. **40**: p. 1-7.
171. Sanderson, H. and M. Thomsen, *Ecotoxicological quantitative structure-activity relationships for pharmaceuticals.* Bull Environ Contam Toxicol, 2007. **79**(3): p. 331-5.
172. Veith, G.D. and S.J. Broderius, *Rules for distinguishing toxicants that cause type I and type II narcosis syndromes.* Environ Health Perspect, 1990. **87**: p. 207-11.

173. Vandenbrouck, T., et al., *Mixtures of similarly acting compounds in Daphnia magna: from gene to metabolite and beyond.* Environ Int, 2010. **36**(3): p. 254-68.
174. Aaronson, D.S. and C.M. Horvath, *A road map for those who don't know JAK-STAT.* Science, 2002. **296**(5573): p. 1653-1655.
175. Liu, W.J., et al., *White spot syndrome virus annexes a shrimp STAT to enhance expression of the immediate-early gene ie1.* J Virol, 2007. **81**(3): p. 1461-71.
176. Antczak, P., et al., *Mapping drug physico-chemical features to pathway activity reveals molecular networks linked to toxicity outcome.* PLoS ONE, 2010. **5**(8): p. e12385.
177. Hauser, R., *Urinary phthalate metabolites and semen quality: a review of a potential biomarker of susceptibility.* International journal of andrology, 2008. **31**(2): p. 112-117.
178. Zhao, C.M. and W.X. Wang, *Importance of surface coatings and soluble silver in silver nanoparticles toxicity to Daphnia magna.* Nanotoxicology, 2011(Journal Article).
179. Zhao, C.M. and W.X. Wang, *Biokinetic uptake and efflux of silver nanoparticles in Daphnia magna.* Environmental science & technology, 2010. **44**(19): p. 7699-7704.
180. Jayakody, C., et al., *Fire-retardant characteristics of water-blown molded flexible polyurethane foam materials.* Journal of Fire Sciences, 2000. **18**(6): p. 430-455.
181. Zota, A.R., et al., *Elevated house dust and serum concentrations of PBDEs in California: unintended consequences of furniture flammability standards?* Environmental science & technology, 2008. **42**(21): p. 8158-8164.
182. Kato, Y., et al., *Development of an RNA interference method in the cladoceran crustacean Daphnia magna.* Dev Genes Evol, 2011. **220**(11-12): p. 337-45.